


2008

# Mass Spectrometry-Based High Throughput Approach for Identification of Molecular Modification of Oxidative Process in Respiratory Diseases

Wei Song
*Cleveland State University*

# MASS SPECTROMETRY-BASED HIGH THROUGHPUT APPROACH FOR IDENTIFICATION OF MOLECULAR MODIFICATION OF OXIDATIVE PROCESS IN RESPIRATORY DISEASES

**WEI SONG**

**Bachelor of Science in Medicinal Chemistry**

**Beijing Medical University**

**June 1996**

**submitted in partial fulfillment of requirements for the degree**

**DOCTOR OF PHILOSOPHY IN CLINICAL-BIOANALYTICAL CHEMISTRY**

**at the**

**CLEVELAND STATE UNIVERSITY**

**November 2007**

**This Dissertation has been approved**

**For the Department of CHEMISTRY**

**And the College of Graduates Studies by**

---

**Dissertation Committee Co-Chairman, Dr. Stanley L. Hazen**

**Department of Cell Biology, Lerner Research Institute, Cleveland Clinic**

---

**Dissertation Committee Co-Chairman, Dr. Lily M. Ng**

**Department of Chemistry, Cleveland State University**

---

**Dissertation Committee Member, Dr. Serpil Erzurum**

**Department of Pathobiology, Lerner Research Institute, Cleveland Clinic**

---

**Dissertation Committee Member, Dr. Baochuan Guo**

**Department of Chemistry, Cleveland State University**

---

**Dissertation Committee Member, Dr. Michael T. Kinter**

**Department of Cell Biology, Lerner Research Institute, Cleveland Clinic**

## DEDICATION AND ACKNOWLEDGEMENTS

I want to thank the Cleveland State University and Lerner Research Institute of Cleveland Clinic Foundation joined program for providing me this golden opportunity to perform my research at Dr. Hazen's Lab. I deeply and gratefully thank my dissertation advisor Dr. Hazen and academic advisor Dr. Ng for their exceptional mentorship, constant support, unlimited encouragement and patience. The training they gave me will be an important part of my future scientific achievements. For everything you have done for me, Dr. Hazen and Dr. Ng, I thank you!

I gratefully acknowledge Dr. Erzurum, Dr. Guo and Dr. Kinter for being on my committee member, and for their support, motivation and valuable input. Their understanding and support play an important role in my research.

I extend my sincere appreciation to Dr. Brennan for her training and assistance in animal study. I want to thank Dr. Citardi for his help in clinical study. I also want to thank Dr. Levison and Dr. Zhang for technical support in Mass Spectrometry. Special thanks are given to Xiaoming Fu and David Schmitt for their assistance. I like to acknowledge all my co-workers and friends in Dr. Hazen's lab for their unlimited support.

I like to thank my husband, Yu for his support, encouragement and unwavering love. Finally, and most importantly, I like to thank my parents for their love, guidance and support.

**MASS SPECTROMETRY-BASED HIGHTHROUGHPUT APPROACH FOR IDENTIFICATION OF MOLECULAR MODIFICATION OF OXIDATIVE PROCESS IN RESPIRATORY DISEASES**

**WEI SONG**

## ABSTRACT

Eosinophil peroxidase (EPO) and myeloperoxidase (MPO) have been implicated in generating reactive species and promoting oxidative modifications in numerous diseases. The detection and identification of potential pathways has been proven extremely challenge due to evanescence nature of these reactive species. An alternative approach to study the involvement of oxidative modification is to detect and quantify the stable molecular fingerprints, like oxidized tyrosine species, in biological matrices.

Previously reported analytical methods for quantifying oxidized amino acids have typically been limited by: low sensitivity, specificity and the failure of detection potential oxidation products generated during sample handling. Using GC/MS in combination with stable isotope dilution, a sensitive and self-quality control assay was developed. Using this isotope-dilution GC/MS and multiple allergen challenge models, we demonstrate that EPO is the major pathway for generating protein-bound 3-bromotyrosine *in vivo*.

However, the need for chemical derivatization of samples increases the possibility that artifactual generation of oxidation products which may interfere with the detection of native levels. Requirement of unique derivatization reagent for each oxidized tyrosine results sample analysis both cumbersome and time/labor intensive. Therefore, we develop a liquid chromatography with on-line electrospray ionization tandem mass

spectrometry (LC-ESI/MS/MS) assay that simultaneously detects and quantifies multiple structurally informative protein oxidation products along with their precursor amino acids. Use of four HPLC systems in multiplex array with column switching permits on-line analyses of only relevant portions of chromatographic profiles and up to four-fold increased throughput efficiency of mass detector usage.

Using this high-throughput multiplexed array-based LC-MS/MS method, we found significant correlations among individual oxidized tyrosine in sera from healthy volunteers. These correlations provide chemical evidence that activated leukocytes utilize various physiological available substrates to participate multiple oxidative modifications *in vivo*. In rhinosinusitis study, significantly elevated protein-bound oxidized tyrosine species were detected in healthy nasal tissue compared to that at the peripheral level. In addition, rhinosinusitis patients had more severe oxidative modification in their nasal tissue. The evidence supports elevated bromination and tyrosylation may contribute to the pathogenesis of rhinosinusitis.

# TABLE OF CONTENTS

## LIST OF TABLES

# LIST OF FIGURES

# CHAPTER I

# PEROXIDASE AND PEROXIDASE CATALYZED OXIDATIVE DAMAGES

Peroxidases are heme-containing enzymes that catalyze the reduction of hydrogen peroxide ($H_2O_2$) and facilitate the generation of various reactive species as part of the innate host defense system [1-3]. The mammalian peroxidase super-family includes eosinophil peroxidase (EPO), lactoperoxidase (LPO), myeloperoxidase (MPO), prostaglandin H1/2 synthases (PGHS-1, PGHS-2) and thyroid peroxidase (TPO) [4]. The major function of EPO and MPO is involved in protecting the host from infectious diseases [5, 6]. Evidences indicate that EPO and MPO may also play a vital role in facilitating oxidative modifications by generating reactive oxygen species in numerous diseases such as asthma, rhinosinuositis, atherosclerosis and multiple sclerosis [7-9].

In this chapter, a brief review includes following topics: (1) Eosinophil peroxidase (EPO) and myeloperoxidase (MPO); (2) Catalytic site of EPO and MPO; (3) Peroxidase catalyzed oxidationand inflammatory diseases.

## 1.1 Eosinophil Peroxidase (EPO) and Myeloperoxidase (MPO)

Eosinophil peroxidase (EPO) and Myeloperoxidase (MPO) share a high degree homology at genomic sequence level and in physiological function. Genetic studies reveal that human EPO and human MPO are encoded by adjacent genes located on human chromosome 17 [4, 10]. DNA sequence studies reveal that EPO and MPO gene both contain 12 exons and 11 introns. Further, human EPO and human MPO have an overall 72.4% homology at nucleotide level and 69.8% homology at amino acids level [11]. Elevated eosinophils, neutrophils and increased EPO, MPO contents are associated with numerous disorder including allergic respiratory diseases, cardiovascular diseases and neurodegenerative disorders [12, 13]. Upon stimulation, eosinophils and neutrophils are recruited to the inflammation sites and release their specific granule proteins, including peroxidases [14, 15]. Peroxidases utilize $H_2O_2$ and various substrates to generate cytotoxic oxidants to fight invading pathogens [16, 17].

### Genetic Properties of MPO and EPO

Genomic studies of MPO and EPO were started in the middle 1980s. Morishita et al. used a synthetic 41-base oligonucleotide, which was decoded from amino acid sequence of human myeloperoxidase, as a probe to isolate MPO cDNA clones from human promyelocytic leukemia HL-60 cell. They identified a 2.6-kilobase nucleotide that contained genetic information for a polypeptide which had 745 amino acids. The calculated molecular weight was estimated of 83 kDa. Human MPO heavy chain was located on the C terminus of this particular polypeptide. [18]. Yamada et al. isolated and characterized a cDNA which encoded the carboxyl-terminal fragment of human MPO

heavy chain. Using this cDNA as a probe, they identified a MPO mRNA fragment with approximately 3.3 kb in length. *In vitro* translation of this MPO mRNA fragment generated a major product, a 74 KDa polypeptide precursor. The identity of this polypeptide precursor was confirmed by co-precipitation with anti-MPO IgG antibody. Antibodies specific for MPO light and heavy chains both recognized this polypeptide precursor. These findings further support that MPO is initially synthesized as a single polypeptide, and then it is further processed into a light chain and a heavy chain [19]. Later, human MPO mRNA was identified by MPO cDNA in human leukemia HL-60 cell. Using in situ hybridization, Chang et al. located human MPO gene on chromosome 17q22-24 [20]. Other studies also localize MPO gene to a region between 17q11-q21 and 17q21-q42 [21]. Interestingly, in mouse, the corresponding myeloperoxidase gene (mMPO) was located on chromosome 11[22].

Sakamaki et al. used northern hybridization and S1 mapping analysis of RNA technique to confirm that EPO gene was only expressed in eosinophilic subline but not neutrophilic subline or in parental human HL-60 cells [11]. Using human MPO cDNA as a probe, the chromosomal gene of human EPO was isolated and studied. This gene contained the genetic information for a polypeptide of 715 amino acids with an estimated molecular weight about 81 KDa. Further, EPO heavy chain and light chain were identified at C and N termini of this polypeptide, respectively. Later, In situ hybridization studies indicated that human EPO gene was located on chromosome 17q23.1 [23].

The high degree homology of human EPO and human MPO at genomic level strongly supports the notion that both genes may originate from the same ancestral gene, or from gene duplication and divergent evolution.

**Biochemical Properties of MPO and EPO**

Human myeloperoxidase (MPO, EC 1.11.1.7), a disulfide-linked dimer with two light chains and two heavy chains, was purified from human leukocytes by three steps including dialysis with a low salt buffer solution, separation by gel filtration chromatography and carboxymethylcellulose chromatography. The molecular weight (MW) of human MPO was estimated to be 118 kDa by sedimentation equilibrium ultracentrifuge [24]. A-Sepharose affinity chromatography was used to purify human MPO from peripheral blood from one donor. The identity of extracted MPO was confirmed by having maximum Soret absorbance at 430 nm. The MW of this human MPO was estimated to be 146 KDa [25]. A rapid isolation procedure was applied to purify human MPO from normal human leukocyte with about 17% yield. The high-spin heme signal in this purified MPO was demonstrated by electron paramagnetic resonance spectroscopy (EPR). The MW of this purified MPO was determined to be 144 KDa by ultracentrifuge [26]. A single polypeptide with MW of 80 KDa was identified as primary translation product of MPO massager RNA (mRNA). Thise proMPO is formed by proteolytic cleavage and N-linked glycosylation. After acquisition of heme group, the proMPO undergoes a sequential of post-translational modifications to form mature MPO that contains a pair of light and heavy chains [27 28].

Human eosinophil peroxidase (EPO, EC 1.11.1.7), a monomer with one light chain and one heavy chain, was purified from eosinophilic leukemia cells by gel filtration

and ion-exchange chromatography. The MW of EPO was determined by gel chromatography and estimated to be 77 KDa. Sodium dodecyl sulfate polyacrylamide gel electrophoresis (SDS-PAGE) analysis revealed that this reduced EPO was composed of one heavy chain and one light chain with MW of 52 KDa and 15 KDa, respectively [29]. Later, EPO was purified from normal leukocytes and also demonstrated similar molecular weight of 72±1 KDa. Other analysis revealed this isolated EPO was composed by heavy chain and light chain with MW of 58 and 14 KDa, respectively [30]. Similar high spin EPR signal of heme group was also observed in purified EPO [31]. Radioimmunoassay revealed that the content of EPO was estimated to be 15.0 μg/10 $^{6}$eosinophils [29]. Carbon 14 labeled leucine was used as a probe to study the biosynthesis of EPO in marrow cells from patients with eosinophilia. Two EPO precursors with MW of 78 and 72 KDa were detected and recognized by anti-EPO antibody. Monensin, an inhibitor of MPO synthesis, did not block the biosynthesis of EPO [32].

The major Soret band of oxidized MPO is observed at 430 nm and shifted to 470 nm after reduction [25]. However, the major Soret band of purified EPO is observed at 412 nm [31]. The unique distorted porphyrin ring structure and positive charged sulfonium ion was observed in MPO. This distinctive structure of MPO is proposed to be the cause of red shift of Soret band, and its distinct affinity for chloride. In site directed mutagenesis studies indicate that the Soret band of MPO will shift back to 411 nm when the Met243 is replaced by either of Thr, Gln or Val. The affinity for chloride is also decreased 100 fold due to the replacement of Met243 in MPO [33].

Colorimetric assays are developed to determine peroxidase activity in biological matrices. MPO can specifically utilize chloride and hydrogen peroxide to oxidize

chromogen like tetramethylbenzidine (TMB) at pH 5.0 in the presence of resorcinol, an EPO inhibitor [34, 35]. Other chromogens were used to measure MPO activity including guaiacol, taurine and o-dianisidine dihydrochloride[35-37]. Unlike MPO, EPO oxidizes bromide instead of chloride under physiological conditions to generate hypobromous acid and its conjugate base hypobromite (HOBr/ $OBr^-$) [38]. EPO activity can be determined by adding o-phenylene diamine at pH 8.0 in the presence of 3 mM bromide and 1 mM hydrogen peroxide [34, 39]. In all these approaches, measured peroxidase activity is significantly affected by pH, the presence of peroxidase inhibitor, and the concentration of chloride, hydrogen peroxide.

Immunochemical study indicates that the structure of EPO is distinct from that of MPO. Antibodies that recognize human EPO do not cross react with human MPO, and vice versa [32].

## 1.2 Catalytic Sites of MPO and EPO

Both MPO and EPO contain heme groups. The heme group contains an iron ion (ferric oxidation state, $Fe^{3+}$) at the center of protoporphyrin IX group. The ferric ion is bound to four pyrrole nitrogen. The fifth coordination position is connected with a histidine residue to form an imidazole side chain. The sixth position is believed to be empty at the distal side of both native MPO and EPO. However, in MPO, histidine 95 at distal side may perform as an acid/base catalyst to assist peroxidase catalyzed oxidation [40, 41].

Low resolution X-ray crystallography (3 Å) study indicates that heme prosthetic group of human MPO contains a bound calcium ion and three asparagine-linked glycosylation. Around the heme prosthetic group, His336 is linked to the heme iron ion

on the proximal side of the heme in human MPO. Simultaneously, His336 is linked to Asn421 through a hydrogen bond [42]. Later, Fiedler et al. elucidated human MPO crystal structure at higher resolution (1.8 Å) and demonstrated that the methyl groups on the pyrrole rings A and C were covalently attached to the carboxyl groups of Glu242 and Asp94, respectively, via ester bonds. The beta carbon of the vinyl group on pyrrole ring A connects with the sulfur atom of Met243 to form a sulfonium ion linkage via a covalent bond. Although the pyrrole ring B and D are still co-planar, ring A and C are bent to the distal side. In addition, each side chain of Gln91, His95 and Arg239 connects with one immobilized water molecule via a hydrogen bond. These three amino acids side chains and the water molecules provide a solvent accessible environment and facilitate the oxidation inside the catalytic site [43]. A similar covalent attachment in human EPO has been identified. Glu241 is covalently attached with the pyrrole ring via an ester bond. However, there is no sulfonium ion linkage in human EPO structure [44].

During the inflammation, MPO/EPO are secreted by activated leukocytes and implicated in host defense. They play an essential role in oxidizing chloride ($Cl^-$), bromide ($Br^-$), iodide ($I^-$), and the thiocyanate ($SCN^-$) to form strong oxidants that kill microorganism as part of the defense function [7, 17, 45-47]. Three major intermediates, the native state of MPO or EPO, Compound I and II are found to catalyze the generation of these reactive oxidants, [40, 48, 49]. Each intermediate has its unique structure and spectral property. Electron paramagnetic resonance (EPR) studies indicate the existence of a ferryl/prophrin radical ($Por^{\bullet+}$ $Fe^{IV}$=O) structure in MPO compound I (Cpd I) [41]. Raman resonance spectroscopy studies confirm the presence of oxyferryl ($Fe^{IV}$=O) structure in MPO compound II (CpdII) [40]

The structures of these intermediates and related reactions have been investigated to understand the fundamental mechanism of peroxidase catalyzed oxidation. In the first step of the catalytic cycle, $H_2O_2$ oxidizes native ferric form of MPO or EPO to corresponding active state Cpd I by transferring two electrons and generating water (Eq.1). Other *in vitro* studies indicate that other hydroxyperoxides like hypochlorous acid (chloride-free media) can also oxidize native peroxidase to Compound I (Cpd I). The reduction potential of Cpd I is about -1.1 V [50, 51].

$$PorFe^{3+} + H_2O_2 \rightarrow Por^{\bullet+}Fe^{IV}=O + H_2O \qquad \text{Eq.1}$$

In the presence of endogenous one-electron donors like nitrite ($NO_2^-$), nitric oxide ($NO^\bullet$) and tyrosine, Compound I can be quickly reduced to Compound II (Eq. 2), and then further to the native ferric enzyme (Eq. 3) via obtaining two sequential one-electron and generating nitro dioxide and tyrosyl radicals respectively [50, 52-54]. However, in the presence of halides and thiocyanide ($SCN^-$), compound I ($Por^{\bullet+}\ Fe^{IV}=O$) coverts to the native form (Pro $Fe^{3+}$) by obtaining two-electron reduction and generating the corresponding hypohalous acid (Eq. 4).

$$^{\bullet+}PorFe^{IV}=O + R \rightarrow PorFe^{IV}=O + R^\bullet \qquad \text{Eq. 2}$$

$$PorFe^{IV}=O + RH + H^+ \rightarrow PorFe^{3+} + R^\bullet +^{\cdot} H_2O \qquad \text{Eq. 3}$$

$$^{\bullet+}PorFeIV=O + X^- + H^+ \rightarrow PorFeI^{3+} + HOX \qquad \text{Eq. 4}$$

R= $NO^\bullet$, $NO_2^-$, Tyr, X= $SCN^-$, $Cl^-$, Br and $I^-$

In addition, researchers also propose the reactive species like $H_2O_2$, superoxide can reduce native MPO to a ferrous intermediate (MPO-$Fe^{2+}$). An inactive state, Compound III (Cpd III, MPO-$Fe^{2+}$-$O_2$) was formed via the binding between MPO-$Fe^{3+}$

and superoxide or MPO-Fe $^{2+}$ with oxygen, respectively [55-58]. It takes longer time for Cpd III to be converted back to the native enzyme form which utilizes two $H_2O_2$ molecules and generate of one $O_2$ molecule [56, 59]. Studies support that Cpd III reacts with $H_2O_2$/ $O_2^{\bullet}$ to re-enter classical peroxidase cycle via Cpd II or native MPO [57, 60]. Using distinct spectroscopic measurement, our lab reported that both ferric (Fe $^{3+}$) and ferrous (Fe $^{2+}$) MPO could reversibly bind to nitric oxide and generated stable low-spin six-coordinate complexes Fe $^{3+}$ –NO and Fe $^{2+}$ –NO, respectively [51].

The scheme of catalytic cycles include three major pathways: (A) the conversions of native ferric peroxidase (MPO) via Compound I, Compound II and back to the native state of MPO; (B) the reaction of MPO (Fe $^{3+}$) with superoxide or MPO (Fe $^{2+}$) with oxygen to generate compound III; (C) the reaction of MPO (Fe $^{3+}$) or MPO (Fe $^{2+}$) with nitric oxide (Figure 1.1). Under certain condition, these reactions can be carried in the opposite direction. Overall, the catalytic cycle of peroxidase starts with the conversion of native enzyme to its active form Compound I by losing two electrons. Compound I can be reduced to the native state ($Fe^{3+}$) either by two-electron reduction or two sequential one-electron reductions.

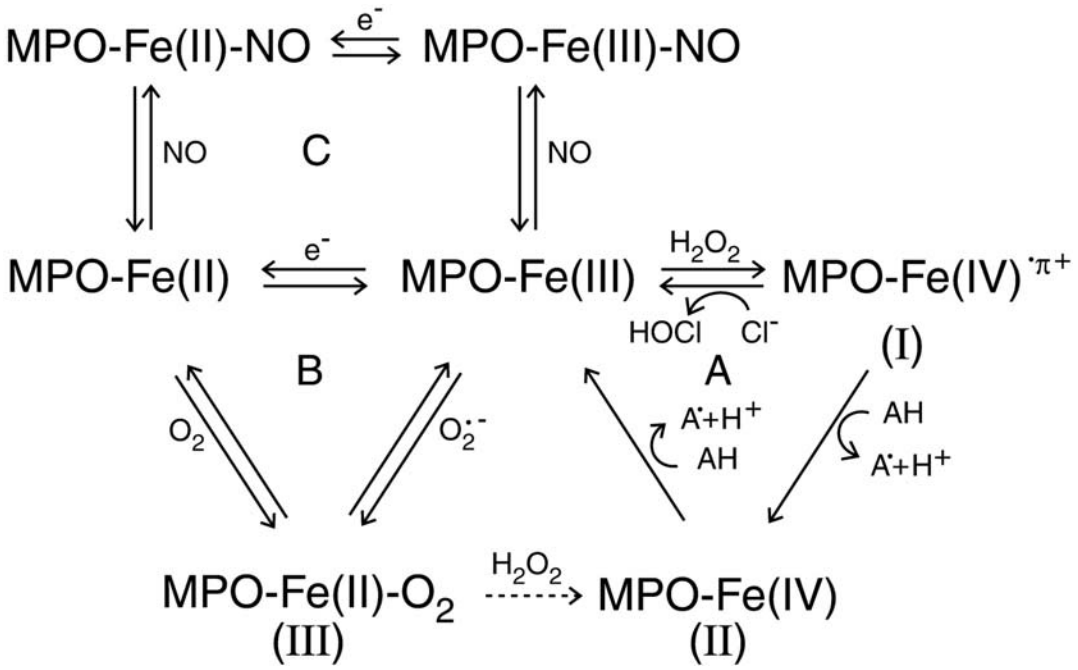


**Figure 1. 1 Catalytic Cycles of MPO**

The proposed MPO catalytic model: (A) Native MPO is converted to active MPO Compound I (Cpd I) by losing two electrons. Compound I can be reduced to the native state ($Fe^{3+}$) either by two-electron reduction or to compound II (Cpd II) by a one-electron reduction. The Compound II is further transformed to the native state via another one-election reduction; (B) Native MPO (FeIII) or its reduced form MPO (FeII) bind with superoxide or oxygen, respectively, to generate an inactive intermediate, compound III (Cpd III); (C) Native MPO (FeIII) or its reduced form MPO (FeII) bind with nitric oxide to form MPO (FeIII)-NO or MPO (FeII)-NO, respectively.

## 1.3 Peroxidases and Diseases

Both EPO and MPO are able to generate cytotoxic oxidants and cause the damage of invading pathogens. However, these reactive oxidants may also associate with host damage. Upon stimulation, eosinophils and neutrophils are recruited to the sites of inflammation and release their unique granule proteins EPO and MPO, respectively. EPO and MPO utilize $H_2O_2$ and available substrates to initiate a cascade of oxidative events. *In vitro* studies demonstrate that MPO/EPO-$H_2O_2$-$X^-$ system are toxic to both gram-negative and gram-positive bacteria [47, 61, 62]. The EPO-$H_2O_2$-$X^-$ system is capable of killing parasites like Schistosoma Mansoni [63]. The primary mechanism for EPO/MPO to promote microbicidal function is based on the peroxidase catalyzed oxidative damage to the pathogen. Microorganism like Schistosomula remains viable when it incubates with EPO alone. The microbicidal function of peroxidase can be accomplished only in the presence of hydrogen peroxide and halide [46, 63, 64]. The cell injury can be inhibited by adding heme-enzyme inhibitor, azide, which supports the catalytic role of the heme group in the peroxidase [47].

The contribution of peroxidases in host defense has been questioned since the majority of peroxidase-deficient subjects rarely suffer any severe infectious diseases. Several reasons may attribute this scenario. First, most of these individuals only lost one particular peroxidase activity, either MPO or EPO but not both [65, 66]. The other peroxidase-dependent or peroxidase-independent oxidants generation, may compensate the loss of one particular peroxidase. In one unique case, a patient was both MPO and EPO deficienct. He did suffere severe cor pulmonale disorder and one of his lungs was completely damaged by the bacteria attack [67]. Second, infectious diseases like Candida

are predominately seen in MPO deficient patients with diabetes mellitus [68]. Utilizing GC/MS and LC/MS/MS, Brennan et al investigated the potential pathways that participate the generation of 3-nitrotyrosine generation *in vivo*. Within multiple inflammation models, the formation of 3-nitrotyrosine were evaluated in EPO or MPO wild type and knockout mice. In some models, MPO or EPO played a dominant role, accounting for the majority of nitrotyrosine generation. However, in other leukocyte-rich acute inflammatory models, no significant protein-bound nitration was observed [69]. Overall, peroxidase does play an important role in host defense against bacteria, fungi and parasites infection.

Other than the beneficial effects of peroxidases in host defense, more and more evidence indicates that peroxidase catalyzed oxidation may lead to host damage. Recent studies indicate that eosinophils and eosinophil peroxidase may involve in the pathogenesis of allergic respiratory diseases like asthma, rhinosinusitis by promoting oxidative modification [9, 70, 71].

Asthma, a common lung disorder in developed countries, is characterized by wheezing, breathlessness, chest tightness and coughing with reversible airway obstruction. In 1998, an estimate of 17 millions Americans suffered from this lung disorder. In addition, 30% of these patients were children [72]. Similarly, rhinosinusitis is an inflammation disease characterized by nasal congestion, itching, sneezing and nasal discharge. In 2001, an estimate of 58 millions Americans suffered rhinosinusitis [73]. The overall direct cost of asthma and chronic rhinosinusitis is estimated over $ 10 billion per year [72, 74].

Eosinophil infiltration and activation are associated with airway allergic responses. First, eosinophilia is predominately observed in asthma and rhinosinusitis patients. Significantly elevated eosinophils were observed in peripheral blood, and sputum recovered from asthmatic patients [70, 71, 75] In rhinosinusitis patients, even if they had negative skin response, elevated eosinophils were detected in peripheral blood and in nasal lavage fluids (NLF) [12, 76]. It is still not clear whether this eosinophilia in patients who suffer respiratory disorder just an epi-phenomenon of allergic disease or a representation of the involvement of eosinophil in the inflammation response. A house mite allergen challenge study was performed in asthmatic subjects and healthy controls. Bronchoalveolar lavage (BAL) was collected 6 hours after allergen challenge. Significantly elevated eosinophils recovered from BAL fluid were observed in asthmatic patients compared to that in the healthy controls in response to the allergen challenge. This finding supports that eosinophils are actively recruited to the lung as a consequence of allergen provocation [13].

In response to cytokine and chemokine stimulation, eosinophils release bioactive molecules, generate reactive species and initiate oxidative modification. Eosinophils are recruited to the inflammation sites and release eosinophil specific granule proteins in response to chemokines stimulation [77, 78]. Chemokines cooperate with cytokines to stimulate eosinophil differentiation, activate cellular response and amplify the immune responses [78-80]. Activated eosinophils releases unique granule proteins including eosinophil cationic protein (ECP), eosinophil peroxidase (EPO) and major basic protein (MBP), and stimulates peripheral mast cell to release histamine [81, 82]. Further, isolated MBP activates neutrophils, basophils and mast cells [83, 84]. In addition, activated

eosinophils release lipids mediator including PAF, $LTC_4/D_4/E_4$ [85-87]. These bioactive lipids initiate the allergic response by contracting smooth muscle, increasing mucous secretion and facilitating granulocytes migration. The details and references are tabulated in Table 1.1.

Peroxidases are the principle enzymes that generate reactive species in allergic diseases like asthma and rhinosinusitis. In the presence of hydrogen peroxide and physiological halide, EPO but not other eosinophil basic granule proteins can cause human lung injuries halides [46]. Eosinophil peroxidase can specifically oxidize bromide even in the presence of 1000 fold higher chloride condition [38]. In aeroallergen lung challenge model, compared to peroxynitrite catalyzed tyrosine nitration, EPO- $H_2O_2$-$NO_2^-$ system is more efficient in generating nitrotyrosine *in vivo*. After allergen challenge, 70% elevated 3-nitrotyroine in $EPO^{+/+}$ animal is originated from EPO-$H_2O_2$-$NO_2^-$ [69].

**Table 1.1 Bioactive Molecules Detected in Asthmatic Patients**

| **Chemokines** | **Abbreviation** | **Reference** |
|---|---|---|
| Regulated upon Activation Normal T-cell Expressed and Secreted | RANTES | [70, 77, 78, 88-90] |
| Macrophage Inflammatory Protein-1α | MIP-1α | |
| Interleukin-8 | IL-8 | |
| **Cytokines** | | |
| Tumor Necrosis Factor-alpha | TNF-α, | [15, 89, 91] |
| Tumor Necrosis Factor-beta | TNF -β | |
| Interleukin-3 | IL-3, | [78-80, 92-94] |
| Interleukin-5 | IL-5, | |
| Granulocyte-macrophage Colony-stimulating Factor | GM-CSF | |
| Platelet-derived Growth Factor-β | PDGF-β | [95, 96] |
| Vascular Endothelial Growth Factor | VEGF | |
| **Granule Cationic Proteins** | | |
| Eosinophil Cationic Protein | ECP | [9, 76, 81-84, 97-99] |
| Eosinophil Derived Neurotoxin | EDN | |
| Eosinophil Peroxidase | EPO | |
| Major Basic Protein | MBP | |
| **Lipid mediators** | | |
| Leukotriene-C4/ D4/ E4 | LTC4/ D4/ E4 | [15, 70, 85-87, 100, 101] |
| Platelet Activating Factor | PAF | |
| Prostaglandin E2 | PGE2 | |

Aromatic amino acid like tyrosine is readily oxidized by peroxidase by losing the phenolic hydrogen and one electron to form tyrosyl radical ($Y^{\cdot}$) [102]. Tyrosyl radical is relative stable since the radical delocalize around the aromatic ring. The tyrosyl radical reacts with free or protein bound tyrosyl residue to form dityrosine. EPO and MPO utilize hydrogen peroxide and various physiological substrates to generate corresponding reactive bromating species (RBS), reactive chlorinating species (RCS), and reactive nitrogen species (RNS) species, catalyze oxidative modification and participate airway remodeling [2, 103-105] (Figure 1.2).

Peroxidase catalyzed oxidative modification is proposed to implicate in the pathogenesis of respiratory disease like asthma and rhinosinusitis. Several clinical studies support that the release of EPO during inflammation response results in extensive oxidation. After a localized allergen challenge, 3-bromotyrosine content recovered from BAL was increased 10-fold, but there were only two- to threefold increases in 3-chlorotyrosine in the mild asthmatics [104]. Aldridge et al. found that protein-bound 3-Bromotyrosine, recovered in sputum from asthmatic patients, was significantly elevated. The levels of this bromination product correlated highly positively with eosinophil peroxidase protein mass ($r = 0.79$, $p < 0.0001$) [106]. In addition, 10-fold increase in protein-bound 3-nitrotyrosine, and 100-fold increase in protein bound 3-bromotyrosine were recovered from BAL of severe asthmatics compared to that from healthy control [107]. Indeed, peroxidase catalyzed oxidation is implicated in promoting oxidative tissue modification in allergic respiratory diseases.

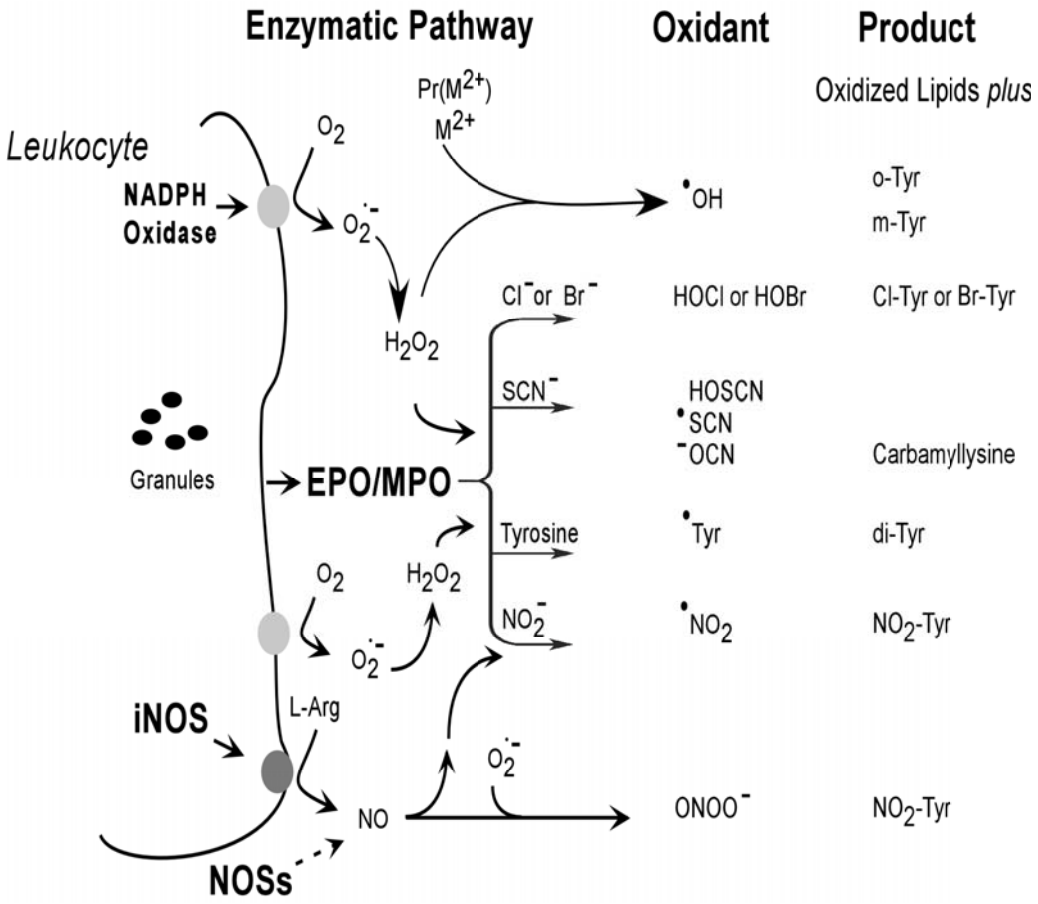


**Figure 1. 2 Potential Enzymatic Pathways for Generating Reactive Oxidants and Oxidation Products**

Each reactive oxidant may result oxidative damage and contribute inflammatory injury. NOS NO synthase, iNOS inducible NO synthase, $M^{2+}$, redox-active metal ion, Pr ($M^{2+}$), protein-bound redox-active metal ion, L-Arg, L-Arginine.

## 1.4 Reference:


1. Nauseef, W. M., Contributions of myeloperoxidase to proinflammatory events: more than an antimicrobial system. Int J Hematol **2001,** 74, (2), 125-33.
2. Zhang, R.; Brennan, M. L.; Shen, Z.; MacPherson, J. C.; Schmitt, D.; Molenda, C. E.; Hazen, S. L., Myeloperoxidase functions as a major enzymatic catalyst for initiation of lipid peroxidation at sites of inflammation. J Biol Chem **2002,** 277, (48), 46116-22.
3. Klebanoff, S. J.; Waltersdorph, A. M.; Rosen, H., Antimicrobial activity of myeloperoxidase. Methods Enzymol **1984,** 105, 399-403.
4. O'Brien, P. J., Peroxidases. Chem Biol Interact **2000,** 129, (1-2), 113-39.
5. Buss, I. H.; Senthilmohan, R.; Darlow, B. A.; Mogridge, N.; Kettle, A. J.; Winterbourn, C. C., 3-Chlorotyrosine as a marker of protein damage by myeloperoxidase in tracheal aspirates from preterm infants: association with adverse respiratory outcome. Pediatr Res **2003,** 53, (3), 455-62.
6. Gujral, J. S.; Hinson, J. A.; Jaeschke, H., Chlorotyrosine protein adducts are reliable biomarkers of neutrophil-induced cytotoxicity in vivo. Comp Hepatol **2004,** 3 Suppl 1, S48.
7. Hoy, A.; Leininger-Muller, B.; Kutter, D.; Siest, G.; Visvikis, S., Growing significance of myeloperoxidase in non-infectious diseases. Clin Chem Lab Med **2002,** 40, (1), 2-8.

8. Kantarci, O. H.; Atkinson, E. J.; Hebrink, D. D.; McMurray, C. T.; Weinshenker, B. G., Association of a myeloperoxidase promoter polymorphism with multiple sclerosis. J Neuroimmunol **2000,** 105, (2), 189-94.

9. Venge, P.; Dahl, R.; Fredens, K.; Peterson, C. G., Epithelial injury by human eosinophils. Am Rev Respir Dis **1988,** 138, (6 Pt 2), S54-7.

10. Petrides, P. E., Molecular genetics of peroxidase deficiency. J Mol Med **1998,** 76, (10), 688-98.

11. Sakamaki, K.; Tomonaga, M.; Tsukui, K.; Nagata, S., Molecular cloning and characterization of a chromosomal gene for human eosinophil peroxidase. J Biol Chem **1989,** 264, (28), 16828-36.

12. Mygind, N.; Dirksen, A.; Johnsen, N. J.; Weeke, B., Perennial rhinitis: an analysis of skin testing, serum IgE, and blood and smear eosinophilia in 201 patients. Clin Otolaryngol **1978,** 3, (2), 189-96.

13. De Monchy, J. G.; Kauffman, H. F.; Venge, P.; Koeter, G. H.; Jansen, H. M.; Sluiter, H. J.; De Vries, K., Bronchoalveolar eosinophilia during allergen-induced late asthmatic reactions. Am Rev Respir Dis **1985,** 131, (3), 373-6.

14. Wardlaw, A. J.; Dunnette, S.; Gleich, G. J.; Collins, J. V.; Kay, A. B., Eosinophils and mast cells in bronchoalveolar lavage in subjects with mild asthma. Relationship to bronchial hyperreactivity. Am Rev Respir Dis **1988,** 137, (1), 62-9.

15. McClenahan, D.; Fagliari, J.; Evanson, O.; Weiss, D., Role of inflammatory mediators in priming, activation, and deformability of bovine neutrophils. Am J Vet Res **2000,** 61, (5), 492-8.

16. Furtmuller, P. G.; Burner, U.; Regelsberger, G.; Obinger, C., Spectral and kinetic studies on the formation of eosinophil peroxidase compound I and its reaction with halides and thiocyanate. Biochemistry **2000,** 39, (50), 15578-84.

17. McCormick, M. L.; Roeder, T. L.; Railsback, M. A.; Britigan, B. E., Eosinophil peroxidase-dependent hydroxyl radical generation by human eosinophils. J Biol Chem **1994,** 269, (45), 27914-9.

18. Morishita, K.; Kubota, N.; Asano, S.; Kaziro, Y.; Nagata, S., Molecular cloning and characterization of cDNA for human myeloperoxidase. J Biol Chem **1987,** 262, (8), 3844-51.

19. Yamada, M.; Hur, S. J.; Hashinaka, K.; Tsuneoka, K.; Saeki, T.; Nishio, C.; Sakiyama, F.; Tsunasawa, S., Isolation and characterization of a cDNA coding for human myeloperoxidase. Arch Biochem Biophys **1987,** 255, (1), 147-55.

20. Chang, K. S.; Schroeder, W.; Siciliano, M. J.; Thompson, L. H.; McCredie, K.; Beran, M.; Freireich, E. J.; Liang, J. C.; Trujillo, J. M.; Stass, S. A., The localization of the human myeloperoxidase gene is in close proximity to the translocation breakpoint in acute promyelocytic leukemia. Leukemia **1987,** 1, (5), 458-62.

21. Miki, T.; Weil, S. C.; Rosner, G. L.; Reid, M. S.; Kidd, K. K., An MPO cDNA clone identifies an RFLP with PstI. Nucleic Acids Res **1988,** 16, (4), 1649.

22. Robinson, T. J.; Morris, D. J.; Ledbetter, D. H., Chromosomal assignment and regional localization of myeloperoxidase in the mouse. Cytogenet Cell Genet **1990,** 53, (2-3), 83-6.

23. Sakamaki, K.; Kanda, N.; Ueda, T.; Aikawa, E.; Nagata, S., The eosinophil peroxidase gene forms a cluster with the genes for myeloperoxidase and lactoperoxidase on human chromosome 17. Cytogenet Cell Genet **2000,** 88, (3-4), 246-8.

24. Matheson, N. R.; Wong, P. S.; Travis, J., Isolation and properties of human neutrophil myeloperoxidase. Biochemistry **1981,** 20, (2), 325-30.

25. Merrill, D. P., Purification of human myeloperoxidase by Concanavalin A-Sepharose affinity chromatography. Prep Biochem **1980,** 10, (2), 133 50.

26. Bakkenist, A. R.; Wever, R.; Vulsma, T.; Plat, H.; van Gelder, B. F., Isolation procedure and some properties of myeloperoxidase from human leucocytes. Biochim Biophys Acta **1978,** 524, (1), 45-54.

27. Nauseef, W. M., Myeloperoxidase biosynthesis by a human promyelocytic leukemia cell line: insight into myeloperoxidase deficiency. Blood **1986,** 67, (4), 865-72.

28. Hansson, M.; Olsson, I.; Nauseef, W. M., Biosynthesis, processing, and sorting of human myeloperoxidase. Arch Biochem Biophys **2006,** 445, (2), 214-24.

29. Carlson, M. G.; Peterson, C. G.; Venge, P., Human eosinophil peroxidase: purification and characterization. J Immunol **1985,** 134, (3), 1875-9.

30. Menegazzi, R.; Zabucchi, G.; Patriarca, P., A simple procedure for the purification of eosinophil peroxidase from normal human blood. J Immunol Methods **1986,** 91, (2), 283-8.

31. Bolscher, B. G.; Plat, H.; Wever, R., Some properties of human eosinophil peroxidase, a comparison with other peroxidases. Biochim Biophys Acta **1984,** 784, (2-3), 177-86.

32. Olsson, I.; Persson, A. M.; Stromberg, K.; Winqvist, I.; Tai, P. C.; Spry, C. J., Purification of eosinophil peroxidase and studies of biosynthesis and processing in human marrow cells. Blood **1985,** 66, (5), 1143-8.

33. Kooter, I. M.; Moguilevsky, N.; Bollen, A.; van der Veen, L. A.; Otto, C.; Dekker, H. L.; Wever, R., The sulfonium ion linkage in myeloperoxidase. Direct spectroscopic detection by isotopic labeling and effect of mutation. J Biol Chem **1999,** 274, (38), 26794-802.

34. Schneider, T.; Issekutz, A. C., Quantitation of eosinophil and neutrophil infiltration into rat lung by specific assays for eosinophil peroxidase and myeloperoxidase. Application in a Brown Norway rat model of allergic pulmonary inflammation. J Immunol Methods **1996,** 198, (1), 1-14.

35. Marcinkiewicz, J.; Chain, B.; Nowak, B.; Grabowska, A.; Bryniarski, K.; Baran, J., Antimicrobial and cytotoxic activity of hypochlorous acid: interactions with taurine and nitrite. Inflamm Res **2000,** 49, (6), 280-9.

36. Vlasova, II; Arnhold, J.; Osipov, A. N.; Panasenko, O. M., pH-Dependent Regulation of Myeloperoxidase Activity. Biochemistry (Mosc) **2006,** 71, (6), 667-77.

37. Bradley, P. P.; Priebat, D. A.; Christensen, R. D.; Rothstein, G., Measurement of cutaneous inflammation: estimation of neutrophil content with an enzyme marker. J Invest Dermatol **1982,** 78, (3), 206-9.

38. Weiss, S. J.; Test, S. T.; Eckmann, C. M.; Roos, D.; Regiani, S., Brominating oxidants generated by human eosinophils. Science **1986,** 234, (4773), 200-3.

39. Strath, M.; Warren, D. J.; Sanderson, C. J., Detection of eosinophils using an eosinophil peroxidase assay. Its use as an assay for eosinophil differentiation factors. J Immunol Methods **1985,** 83, (2), 209-15.

40. Oertling, W. A.; Hoogland, H.; Babcock, G. T.; Wever, R., Identification and properties of an oxoferryl structure in myeloperoxidase compound II. Biochemistry **1988,** 27, (15), 5395-400.

41. Ortiz de Montellano, P. R., Catalytic sites of hemoprotein peroxidases. Annu Rev Pharmacol Toxicol **1992,** 32, 89-107.

42. Zeng, J.; Fenna, R. E., X-ray crystal structure of canine myeloperoxidase at 3 A resolution. J Mol Biol **1992,** 226, (1), 185-207.

43. Fiedler, T. J.; Davey, C. A.; Fenna, R. E., X-ray crystal structure and characterization of halide-binding sites of human myeloperoxidase at 1.8 A resolution. J Biol Chem **2000,** 275, (16), 11964-71.

44. Oxvig, C.; Thomsen, A. R.; Overgaard, M. T.; Sorensen, E. S.; Hojrup, P.; Bjerrum, M. J.; Gleich, G. J.; Sottrup-Jensen, L., Biochemical evidence for heme linkage through esters with Asp-93 and Glu-241 in human eosinophil peroxidase. The ester with Asp-93 is only partially formed in vivo. J Biol Chem **1999,** 274, (24), 16953-8.

45. Furtmuller, P. G.; Obinger, C.; Hsuanyu, Y.; Dunford, H. B., Mechanism of reaction of myeloperoxidase with hydrogen peroxide and chloride ion. Eur J Biochem **2000,** 267, (19), 5858-64.

46. Agosti, J. M.; Altman, L. C.; Ayars, G. H.; Loegering, D. A.; Gleich, G. J.; Klebanoff, S. J., The injurious effect of eosinophil peroxidase, hydrogen peroxide, and halides on pneumocytes in vitro. J Allergy Clin Immunol **1987,** 79, (3), 496-504.

47. Persson, T.; Andersson, P.; Bodelsson, M.; Laurell, M.; Malm, J.; Egesten, A., Bactericidal activity of human eosinophilic granulocytes against Escherichia coli. Infect Immun **2001,** 69, (6), 3591-6.

48. Marquez, L. A.; Huang, J. T.; Dunford, H. B., Spectral and kinetic studies on the formation of myeloperoxidase compounds I and II: roles of hydrogen peroxide and superoxide. Biochemistry **1994,** 33, (6), 1447-54.

49. Marquez, L. A.; Dunford, H. B., Reaction of compound III of myeloperoxidase with ascorbic acid. J Biol Chem **1990,** 265, (11), 6074-8.

50. Abu-Soud, H. M.; Hazen, S. L., Nitric oxide is a physiological substrate for mammalian peroxidases. J Biol Chem **2000,** 275, (48), 37524-32.

51. Abu-Soud, H. M.; Hazen, S. L., Nitric oxide modulates the catalytic activity of myeloperoxidase. J Biol Chem **2000,** 275, (8), 5425-30.

52. Furtmuller, P. G.; Jantschko, W.; Regelsberger, G.; Obinger, C., Spectral and kinetic studies on eosinophil peroxidase compounds I and II and their reaction with ascorbate and tyrosine. Biochim Biophys Acta **2001,** 1548, (1), 121-8.

53. Furtmuller, P. G.; Arnhold, J.; Jantschko, W.; Pichler, H.; Obinger, C., Redox properties of the couples compound I/compound II and compound II/native enzyme of human myeloperoxidase. Biochem Biophys Res Commun **2003,** 301, (2), 551-7.

54. Burner, U.; Furtmuller, P. G.; Kettle, A. J.; Koppenol, W. H.; Obinger, C., Mechanism of reaction of myeloperoxidase with nitrite. J Biol Chem **2000,** 275, (27), 20597-601.

55. Cuperus, R. A.; Muijsers, A. O.; Wever, R., The superoxide dismutase activity of myeloperoxidase; formation of compound III. Biochim Biophys Acta **1986,** 871, (1), 78-84.

56. Cuperus, R. A.; Hoogland, H.; Wever, R.; Muijsers, A. O., The effect of D-penicillamine on myeloperoxidase: formation of compound III and inhibition of the chlorinating activity. Biochim Biophys Acta **1987,** 912, (1), 124-31.

57. Kettle, A. J.; Winterbourn, C. C., Superoxide modulates the activity of myeloperoxidase and optimizes the production of hypochlorous acid. Biochem J **1988,** 252, (2), 529-36.

58. Kettle, A. J.; Sangster, D. F.; Gebicki, J. M.; Winterbourn, C. C., A pulse radiolysis investigation of the reactions of myeloperoxidase with superoxide and hydrogen peroxide. Biochim Biophys Acta **1988,** 956, (1), 58-62.

59. Kohler, H.; Taurog, A.; Dunford, H. B., Spectral studies with lactoperoxidase and thyroid peroxidase: interconversions between native enzyme, compound II, and compound III. Arch Biochem Biophys **1988,** 264, (2), 438-49.

60. Winterbourn, C. C.; Garcia, R. C.; Segal, A. W., Production of the superoxide adduct of myeloperoxidase (compound III) by stimulated human neutrophils and its reactivity with hydrogen peroxide and chloride. Biochem J **1985,** 228, (3), 583-92.

61. Miyasaki, K. T.; Wilson, M. E.; Genco, R. J., Killing of Actinobacillus actinomycetemcomitans by the human neutrophil myeloperoxidase-hydrogen peroxide-chloride system. Infect Immun **1986,** 53, (1), 161-5.

62. Miyasaki, K. T.; Zambon, J. J.; Jones, C. A.; Wilson, M. E., Role of high-avidity binding of human neutrophil myeloperoxidase in the killing of Actinobacillus actinomycetemcomitans. Infect Immun **1987,** 55, (5), 1029-36.

63. Jong, E. C.; Chi, E. Y.; Klebanoff, S. J., Human neutrophil-mediated killing of schistosomula of Schistosoma mansoni: augmentation by schistosomal binding of eosinophil peroxidase. Am J Trop Med Hyg **1984,** 33, (1), 104-15.

64. Klebanoff, S. J.; Shepard, C. C., Toxic effect of the peroxidase-hydrogen peroxide-halide antimicrobial system on Mycobacterium leprae. Infect Immun **1984,** 44, (2), 534-6.

65. Nakagawa, T.; Ikemoto, T.; Takeuchi, T.; Tanaka, K.; Tanigawa, N.; Yamamoto, D.; Shimizu, A., Eosinophilic peroxidase deficiency: Identification of a point mutation (D648N) and prediction of structural changes. Hum Mutat **2001,** 17, (3), 235-6.

66. Nauseef, W. M., Myeloperoxidase deficiency. Hematol Oncol Clin North Am **1988,** 2, (1), 135-58.

67. Kutter, D., Prevalence of myeloperoxidase deficiency: population studies using Bayer-Technicon automated hematology. J Mol Med **1998,** 76, (10), 669-75.

68. Parry, M. F.; Root, R. K.; Metcalf, J. A.; Delaney, K. K.; Kaplow, L. S.; Richar, W. J., Myeloperoxidase deficiency: prevalence and clinical significance. Ann Intern Med **1981,** 95, (3), 293-301.

69. Brennan, M. L.; Wu, W.; Fu, X.; Shen, Z.; Song, W.; Frost, H.; Vadseth, C.; Narine, L.; Lenkiewicz, E.; Borchers, M. T.; Lusis, A. J.; Lee, J. J.; Lee, N. A.; Abu-Soud, H. M.; Ischiropoulos, H.; Hazen, S. L., A tale of two controversies: defining both the role of peroxidases in nitrotyrosine formation in vivo using eosinophil peroxidase and myeloperoxidase-deficient mice, and the nature of peroxidase-generated reactive nitrogen species. J Biol Chem **2002,** 277, (20), 17415-27.

70. Romagnoli, M.; Vachier, I.; Tarodo de la Fuente, P.; Meziane, H.; Chavis, C.; Bousquet, J.; Godard, P.; Chanez, P., Eosinophilic inflammation in sputum of poorly controlled asthmatics. Eur Respir J **2002,** 20, (6), 1370-7.

71. Bousquet, J.; Chanez, P.; Lacoste, J. Y.; Barneon, G.; Ghavanian, N.; Enander, I.; Venge, P.; Ahlstedt, S.; Simony-Lafontaine, J.; Godard, P.; et al., Eosinophilic inflammation in asthma. N Engl J Med **1990,** 323, (15), 1033-9.

72. Forecasted State-Specific Estimates of Self-Reported Asthma Prevalence -- United States, 1998. Morbidity and Mortality Weekly Report **1998,** 47, (47), 1022-25.

73. Settipane, R. A., Demographics and epidemiology of allergic and nonallergic rhinitis. Allergy Asthma Proc **2001,** 22, (4), 185-9.

74. Murphy, M. P.; Fishman, P.; Short, S. O.; Sullivan, S. D.; Yueh, B.; Weymuller, E. A., Jr., Health care utilization and cost among adults with chronic rhinosinusitis enrolled in a health maintenance organization. Otolaryngol Head Neck Surg **2002,** 127, (5), 367-76.

75. Yamada, H.; Yamaguchi, M.; Yamamoto, K.; Nakajima, T.; Hirai, K.; Morita, Y.; Sano, Y., Eotaxin in induced sputum of asthmatics: relationship with eosinophils and eosinophil cationic protein in sputum. Allergy **2000,** 55, (4), 392-7.

76. Rasp, G.; Thomas, P. A.; Bujia, J., Eosinophil inflammation of the nasal mucosa in allergic and non-allergic rhinitis measured by eosinophil cationic protein levels in native nasal fluid and serum. Clin Exp Allergy **1994,** 24, (12), 1151-6.

77. Schweizer, R. C.; Welmers, B. A.; Raaijmakers, J. A.; Zanen, P.; Lammers, J. W.; Koenderman, L., RANTES- and interleukin-8-induced responses in normal human eosinophils: effects of priming with interleukin-5. Blood **1994,** 83, (12), 3697-704.

78. Dahinden, C. A.; Geiser, T.; Brunner, T.; von Tscharner, V.; Caput, D.; Ferrara, P.; Minty, A.; Baggiolini, M., Monocyte chemotactic protein 3 is a most effective basophil- and eosinophil-activating chemokine. J Exp Med **1994,** 179, (2), 751-6.

79. Kita, H.; Ohnishi, T.; Okubo, Y.; Weiler, D.; Abrams, J. S.; Gleich, G. J., Granulocyte/macrophage colony-stimulating factor and interleukin 3 release from human peripheral blood eosinophils and neutrophils. J Exp Med **1991,** 174, (3), 745-8.

80. Kita, H.; Weiler, D. A.; Abu-Ghazaleh, R.; Sanderson, C. J.; Gleich, G. J., Release of granule proteins from eosinophils cultured with IL-5. J Immunol **1992,** 149, (2), 629-35.

81. Zheutlin, L. M.; Ackerman, S. J.; Gleich, G. J.; Thomas, L. L., Stimulation of basophil and rat mast cell histamine release by eosinophil granule-derived cationic proteins. J Immunol **1984,** 133, (4), 2180-5.

82. Henderson, W. R.; Chi, E. Y.; Jong, E. C.; Klebanoff, S. J., Mast cell-mediated tumor-cell cytotoxicity. Role of the peroxidase system. J Exp Med **1981,** 153, (3), 520-33.

83. O'Donnell, M. C.; Ackerman, S. J.; Gleich, G. J.; Thomas, L. L., Activation of basophil and mast cell histamine release by eosinophil granule major basic protein. J Exp Med **1983,** 157, (6), 1981-91.

84. Popken-Harris, P.; Thomas, L.; Oxvig, C.; Sottrup-Jensen, L.; Kubo, H.; Klein, J. S.; Gleich, G. J., Biochemical properties, activities, and presence in biologic fluids of eosinophil granule major basic protein. J Allergy Clin Immunol **1994,** 94, (6 Pt 2), 1282-9.

85. Tedla, N.; Bandeira-Melo, C.; Tassinari, P.; Sloane, D. E.; Samplaski, M.; Cosman, D.; Borges, L.; Weller, P. F.; Arm, J. P., Activation of human eosinophils through leukocyte immunoglobulin-like receptor 7. Proc Natl Acad Sci U S A **2003,** 100, (3), 1174-9.

86. Oshiro, T.; Kakuta, Y.; Shimura, S.; Nara, M.; Shirato, K., Characterization of platelet-activating factor-induced cytosolic calcium mobilization in human eosinophils. Clin Exp Allergy **2000,** 30, (5), 699-705.

87. Raab, Y.; Sundberg, C.; Hallgren, R.; Knutson, L.; Gerdin, B., Mucosal synthesis and release of prostaglandin E2 from activated eosinophils and macrophages in ulcerative colitis. Am J Gastroenterol **1995,** 90, (4), 614-20.

88. Meurer, R.; Van Riper, G.; Feeney, W.; Cunningham, P.; Hora, D., Jr.; Springer, M. S.; MacIntyre, D. E.; Rosen, H., Formation of eosinophilic and monocytic intradermal inflammatory sites in the dog by injection of human RANTES but not

human monocyte chemoattractant protein 1, human macrophage inflammatory protein 1 alpha, or human interleukin 8. J Exp Med **1993,** 178, (6), 1913-21.

89. Costa, J. J.; Matossian, K.; Resnick, M. B.; Beil, W. J.; Wong, D. T.; Gordon, J. R.; Dvorak, A. M.; Weller, P. F.; Galli, S. J., Human eosinophils can express the cytokines tumor necrosis factor-alpha and macrophage inflammatory protein-1 alpha. J Clin Invest **1993,** 91, (6), 2673-84.

90. Simon, H. U.; Yousefi, S.; Weber, M.; Simon, D.; Holzer, C.; Hartung, K.; Blaser, K., Human peripheral blood eosinophils express and release interleukin-8. Int Arch Allergy Immunol **1995,** 107, (1-3), 124-6.

91. Levi-Schaffer, F.; Garbuzenko, E.; Rubin, A.; Reich, R.; Pickholz, D.; Gillery, P.; Emonard, H.; Nagler, A.; Maquart, F. A., Human eosinophils regulate human lung- and skin-derived fibroblast properties in vitro: a role for transforming growth factor beta (TGF-beta). Proc Natl Acad Sci U S A **1999,** 96, (17), 9660-5.

92. Stern, M.; Meagher, L.; Savill, J.; Haslett, C., Apoptosis in human eosinophils. Programmed cell death in the eosinophil leads to phagocytosis by macrophages and is modulated by IL-5. J Immunol **1992,** 148, (11), 3543-9.

93. Calhoun, W. J.; Sedgwick, J.; Busse, W. W., The role of eosinophils in the pathophysiology of asthma. Ann N Y Acad Sci **1991,** 629, 62-72.

94. Kramer, M. F.; Rasp, G., Nasal polyposis: eosinophils and interleukin-5. Allergy **1999,** 54, (7), 669-80.

95. Leonardi, A.; Brun, P.; Tavolato, M.; Abatangelo, G.; Plebani, M.; Secchi, A. G., Growth factors and collagen distribution in vernal keratoconjunctivitis. Invest Ophthalmol Vis Sci **2000,** 41, (13), 4175-81.

96. Horiuchi, T.; Weller, P. F., Expression of vascular endothelial growth factor by human eosinophils: upregulation by granulocyte macrophage colony-stimulating factor and interleukin-5. Am J Respir Cell Mol Biol **1997,** 17, (1), 70-7.

97. Fredens, K.; Dahl, R.; Venge, P., The Gordon phenomenon induced by the eosinophil cationic protein and eosinophil protein X. J Allergy Clin Immunol **1982,** 70, (5), 361-6.

98. Kokuludag, A.; Sin, A.; Terzioglu, E.; Saydam, G.; Sebik, F., Elevation of serum eosinophil cationic protein, soluble tumor necrosis factor receptors and soluble intercellular adhesion molecule-1 levels in acute bronchial asthma. J Investig Allergol Clin Immunol **2002,** 12, (3), 211-4.

99. Patella, V.; de Crescenzo, G.; Marino, I.; Genovese, A.; Adt, M.; Gleich, G. J.; Marone, G., Eosinophil granule proteins are selective activators of human heart mast cells. Int Arch Allergy Immunol **1997,** 113, (1-3), 200-2.

100. Foegh, M. L.; Maddox, Y. T.; Ramwell, P. W., Human peritoneal eosinophils and formation of arachidonate cyclooxygenase products. Scand J Immunol **1986,** 23, (5), 599-603.

101. Bartemes, K. R.; McKinney, S.; Gleich, G. J.; Kita, H., Endogenous platelet-activating factor is critically involved in effector functions of eosinophils stimulated with IL-5 or IgG. J Immunol **1999,** 162, (5), 2982-9.

102. Marquez, L. A.; Dunford, H. B., Kinetics of oxidation of tyrosine and dityrosine by myeloperoxidase compounds I and II. Implications for lipoprotein peroxidation studies. J Biol Chem **1995,** 270, (51), 30434-40.

103. Shen, Z.; Mitra, S. N.; Wu, W.; Chen, Y.; Yang, Y.; Qin, J.; Hazen, S. L., Eosinophil peroxidase catalyzes bromination of free nucleosides and double-stranded DNA. Biochemistry **2001,** 40, (7), 2041-51.

104. Wu, W.; Samoszuk, M. K.; Comhair, S. A.; Thomassen, M. J.; Farver, C. F.; Dweik, R. A.; Kavuru, M. S.; Erzurum, S. C.; Hazen, S. L., Eosinophils generate brominating oxidants in allergen-induced asthma. J Clin Invest **2000,** 105, (10), 1455-63.

105. Wu, W.; Chen, Y.; Hazen, S. L., Eosinophil peroxidase nitrates protein tyrosyl residues. Implications for oxidative damage by nitrating intermediates in eosinophilic inflammatory disorders. J Biol Chem **1999,** 274, (36), 25933-44.

106. Aldridge, R. E.; Chan, T.; van Dalen, C. J.; Senthilmohan, R.; Winn, M.; Venge, P.; Town, G. I.; Kettle, A. J., Eosinophil peroxidase produces hypobromous acid in the airways of stable asthmatics. Free Radic Biol Med **2002,** 33, (6), 847-56.

107. MacPherson, J. C.; Comhair, S. A.; Erzurum, S. C.; Klein, D. F.; Lipscomb, M. F.; Kavuru, M. S.; Samoszuk, M. K.; Hazen, S. L., Eosinophils are a major source of nitric oxide-derived oxidants in severe asthma: characterization of pathways available to eosinophils for generating reactive nitrogen species. J Immunol **2001,** 166, (9), 5763-72.

# CHAPTER II

# METHODS FOR ANALYSIS OF OXIDIZED TYROSINE SPECIES

Peroxidase catalyzed oxidative modifications are implicated in various physiological and pathological processing like aging, allergic response and neurodegenerative disorders [1-3]. Both *in vitro* and *in vivo* studies support reactive intermediates generated by MPO/EPO reacting with a variety of targets including protein, lipid and genetic materials [4-9]. It is extremely important to understand the operational mechanisms of peroxidase induced oxidation because it may not only provide information on the involvement of oxidative modification in disease development, but may also offer insights into possible strategies to slow or stop oxidative modification.

Reliable analytical techniques are needed to detect and quantify those reactive species including reactive brominating species (RBS), reactive chlorinating species (RCS) and reactive nitrogen species (RNS). However, it is extreme challenges to monitor the generation and reaction of these reactive intermediates *in vivo* due to the transient nature of these reactive intermediates. As an alternative approach, most studies

are focused on detecting and quantifying stable end-products of each distinct oxidative pathway from normal and pathological specimens[4-9]. Protein oxidation has been intensively investigated since the last decade due to the following reasons: (1) protein is the major scavenger of oxidative free radical species both in intra and extra cellular environments [1]; (2) protein has a longer half-time compared with other macromolecules and may preserve more structural changes [10]; (3) the modification on the protein may associate with the change of the corresponding enzymatic function and may initiate a cascade biological event [1, 11, 12]. Although various amino acid residues are subjected to reactive oxygen species attack, aromatic amino acid residues like tyrosine, phenylalanine and tryptophan are more vulnerable to free radical induced oxidation [13, 14] For example, 3-Bromotyrosine can be generated by the reaction of tyrosine with HOBr/$OBr^-$ which may originate from the EPO/MPO-$H_2O_2$-$Br^-$ system [15]. 3-Chlorotyrosine is the product of tyrosine reacting with HOCl/$OCl^-$ or with species such as chlorine ($Cl_2$) [16, 17]. 3-Nitrotyrosine is generated when reactive nitrogen species react with free tyrosine or tyrosine residue [6, 7, 18]. Dityrosine is formed by radical-radical addition reaction via a tyrosyl radical generating system [19, 20]. Hydroxyl radical oxidizes phenylalanine to generate non physiologic tyrosine species, *m*-tyrosine and *o*-tyrosine [13, 21]. All these oxidized tyrosine species resist to change during acid hydrolysis. Indeed, these oxidized tyrosine species are unique molecular fingerprint to study potential the mechanisms of protein oxidation.

## 2.1 Antibody-based Immunostaining and ELISA Assays

A variety of approaches including immunohistochemical and enzyme-linked immunosorbent assay (ELISA) have been developed by using commercially available polyclonal and/or monoclonal antibodies to recognize oxidized tyrosine species. Antibodies which specifically recognized oxidized tyrosine species including 3-nitrotyrosine, Dityrosine, 3-chlorotyrosine have been used to detect and localize these oxidation markers *in vivo* [22-27].

Immunostaining offers a way of localizing oxidized tyrosine species within biological matrices [28]. Using 3-nitrotyrosine (3-$NO_2$Y) specific antibody and immunohistochemical staining, elevated 3-$NO_2$Y was detected in myocardium from patients with myocarditis [23], in atherosclerotic lesions of human coronary arteries [29, 30], in the lower neuron from multiple sclerosis patients [31], in Lewy body core from patients suffered Alzheimer's disease or Parkinson's disease [32, 33] and in the lung tissue from patients with adult respiratory distress syndrome (ARDS) [34]. Similarly, dityrosine was detected in lipofuscin from aged human brain [24]. In the mice endotoxemia model, 3-Chlorotyrosine was detected in liver tissue and co-localized with neutrophils [27].

ELISA assay is a powerful tool to evaluate relative amounts of oxidized tyrosine species *in vivo*. Detection of oxidized tyrosine residue requires minimum sample handling procedures including incubation, washing and reaction. In addition, there is no artifact generation during sample processing and the oxidized protein remains intact and may use for further investigation. Using an ELISA assay, 3-nitrotyrosine was only detected in plasma from type II diabetic patients (n= 40, 0.251±0.141 μM) [35]. Elevated

3-nitrotyrosine (1.27±1.03 μM) was detected in plasma samples from celiac disease patients but not in that from controls [36] [37]. Recently, several studies reported using competitive enzyme-linked immunosorbent assay (c-ELISA) to quantify nitrated protein in plasma and other biological fluids [38, 39]. Other studies reported the detection of 3-nitrotyrosine residue in various matrixes including bovine serum albumin (BSA), human serum albumin (HSA), $\alpha_1$-antiprotease inhibitor, pepsinogen and fibrinogen. To quantify nitrated protein, a standard curve was constructed by determining the binding of the anti-3-$NO_2$Y antibody to the immobilized antigen (nitrated protein) in the presence of a serial dilution of nitrated BSA or corresponding nitrated protein solutions (Fig 2.1). Their assay demonstrates the high affinity between 3-$NO_2$Y residue and polyclonal antibody. 95.8% antibody binding was inhibited by 10 mM of 3-$NO_2$Y but only 3.3% inhibition was observed in the presence of the 10 mM of tyrosine. But the specificity of this assay may be challenged due to the extremely low abundance of 3-$NO_2$Y compared with tyrosine (3-$NO_2$Y:Y, approximately 0.1-1:$10^6$)[40]. In addition, the high affinity binding between antibody and 3-$NO_2$Y residue may also be altered by the environment of 3-$NO_2$Y residue, distinct protein structure, sample amount, and other components that may cross react with the antibody. The half maximal inhibition concentration ($IC_{50}$) values for different nitrated protein were varied from 5-100 nM [41].

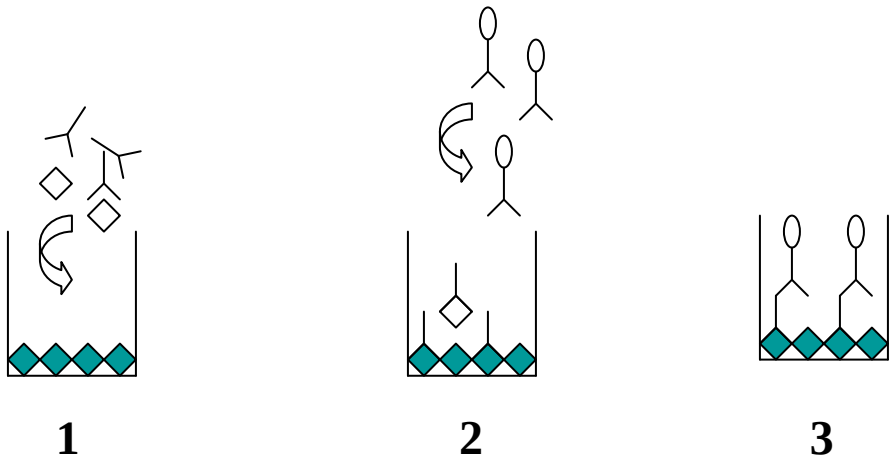


**Figure 2. 1 Schematic Diagram of Competitive ELISA**

◆ Nitrated BSA (immobilized antigen); ◇ nitrated BSA (standard) or nitrated protein in sample; Rabbit anti-nitrotyrosine IgG; HRP conjugated donkey anti-rabbit Ig G. Briefly, the 96-well plate was blocked with nitrated BSA. A PBS solution containing polyclonal rabbit anti-nitrotyrosine Ig G was mixed with variable amount of nitrated BSA and incubated with immobilized nitrated BSA. The rabbit anti-nitrotyrosine Ig G was bound with either immobilized nitrated BSA or nitrated BSA in PBS solution. After a sequential washing, incubating donkey anti-rabbit Ig G antibody was applied to bind with rabbit anti-nitrotyrosine Ig G which was bound with immobilized nitrated BSA. After washing, distinct color was developed and detected at 490 nm.

However, cross-reactivity and semi-quantitative nature dramatically limits the utilization of this technique for quantification purpose [38, 41]. Although the antibodies were developed to target a distinct oxidized tyrosine residue, the abilities of these antibodies to specifically recognize this unique oxidation product, especially in complex biological matrixes, were little tested. The identity of recognized antigen may be queried because there is no direct structural information of this antigen available in the assay. Further more, there is no immunochemical assay yet available that can simultaneously quantify multiple oxidized tyrosine species and their precursors.

## 2.2 Analytical-based Quantitative Assays

Analytical approaches include sample extraction, separation, and quantification of the protein-bound oxidized tyrosine species. High performance liquid chromatography (HPLC) and gas chromatography (GC) are commonly used to separate oxidized tyrosine species in the protein hydrolysate [2, 8, 15-18, 20, 42-45]. Detection techniques can be selected based on the requirement for selectivity, precision and detection limit. Currently, on-line detectors include ultraviolet-visible detector (UV), fluorescence detector, electrochemical detection detector (ECD) and mass spectrometer (MS).

### 2.2.1 Protein Hydrolysis

Peroxidase catalyzed oxidation generate both free and protein bound oxidized tyrosine species. To analyzing protein-bound oxidized tyrosine species, protein is separated from salts and hydrolyzed into amino acid residues. Protein was commonly hydrolyzed to yield free amino acids under 6 M HCl at 110 ˚C for about 24 hours [46-48]. Further investigations indicate that tyrosine can be easily nitrated when co-incubate with

trace amount of nitrite or nitrate ions in acidic condition at elevated temperature [40, 49]. Trace amount of nitrite ion (10 μM) induces significant tyrosine nitration (up to 250 fold increase). However, this nitration can be significantly reduced by adding 1% phenol or 1% butylated hydroxytoluene (BHT) into this acidic system [50, 51]. Similar tyrosine chlorination and bromination were noticed in acidic condition in the presence of the corresponding anion ions, chloride and bromide, respectively [15, 52].

Several approaches are carried out to eliminate potential artifacts generation during protein hydrolysis. First, all the glassware should be carefully cleaned to create a clean environment (nitrite, nitrate, chloride and bromide free). The general procedure includes rinsing with HPLC grade water, and baking at 500 degree over 12 hours to reduce the anions [17, 52]. Second, techniques including dialysis, protein precipitation and strong cation ion exchange chromatography, are used to separate protein from water soluble salts prior to acidic hydrolysis [52-54]. Third, oxidation scavengers including phenol and BHT are added into the system to reduce artifact generation [50]. Finally multiple protein hydrolysis techniques are developed to meet individual purpose. For example, hydrobromic acid (HBr) or methanesulfonic acid (MSA) instead of hydrochloric acid is used to eliminate chloride ion in system [2, 17]. Mild enzymatic digestion in neutral condition (pH=7.2) was performed and no artifact was detected [40, 50]. However, the potential limitations of enzymatic digestion include low yield of protein hydrolysis and the contribution of tyrosine and oxidized tyrosine species from autolysis of protease itself [49, 50]. Alkaline hydrolysis also demonstrated that no artifact was generated during processing. However, multiple interference peaks of 3-nitrotyrosine were observed and additional derivatization step (acidic condition) was required [55]. In addition, the

degradation of oxidized tyrosine species was observed during alkaline hydrolysis [56, 57]. Although these procedures were proved effectively reduced tyrosine residue oxidation during hydrolysis, none of these methods can guarantee no artifact generation during protein hydrolysis. To monitor the artifact generation, unique isotope labeled tyrosine species ($^{13}C_9$, $^{15}N_1$ Tyr and $^{2}H_4$ Tyr respectively) were added prior to protein hydrolysis and served as chemical detectors of preparative oxidation [18 55]. Compared to the natural abundance tyrosine, the isotope labeled tyrosine species are structurally identical except for the extra molecular weight. During sample preparation, if trace amount anion ions are left in the hydrolysis chamber, natural abundance tyrosine ($^{12}C_9$, $^{14}N_1$ Tyr) and the corresponding isotope labeled tyrosine ($^{13}C_9$, $^{15}N_1$ Tyr or $^{2}H_4$ Tyr) will be oxidized at the same reaction rate to generate distinct oxidation products which can be distinguished by the mass spectrometer only [18, 52, 55]. In deed, isotope labeled tyrosine serves as an internal quality controller for potential *ex vivo* oxidized tyrosine generation to insure that the final result only represents oxidation stress *in vivo*.

### 2.2.2 Sample Purification and Derivatization

Due to the complexity of biological matrixes, purification and derivatization are essential steps for quantification of free or protein-bound tyrosine species. Purification is used to remove extra acid, salt and unwanted debris from biological matrix. Derivatization is a critical step that can modify the structure of analyte to get better separation and sensitivity.

Protein precipitation (PPT), liquid-liquid extraction (LLE) and solid phase extraction (SPE) are commonly used to desalt and to remove macromolecules and potential interference substances. Organic solvents like acetonitrile, chloroform,

methanol and diethyl ether were used to isolate protein in tissue homogenate, plasma, and other biological fluids [18, 40, 52, 55]. Protein dissolves in solvent with large dielectric constant like water. Organic solvents with smaller dielectric constant, like acetonitrile and methanol, significantly decrease protein solubility and induce protein precipitation [58]. The smaller the dielectric constant of the final solution, the lower solubility of the protein will be. In addition, decreased temperature also facilitates protein precipitation. Protein pellet is obtained by centrifuging at 4000~9000 g [55 18]. The supernatant (for free amino acid) or protein pellet (for protein bound amino acid residue) are recovered.

Liquid-liquid extraction (LLE) is a powerful tool to separate an analyte from a mixture or to remove unwanted interference compounds. The separation is achieved based on the difference in solubility of the analyte in two immiscible liquid phases (aqueous phase and organic phase). The more hydrophobic of the analyte, the better extraction efficiency is achieved by LLE. Extracted analyte is easily recovered by separating the liquid layer. The extraction efficiency of analyte (E) is determined by equation 2.1:

$$E = \frac{K_D V}{1 + K_D V} \qquad 2.1$$

$K_D$ is the partition coefficient of the analyte in the organic and aqueous phases ($C_o/C_{aq}$); V is the volume ratio of two phases ($V_o/V_{aq}$). To get better extraction efficiency, the organic solvent is selected with bigger $K_D$ value and larger volume. Successive multiple extractions give a better recovery. Using chloroform as the extraction reagent, about 93% of the free dityrosine was extracted from cerebrospinal fluid [59]. Other reagents like

mixture of chloroform/methanol (v:v, 2:1) were used to extract 3-nitrotyrosine from human plasma [55].

Solid phase extraction (SPE) is commonly used to remove water soluble strong acid/base. The 3 mL SPE cartridge with 100-500 mg packing material was commonly used. The packing material of SPE column is often in irregular shape with diameters above 50 μm (10-20 fold larger than HPLC packing material). The separation mechanism of SPE is similar to that of HPLC column. First the analyte is loaded on a pre-conditioned cartridge. The analytes and unwanted debris are separated by choosing appropriate washing and eluting solvents. The eluted analytes are analyzed directly or dried under vacuum and then reconstituted prior to quantitation. Compared with LLE, SPE demonstrates a better separation of analyte from interferences, easier collection of analyte fraction and less organic solvent usage. In addition, automation can easily be adapted using SPE column. Different adsorbents, extraction mechanism were investigated to improve the recovery and eliminate interference peak of analytes in different matrices. In addition, different washing, elution solvents were compared. Reverse phase C-18 SPE column is one of the commonly used cartridges to remove excess acid and potential debris in protein hydrolysate [6, 17, 18, 43, 45, 52, 60]. Further purification is achieved by using additional chrom P cartridge right after C-18 SPE extraction [61]. Frost et al used a polymeric resin based $ENV^+$ cartridge to remove interference of 3-nitrotyrosine [55]. Anion exchange column (AG1-XS8) was used to purify 3-nitrotyroisne in protein hydrolysate [62]. Tandem octadecylsilyl and aminopropylsilyl cartridges were applied to isolate tyrosine and nitrotyrosine respectively

in protein hydrolysate [63]. Aminopropyl cartridge was used to isolate dityrosine, ortho-tyrosine and nitrotyrosine in cat urine [64].

Derivatization is a method of chemically transforming the analyte into a new compound which has different volatility, thermo-stability and better chromatographic behavior to fit the requirement of quantitation [65]. For GC based assay, the derivatization step is an essential step to eliminate the presence of polar group like OH, $NH_2$ and COOH. The carboxylic acid group (COOH) of tyrosine and oxidized tyrosine are converted to the corresponding ester derivative by reacting with 1-propanol at acidic condition (HCl or HBr) at 65 °C for 20~ 30 minutes [2, 52]. The resulting solutions further react with heptafluorobutyric anhydride (HFBA), pentafluoropropionic anhydride (PFPA) and trifluoroacetic anhydride (TFAA) in the presence of ethyl acetate [52 2, 51]. N-(t-butyl-dimethylsilyl)-N-methyltrifluoroacetamide chlorosilane (TBDMS) was used to protect hydroxyl group to form an ether derivative [55]. However several steps including acetylation, o-deacetylation and reduction were required to achieve a better separation and lower detection limit [40]. The complexity of derivatization procedures may introduce potential artifacts generation, especially under acidic conditions [49]. Chemical derivatization of analyte prior to HPLC system gave a lower detection limit and better chromatographic behavior. Butylation of o-tyrosine and nitrotyrosine dramatically improved their sensitivity. MS response of o-tyrosine and nitrotyrosine were increased 7 and 6 fold respectively. However, butylation of o,o'-dityrosine did not improve the sensitivity due to the side reactions. The limit of quantitation (LOQ) of $NO_2$-Tyr butyl ester, o-Tyr butyl ester, and di-Tyr in cat urine samples were reported at 14.5, 28.2 and 140.9 nM, respectively [64].

## 2.3 HPLC with on-line Ultraviolet-visible and Fluorescence Detector

HPLC is a common technique for separation. A number of LC detectors including ultraviolet-visible (UV), fluorescence detector, electrochemical detector (ECD) and mass spectrometer (MS) are developed to accomplish different requirements. Both UV and fluorescence detectors have been used to quantify free oxidized tyrosine species based on specific absorbance at acidic or basic condition.

Using an UV detector, Kaur et al. detected 3-nitrotyrosine in serum and synovial fluid from rheumatoid arthritis patients but not in that from controls. Later, this method was adopted to determine plasma level 3-nitrotyrosine in chronic renal failure patients [66]. A higher plasma level of 3-nitrotyrosine was detected in patients with septic shock (173.9 μM) than those without shock (75.6 μM). In addition, no 3-nitrotyrosine was detected in control plasma. The detection limits were reported to be 0.2 -0.6 μM [66, 67]. Protein-bound nitrotyrosine was detected based on its characteristic spectral absorbance in alkaline or acidic solutions. After treated with peroxynitrite or tetranitromethane, oxidized bovine Cu-Zn superoxide dismutase have a maxima absorbance at 438 nm in basic solution (pH 9.5) and a secondary peak at 356 nm in acidic condition (pH 3.5) [7]. After exposure to a 100-fold molar excess of peroxintirite, glutathione reductase also exhibits absorbance at approximately 423 nm, indicating the presence of 3-Nitrotyrosine residue [68]. Using HPLC with online UV detector (280 nm, pH=2.5), Wu et al reported the generation of 3-bromotyrosine and 3,5-dibromotyrosine by incubating HOBr or N-bromo, or N,N-dibromoamine with 2 mM tyrosine solution [15].

Using pre-column derivatization techniques, the amino groups of 3-nitrotyrosine or dityrosine are reacted with fluorescence active compounds including 7-fluoro-4-

nitrobenzo-2-oxa-1, 3-diazole, o-phthalaldehyde and 4'-Dimethylaminoazobenzene-4-sulfonyl chloride. The derivatized tyrosine species can be detected by the fluorescence detector [69, 70]. The detection limits of these assays were reported at 0.1-1 pmol level. Compared to the UV detection, fluorescence detection has lower background, better the sensitivity and selectivity. But these two approaches are limited for identification of any *ex vivo* generated trace level oxidized tyrosine species during sample preparation.

## 2.4 HPLC with On-line Electrochemical Detector

Electrochemical detector (ECD) was widely applied to detect and quantified 3-nitrotyrosine [71, 72], 3- Chlorotyrosine [73], dityrosine [74], meta- and ortho-tyrosine [75, 76]. A better selectivity and lower detection limit is achieved by combining HPLC separation system and sensitive electrochemical detector.

Using HPLC-ECD system, 3-nitrotyrosine was detected by passing through reduction potential and then following oxidation potential. Elevated plasma level 3-nitrotyrosine was observed after lipopolysaccharide (LPS) administration [71]. Hensley et al reported an assay using ECD detector to quantify tyrosine, 3-nitrotyrosine and 3,4-dihydroxyphenylalanine (3,4-Dopa) simultaneously [77]. Later, they observed elevated dityrosine and 3-nitrotyrosine in the hippocampus and neocortical regions of the brain and ventricular cerebrospinal fluid form Alzheimer patient compared to that from healthy control [72].

To achieve a lower detection limit, 3-nitrotyrosine was modified to N-acetyl-amino-tyrosine before loading HPLC-ECD system. The separation was significantly improved after 3-nitrotyrosine acetylation, o-deacetylation and reduction. In addition, the detection limit was reported at 20 fmol [40, 50]. Other assays used ECD detector to quantify

3-chlorotyrosine, dityrosine, meta-tyrosine and ortho-tyrosine generated *in vitro* and *in vivo* [73-76].

## 2.5 Mass Spectrometry-based Assay

Mass spectrometry (MS) is a powerful analytical technique that is widely used for identification, quantitation and clarification of structural properties of interested analyte(s). Mass spectrometer is divided into three major parts: ionization chamber (ion source), ion analyzer and detector (Fig 2.2). Once the sample is introduced into an ionization chamber, the gas phase cation or anion ions are generated. The resulting ions are separated in the mass analyzer according to their mass charge ratio (m/z). Once the ion which contains selected m/z ratio reaches the detector, an electronic signal will be generated and recorded by the data system. Compared with other LC detector, mass spectrometer is more expensive, less user friendly. But unique selectivity and sensitivity of mass spectrometry offer an ability to quickly detect and quantify interested compound which only require minimal sample preparation, even for complex biological matrix like tissue homogenate, plasma etc[78].

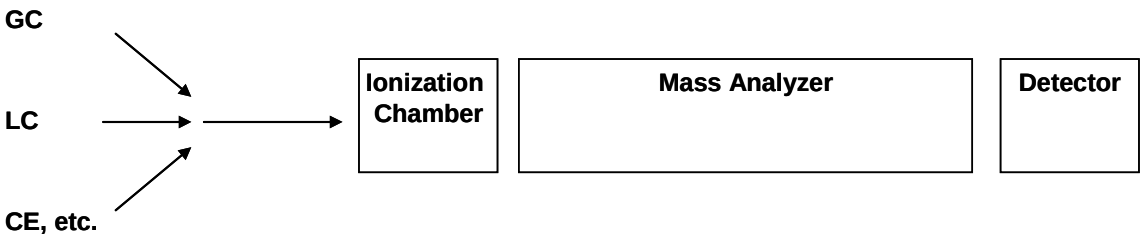


**Figure 2. 2 Schematic Diagram of Mass Spectrometer**

Analytes are introduced into ionization chamber by several separation techniques including gas chromatography (GC), liquid chromatography (LC), and capillary electrophoresis (CE). Once cation (positive) or anion (negative) ions were generated in ionization chamber, these ions were transported into ion analyzer and sorted according their m/z ratios. Only the ion with correct m/z ratio can pass through the ion analyzer and reach the detector.

Various ionization techniques, including electron impact (EI), chemical ionization (CI), negative-ion chemical ionization (NICI) electrospray ionization (ESI) and atmospheric pressure chemical ionization (APCI), may be used to detect and quantify biomarkers like oxidized tyrosine species [62, 79-83]. In electron impact (EI) ionization mode, the high-energy electron (~70 ev) is generate from electrically heated filament. Then the high-energy electrons collide with gas phase analyte. One electron from neutral molecule (A) is knocked out, and the positive charge ion ($A^+$) is generated. This ionization process may generate either molecular ion ($A^+$) or fragment ions ($B^+$ or $C^+$) dependent on applied electron energy, source temperature and the structure of the analyte, (Equation 2.2).

$$A + e \rightarrow A^+ + 2e$$

$$A + e \rightarrow B^+ + C^+ + 3e \qquad \text{(Eq.2.2)}$$

Later chemical ionization (CI), a softer ionization technique, was adopted for quantitation of 3-nitrotyrosine. The CI technique starts with reagent gas being ionized by electron impact ionization. Then the electronic charge is transferred from reagent gas ion to the gas phase analyte molecule through ion-molecule reaction to generate analyte ion. Negative-ion chemical ionization (NICI) is similar to CI technique. However, the reagent gas serves as the buffer gas to slow down the high-energy electrons so that some electrons have just the right energy to be captured by analyte molecules.

Atmospheric pressure ionization (API), the ionization technique that occurs under atmospheric pressure (760 mm Hg), includes electrospray ionization (ESI), atmospheric pressure chemical ionization (APCI) and atmospheric pressure photo ionization (APPI). The first two ionization techniques, ESI and APCI, are more commonly used in detection

and quantitation of polar molecules like oxidized tyrosine species [84]. In electrospray ionization (ESI), analyte solution is pushed through a narrow charged capillary interface and sprayed as very fine mist of charged droplets. Warm high purity nitrogen flow is commonly used to facilitate liquid evaporation. As a consequence of evaporation, the droplet surface charge density is increased. A phenomenon referred as Coulombic Fission is occurred and the gas phase ion is generated. ESI works well for polar, charged compounds with small and large molecular weights. Multiple charge ions are commonly observed in ESI spectrum. Atmospheric pressure chemical ionization (APCI) is more frequently used to anlayze less-polar compound. The sample solution is heated and sprayed with high flow rate nitrogen to form aerosol mist. The corona discharge needle is used to ionize the analyte. Compared with ESI, APCI is essentially a gas-phase ionization technique.

Numerous of mass analyzers are developed to accommodate the requirements on mass range, accuracy and precision. Magnetic sector mass spectrometer (double-focusing mass spectrometer) provides high sensitivity and resolution by separating of ions based on their passages through the perpendicular electric and magnetic fields. Time-of-flight (TOF) mass spectrometer measures the time that is required for the accelerate analyte ions to pass through a constant length tube. It provides a moderate mass resolution over a larger mass range. Ion trap mass spectrometer retains ions into a small region (ion trap) between a ring electrode and two end cap electrodes by specific oscillating electronic field. By changing the potential on the end caps, the ions within a specific m/z range can be trapped in or ejected out of the ion trap. Ion trap mass spectrometer is widely used because of its ability of performing a sequential MS/MS

reaction modes to provide valuable structure information [85]. However, Quadrupole mass spectrometer is the most commonly used mass spectrometer for quantitation purpose. Quadrupole mass spectrometer contains four parallel cylindrical rods that surround the ion paths. Radio-frequency (RF) voltage and direct current (DC) voltage are applied on the quadrupole rods to permit the ion with particular m/z ratio passing through this electronic field. Only the selected ion with specific m/z ratio has a stable trajectory and reaches the detector. Other ions with different m/z ratios have unstable oscillations that increase in amplitude until they collide with quadrupole rods [86 87].

As mentioned previously, both single and triple quadrupole mass spectrometers are widely used for quantitation of oxidized tyrosine species. A schematic diagram of a typical triple quadrupole mass spectrometer is presented in figure 2.3. A triple quadrupole mass spectrometer includes of three quadrupoles. The system includes two mass filters (the first and third quadrupole, $Q_1$ and $Q_3$ respectively) and a collision cell (the second quadrupole, $Q_2$). Triple quadrupole can be operated in different modes including $Q_1$ scan ($Q_1$), single ion monitoring (SIM), parent ion scan, daughter ion scan, neutral loss and multiple reaction monitoring (MRM) to accommodate analysis requirement. In $Q_1$ scan ($Q_1$), $Q_1$ is set at a scan mode, which allows $Q_1$ to filter one m/z each time sequentially. For triple quadrupole, both $Q_2$ and $Q_3$ are set at standby mode and there is no collision-activated dissociation (CAD) gas present in $Q_2$. Thereby the ion passes through $Q_2$ and $Q_3$ directly and reach detector to generate the corresponding signal. $Q_1$ scan provides the mass spectra in a specific mass range. Q1 scan is commonly used to determine the m/z ratio of molecular ion due to the limitation of low sensitivity. In single ion monitoring (SIM) mode, $Q_1$ is set to monitor one target ion with specific

m/z ratio and both $Q_2$ and $Q_3$ are set in standby mode. Only ion with specific m/z ratio can pass through quadrupole ($Q_1$) and reach the detector. SIM mode detects and quantifies one particular ion, which dramatically improve the sensitivity. Since only the ion with selected m/z ratio can pass through $Q_1$, the background noise is significantly decreased. In parent scan mode, $Q_1$ operates in scanning mode and transmits ion with sequential m/z ratio into the collision cell ($Q_2$). When the ions enter $Q_2$, they collide with the neutral CAD gas molecules and generate corresponding fragment ions. The fragmented ions (daughter ions) are then transported to $Q_3$, which is set at SIM mode for the daughter ion with particular m/z ratio. Similarly, in daughter scan mode, $Q_1$ is set at SIM mode to isolate one particular ion (parent ion). After the collision in $Q_2$ cell, the corresponding fragmented ions (daughter ions) are transported to $Q_3$. The $Q_3$ operates in scanning mode and filters each distinct m/z ratio successively. The resulting daughter spectrum of the selected parent ion provides valuable structure information. Daughter scan provides potential ion pair transitions that may be used in MRM mode. Neutral loss is applied to identify compounds that lost a specific uncharged group during either a rearrangement process or collision induced dissociation (CID). In neutral loss mode, both $Q_1$ and $Q_3$ operate in scanning modes with the particular difference ($\Delta$m). The detector responses to the ion that loss (or gain for neutral gain) the selected uncharged group ($\Delta$m) in $Q_2$. Multiple reaction monitoring (MRM) is designed to detect and quantify a specific analyte in complex matrices. In MRM mode, both $Q_1$ and $Q_3$ are set at SIM mode. The ion with specific m/z ratio is isolated by $Q_1$ first. Then this parent ion is collided with CAD gas in $Q_2$ cell and generated corresponding daughter ion (s). Only selected daughter ion(s) can pass through $Q_3$ and reach the detector. Both SIM and MRM

mode are widely used in quantitation of oxidized tyrosine species due to their exceptional sensitivity. Compared with SIM mode, MRM is more sensitive and provides better specificity.

In current mass spectrometer, the detector generates electronic current which is proportional to the mass abundance of each specific m/z ratio. Commonly used ion detectors include electron multiplier, photomultiplier, Faraday cup and microchannel plate detector [87].

## 2.6 Analytical Methods of Quantitation of Oxidized Tyrosine Species

Numerous assays based on gas chromatography with on-line mass spectrometer (GC/MS or GC/MS/MS) were developed to analyze oxidized tyrosine level at physiological and pathological conditions. GC/MS offers better separation and higher sensitivity. One limitation of GC/MS technique is that all the analytes has to be the gas phase prior to separation and detection. To analyze polar compounds like oxidized tyrosine species by GC/MS system, various chemical derivatization reagents were employed to increase analyses' volatility and ionization efficiency [88 6, 16, 17, 43-45].

Using GC combined stable isotope dilution mass spectrometry, the detection limit of 3-Chlorotyrosine was 50 attomole with coefficients of variance (CV) within 3% [52]. 3-chlorotyrosine was detected in normal aortic intima. The level of 3-chlorotyroisne was 30-fold higher in LDL isolated from atherosclerotic intima than that from circulating LDL [16]. A fully validated GC/MS/MS assay was developed to detect and quantify 3-nitrotyrosine in human plasma. The internal standard was purified by HPLC to eliminate nitrate and nitrite to avoid artifacts generation during sample preparation. Using this technique, basal level 3-nitrotyrosine was determined in 11 healthy volunteers [89].

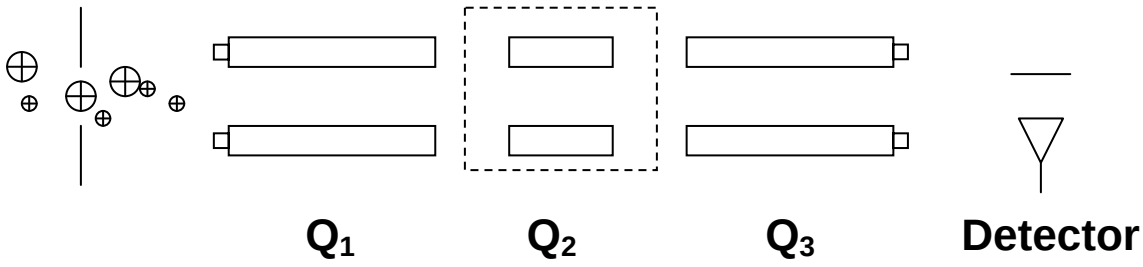


| Mode | $Q_1$ | $Q_2$ | $Q_3$ |
|---|---|---|---|
| $Q_1$ Scan | Scan | Off | Off |
| SIM | Static | Off | Off |
| Parent Scan | Scan | Collision | Static |
| Daughter Scan | Static | Collision | Scan |
| Neutral Loss | Scan | Collision | Scan |

**Figure 2. 3 Schematic Diagram of Typical Triple-quadrupole Mass Spectrometer and Its Operation Modes**

Typical triple-quadrupole includes two mass filters $Q_1$ and $Q_3$ and one collision cell $Q_2$. Numerous modes including $Q_1$ san, SIM, parent scan, daughter scan, MRM and neutral loss can be achieved by adjusting individual quadrupole setting (detail see table).

100-fold elevated dityrosine was observed in LDL isolated atherosclerotic lesions compared to the circulating LDL. No similar increase of meta-tyrosine or ortho-tyrosine was detected [43]. Dityrosine and ortho-tyrosine were also detected in mouse heart, muscle, brain, liver and urine sample [44, 45]. At basal level, 3-bromotyrosine in bronchoalveolar lavage (BAL) proteins recovered from mildly allergic asthmatic individuals was slightly higher than that from controls. After a localized allergen challenge, in BAL protein, 3-bromotyrosine content was increased 10-fold, but only two- to threefold increases in 3-chlorotyrosine [2].

In these studies, the accuracy and sensitivity were significantly improved by utilizing isotope labeled internal standard ($^{13}C$ labeled or $^{2}H$ labeled isotopmer) combining multiple reaction monitoring mode (MRM), [88, 90].. HPLC with on-line electrospray ionization mass spectrometry or tandem mass spectrometry (HPLC/ESI/MS or HPLC/ESI/MS/MS) assay has several advantages compared with GC/MS assay. Chemical derivatization procedure becomes an optional step to improve sensitivity. But majority LC/MS assay skip this step to eliminate the potential sample loss, contamination and side reactions [79]. Sample preparation is dramatically simplified and the efficiency is significantly improved [88].

LC/MS/MS assays for detecting oxidized tyrosine species in different matrices were explored. A simple and sensitive LC/MS/MS assay was used to detect 3-nitrotyrosine in rat brain tissue. The detection limit was below 10 nM[81]. Free 3-nitrotyrosine, 3-bromotyrosine and 3-chlorotyrosine were detected in plasma from healthy volunteers [79]. Yi et al. developed a LC/MS/MS assay to detect and quantify 3-nitrotyrosine and tyrosine simultaneously. HPLC condition was optimized to detect 3-

nitrotyrosine even in presence of 100,000-fold higher tyrosine. The detection limit for standard samples was 0.5 pg/μL (s/n>3) with a linear range from 0.5-100 pg/μL [49]. After peroxynitrite treatment, 3-nitrotyrosine and 3, 5-dinitrotyrosine were observed in peptides like leucine-enkephalin (YGGFL), V3 loop (GPGRAF), and LVV-hemorphin7 (LVVYPWTQRF) [91].

Protein bound dityrosine in milk powder was analyzed by LC-ESI/MS/MS. The mean recovery of dityrosine from milk powder was about 90%. The limit of detection (LOD) and limit of quantitation (LOQ) for protein bound dityrosine (diTyr/Tyr) were set at 2 μmol/mol and at 6 μmol/mol [92].

HPLC combined atmospheric pressure chemical ionization-tandem mass spectrometry (HPLC-APCI-MS/MS) system was also utilized to detect tyrosine, dityrosine, simultaneously. The linearity of each analyte was larger than 0.98. The limits of quantitation (LOQ) of tyrosine, dityrosine, in human urine sample were 1 μM, 50 nM, respectively [82].

Other applications include detecting plasma level 3-nitrotyrosine and 3-chlorotyrosine in preterm infants with clinically documented bronchopulmonary dysplasia [93] Significantly elevated 3-Bromotyrosine was detected in sputum supernatants recovered from mild to moderate asthma compared to that from controls. But no significant increase of protein bound 3-chlorotyrosine and carbonyl were observed between two groups [94]. Elevated protein bound 3-chlorotyrosine also were recovered from tracheal aspirate in low weight infants (n=69) compared to the controls with regular weight. In addition, these 3-chlorotyrosine levels were strongly correlated with myeloperoxidase activity ($r^2 = 0.75$, $p < 0.0001$) [95]. Using HPLC-MS/MS, 3-

chlorotyrosine was detected in HDL recovered from human aortic atherosclerotic lesion [96]. Also elevated dityrosine was detected by LC/MS in brain of Alzheimer's disease (AD) patients [97].

## 2.7 Conclusions

To further understand the mechanism of EPO/MPO induced oxidative damage both *in vitro* and *in vivo*, the level of an array of oxidized tyrosine species and their precursors need carefully investigate. GC/MS, LC/MS and LC/MS/MS are highly sensitive and specific approaches to study these oxidation products in biological specimens. Mass spectrometer provides specific structure information of each analyte. Compared to antibody based immunochemical assay, mass spectrometry based assay has a better sensitivity and specificity. Overall GC or LC/MS/MS approach is superior to immunochemical methods and other chemical detection approaches by providing specific structural information, improved sensitivity and simplicity of sample preparation.

Here we demonstrate the unique character of mass spectrometry based assay to quantify multiple oxidized tyrosine species in various biological specimen. First, it can simultaneously detect and quantify six oxidized tyrosine species and the corresponding precursors. As illustrated in figure 1.2, activated eosinophil and neutrophil releases its unique granule protein EPO and MPO, respectively. EPO or MPO utilizes hydrogen peroxide and various physiological substrates to generate corresponding reactive bromating species (RBS), reactive chlorinating species (RCS), and reactive nitrogen species (RNS) species. These reactive species participate in oxidative modification and involve in inflammatory injury. To study the operational mechanism of EPO and MPO catalyzed oxidative modification, multiple oxidative products are investigated to re-

construct the oxidative damage *in vivo*. Other GC/MS and LC/MS assays can only detect one or several oxidized tyrosine species. To obtain the over all oxidation products, several assays are required. In our assay, detection and quantitation of multiple analytes is achieved by multiple-channel monitoring. It quantifies six oxidized tyrosine species and the corresponding precursors simultaneously, which provides a snapshot of EPO or MPO induced oxidative stress in vivo.

Second, unique isotope-labeled internal standards were used to insure the quality of data. The preparation lost was calibrated by adding the isotopically labeled internal standard. [$^{13}C_6$] ring isotopically labeled oxidized tyrosine and universally labeled tyrosine, phenylalanine (i.e. all carbons $^{13}C$, all nitrogen $^{15}N$) as the internal standard prior to protein hydrolysis. Unique universally labeled oxidized tyrosine species serve internal quality control to monitor artifact generation. Multiple distinct natural abundance oxidized tyrosine species were identified and quantified by the corresponding [$^{13}C_6$] ring labeled isotopomer, while simultaneously the ions possessing the anticipated m/z transitions for universally labeled oxidized amino acids were monitored as an indicator of the generation of preparative oxidation products.

Finally these mass spectrometry based approaches can be used to detect oxidized tyrosine species and their precursors, tyrosine and phenylalanine respectively, in different biological matrices including plasma, BAL, CSF and tissue. High sensitivity and reproducibility ensures that our assay is a powerful tool to explore the free radical induced oxidation *in vivo*. These unique properties suggest protein-bound oxidized residues can serve as molecular probes to identify the underlying oxidation pathways in diseases like atherosclerosis and cancer.

## 2.8 Reference:


1. Stadtman, E. R., Protein oxidation and aging. Science **1992,** 257, (5074), 1220-4.
2. Wu, W.; Samoszuk, M. K.; Comhair, S. A.; Thomassen, M. J.; Farver, C. F.; Dweik, R. A.; Kavuru, M. S.; Erzurum, S. C.; Hazen, S. L., Eosinophils generate brominating oxidants in allergen-induced asthma. J Clin Invest **2000,** 105, (10), 1455-63.
3. Brennan, M.; Gaur, A.; Pahuja, A.; Lusis, A. J.; Reynolds, W. F., Mice lacking myeloperoxidase are more susceptible to experimental autoimmune encephalomyelitis. J Neuroimmunol **2001,** 112, (1-2), 97-105.
4. Shen, Z.; Wu, W.; Hazen, S. L., Activated leukocytes oxidatively damage DNA, RNA, and the nucleotide pool through halide-dependent formation of hydroxyl radical. Biochemistry **2000,** 39, (18), 5474-82.
5. Shen, Z.; Mitra, S. N.; Wu, W.; Chen, Y.; Yang, Y.; Qin, J.; Hazen, S. L., Eosinophil peroxidase catalyzes bromination of free nucleosides and double-stranded DNA. Biochemistry **2001,** 40, (7), 2041-51.
6. Wu, W.; Chen, Y.; Hazen, S. L., Eosinophil peroxidase nitrates protein tyrosyl residues. Implications for oxidative damage by nitrating intermediates in eosinophilic inflammatory disorders. J Biol Chem **1999,** 274, (36), 25933-44.
7. Ischiropoulos, H.; Zhu, L.; Chen, J.; Tsai, M.; Martin, J. C.; Smith, C. D.; Beckman, J. S., Peroxynitrite-mediated tyrosine nitration catalyzed by superoxide dismutase. Arch Biochem Biophys **1992,** 298, (2), 431-7.

8. Zhang, R.; Brennan, M. L.; Shen, Z.; MacPherson, J. C.; Schmitt, D.; Molenda, C. E.; Hazen, S. L., Myeloperoxidase functions as a major enzymatic catalyst for initiation of lipid peroxidation at sites of inflammation. J Biol Chem **2002,** 277, (48), 46116-22.

9. Agosti, J. M.; Altman, L. C.; Ayars, G. H.; Loegering, D. A.; Gleich, G. J.; Klebanoff, S. J., The injurious effect of eosinophil peroxidase, hydrogen peroxide, and halides on pneumocytes in vitro. J Allergy Clin Immunol **1987,** 79, (3), 496-504.

10. Gebicki, S.; Gebicki, J. M., Formation of peroxides in amino acids and proteins exposed to oxygen free radicals. Biochem J **1993,** 289 (Pt 3), 743-9.

11. Dean, R. T.; Fu, S.; Stocker, R.; Davies, M. J., Biochemistry and pathology of radical-mediated protein oxidation. Biochem J **1997,** 324 (Pt 1), 1-18.

12. Marquez, L. A.; Dunford, H. B., Kinetics of oxidation of tyrosine and dityrosine by myeloperoxidase compounds I and II. Implications for lipoprotein peroxidation studies. J Biol Chem **1995,** 270, (51), 30434-40.

13. Maskos, Z.; Rush, J. D.; Koppenol, W. H., The hydroxylation of phenylalanine and tyrosine: a comparison with salicylate and tryptophan. Arch Biochem Biophys **1992,** 296, (2), 521-9.

14. Sarchielli, P.; Galli, F.; Floridi, A.; Gallai, V., Relevance of protein nitration in brain injury: a key pathophysiological mechanism in neurodegenerative, autoimmune, or inflammatory CNS diseases and stroke. Amino Acids **2003,** 25, (3-4), 427-36.

15. Wu, W.; Chen, Y.; d'Avignon, A.; Hazen, S. L., 3-Bromotyrosine and 3,5-dibromotyrosine are major products of protein oxidation by eosinophil peroxidase: potential markers for eosinophil-dependent tissue injury in vivo. Biochemistry **1999,** 38, (12), 3538-48.

16. Hazen, S. L.; Heinecke, J. W., 3-Chlorotyrosine, a specific marker of myeloperoxidase-catalyzed oxidation, is markedly elevated in low density lipoprotein isolated from human atherosclerotic intima. J Clin Invest **1997,** 99, (9), 2075-81.

17. Hazen, S. L.; Hsu, F. F.; Mueller, D. M.; Crowley, J. R.; Heinecke, J. W., Human neutrophils employ chlorine gas as an oxidant during phagocytosis. J Clin Invest **1996,** 98, (6), 1283-9.

18. Brennan, M. L.; Wu, W.; Fu, X.; Shen, Z.; Song, W.; Frost, H.; Vadseth, C.; Narine, L.; Lenkiewicz, E.; Borchers, M. T.; Lusis, A. J.; Lee, J. J.; Lee, N. A.; Abu-Soud, H. M.; Ischiropoulos, H.; Hazen, S. L., A tale of two controversies: defining both the role of peroxidases in nitrotyrosine formation in vivo using eosinophil peroxidase and myeloperoxidase-deficient mice, and the nature of peroxidase-generated reactive nitrogen species. J Biol Chem **2002,** 277, (20), 17415-27.

19. Goldstein, S.; Czapski, G.; Lind, J.; Merenyi, G., Tyrosine nitration by simultaneous generation of NO and O-(2) under physiological conditions. How the radicals do the job. J Biol Chem **2000,** 275, (5), 3031-6.

20. Winterbourn, C. C.; Pichorner, H.; Kettle, A. J., Myeloperoxidase-dependent generation of a tyrosine peroxide by neutrophils. Arch Biochem Biophys **1997,** 338, (1), 15-21.

21. Nair, U. J.; Nair, J.; Friesen, M. D.; Bartsch, H.; Ohshima, H., Ortho- and meta-tyrosine formation from phenylalanine in human saliva as a marker of hydroxyl radical generation during betel quid chewing. Carcinogenesis **1995,** 16, (5), 1195-8.

22. Ye, Y. Z.; Strong, M.; Huang, Z. Q.; Beckman, J. S., Antibodies that recognize nitrotyrosine. Methods Enzymol **1996,** 269, 201-9.

23. Kooy, N. W.; Lewis, S. J.; Royall, J. A.; Ye, Y. Z.; Kelly, D. R.; Beckman, J. S., Extensive tyrosine nitration in human myocardial inflammation: evidence for the presence of peroxynitrite. Crit Care Med **1997,** 25, (5), 812-9.

24. Kato, Y.; Maruyama, W.; Naoi, M.; Hashizume, Y.; Osawa, T., Immunohistochemical detection of dityrosine in lipofuscin pigments in the aged human brain. FEBS Lett **1998,** 439, (3), 231-4.

25. Kato, Y.; Wu, X.; Naito, M.; Nomura, H.; Kitamoto, N.; Osawa, T., Immunochemical detection of protein dityrosine in atherosclerotic lesion of apo-E-deficient mice using a novel monoclonal antibody. Biochem Biophys Res Commun **2000,** 275, (1), 11-5.

26. Chapman, A. L.; Senthilmohan, R.; Winterbourn, C. C.; Kettle, A. J., Comparison of mono- and dichlorinated tyrosines with carbonyls for detection of hypochlorous acid modified proteins. Arch Biochem Biophys **2000,** 377, (1), 95-100.

27. Gujral, J. S.; Hinson, J. A.; Jaeschke, H., Chlorotyrosine protein adducts are reliable biomarkers of neutrophil-induced cytotoxicity in vivo. Comp Hepatol **2004,** 3 Suppl 1, S48.

28. Berger, T.; Rubner, P.; Schautzer, F.; Egg, R.; Ulmer, H.; Mayringer, I.; Dilitz, E.; Deisenhammer, F.; Reindl, M., Antimyelin antibodies as a predictor of clinically definite multiple sclerosis after a first demyelinating event. N Engl J Med **2003,** 349, (2), 139-45.

29. Beckmann, J. S.; Ye, Y. Z.; Anderson, P. G.; Chen, J.; Accavitti, M. A.; Tarpey, M. M.; White, C. R., Extensive nitration of protein tyrosines in human atherosclerosis detected by immunohistochemistry. Biol Chem Hoppe Seyler **1994,** 375, (2), 81-8.

30. Cromheeke, K. M.; Kockx, M. M.; De Meyer, G. R.; Bosmans, J. M.; Bult, H.; Beelaerts, W. J.; Vrints, C. J.; Herman, A. G., Inducible nitric oxide synthase colocalizes with signs of lipid oxidation/peroxidation in human atherosclerotic plaques. Cardiovasc Res **1999,** 43, (3), 744-54.

31. Hill, K. E.; Zollinger, L. V.; Watt, H. E.; Carlson, N. G.; Rose, J. W., Inducible nitric oxide synthase in chronic active multiple sclerosis plaques: distribution, cellular expression and association with myelin damage. J Neuroimmunol **2004,** 151, (1-2), 171-9.

32. Good, P. F.; Hsu, A.; Werner, P.; Perl, D. P.; Olanow, C. W., Protein nitration in Parkinson's disease. J Neuropathol Exp Neurol **1998,** 57, (4), 338-42.

33. Good, P. F.; Werner, P.; Hsu, A.; Olanow, C. W.; Perl, D. P., Evidence of neuronal oxidative damage in Alzheimer's disease. Am J Pathol **1996,** 149, (1), 21-8.

34. Haddad, I. Y.; Pataki, G.; Hu, P.; Galliani, C.; Beckman, J. S.; Matalon, S., Quantitation of nitrotyrosine levels in lung sections of patients and animals with acute lung injury. J Clin Invest **1994,** 94, (6), 2407-13.

35. Ceriello, A.; Mercuri, F.; Quagliaro, L.; Assaloni, R.; Motz, E.; Tonutti, L.; Taboga, C., Detection of nitrotyrosine in the diabetic plasma: evidence of oxidative stress. Diabetologia **2001,** 44, (7), 834-8.

36. ter Steege, J. C.; Koster-Kamphuis, L.; van Straaten, E. A.; Forget, P. P.; Buurman, W. A., Nitrotyrosine in plasma of celiac disease patients as detected by a new sandwich ELISA. Free Radic Biol Med **1998,** 25, (8), 953-63.

37. Onorato, J. M.; Thorpe, S. R.; Baynes, J. W., Immunohistochemical and ELISA assays for biomarkers of oxidative stress in aging and disease. Ann N Y Acad Sci **1998,** 854, 277-90.

38. Khan, J.; Brennand, D. M.; Bradley, N.; Gao, B.; Bruckdorfer, R.; Jacobs, M., 3-Nitrotyrosine in the proteins of human plasma determined by an ELISA method. Biochem J **1998,** 332 (Pt 3), 807-8.

39. Torreilles, J.; Romestand, B., In vitro production of peroxynitrite by haemocytes from marine bivalves: C-ELISA determination of 3-nitrotyrosine level in plasma proteins from Mytilus galloprovincialis and Crassostrea gigas. BMC Immunol **2001,** 2, 1.

40. Shigenaga, M. K.; Lee, H. H.; Blount, B. C.; Christen, S.; Shigeno, E. T.; Yip, H.; Ames, B. N., Inflammation and NO(X)-induced nitration: assay for 3-nitrotyrosine by HPLC with electrochemical detection. Proc Natl Acad Sci U S A **1997,** 94, (7), 3211-6.

41. Khan, J.; Brennand, D. M.; Bradley, N.; Gao, B.; Bruckdorfer, R.; Jacobs, M., 3-Nitrotyrosine in the proteins of human plasma determined by an ELISA method. Biochem J **1998,** 330 (Pt 2), 795-801.

42. Imam, S. Z.; el-Yazal, J.; Newport, G. D.; Itzhak, Y.; Cadet, J. L.; Slikker, W., Jr.; Ali, S. F., Methamphetamine-induced dopaminergic neurotoxicity: role of peroxynitrite and neuroprotective role of antioxidants and peroxynitrite decomposition catalysts. Ann N Y Acad Sci **2001,** 939, 366-80.

43. Leeuwenburgh, C.; Rasmussen, J. E.; Hsu, F. F.; Mueller, D. M.; Pennathur, S.; Heinecke, J. W., Mass spectrometric quantification of markers for protein oxidation by tyrosyl radical, copper, and hydroxyl radical in low density lipoprotein isolated from human atherosclerotic plaques. J Biol Chem **1997,** 272, (6), 3520-6.

44. Leeuwenburgh, C.; Wagner, P.; Holloszy, J. O.; Sohal, R. S.; Heinecke, J. W., Caloric restriction attenuates dityrosine cross-linking of cardiac and skeletal muscle proteins in aging mice. Arch Biochem Biophys **1997,** 346, (1), 74-80.

45. Leeuwenburgh, C.; Hansen, P. A.; Holloszy, J. O.; Heinecke, J. W., Oxidized amino acids in the urine of aging rats: potential markers for assessing oxidative stress in vivo. Am J Physiol **1999,** 276, (1 Pt 2), R128-35.

46. Huggins, T. G.; Wells-Knecht, M. C.; Detorie, N. A.; Baynes, J. W.; Thorpe, S. R., Formation of o-tyrosine and dityrosine in proteins during radiolytic and metal-catalyzed oxidation. J Biol Chem **1993,** 268, (17), 12341-7.

47. Ischiropoulos, H.; al-Mehdi, A. B.; Fisher, A. B., Reactive species in ischemic rat lung injury: contribution of peroxynitrite. Am J Physiol **1995,** 269, (2 Pt 1), L158-64.

48. Salman-Tabcheh, S.; Guerin, M. C.; Torreilles, J., Nitration of tyrosyl-residues from extra- and intracellular proteins in human whole blood. Free Radic Biol Med **1995,** 19, (5), 695-8.

49. Yi, D.; Ingelse, B. A.; Duncan, M. W.; Smythe, G. A., Quantification of 3-nitrotyrosine in biological tissues and fluids: generating valid results by eliminating artifactual formation. J Am Soc Mass Spectrom **2000,** 11, (6), 578-86.

50. Shigenaga, M. K., Quantitation of protein-bound 3-nitrotyrosine by high-performance liquid chromatography with electrochemical detection. Methods Enzymol **1999,** 301, 27-40.

51. Morton, L. W.; Puddey, I. B.; Croft, K. D., Comparison of nitration and oxidation of tyrosine in advanced human carotid plaque proteins. Biochem J **2003,** 370, (Pt 1), 339-44.

52. Hazen, S. L.; Crowley, J. R.; Mueller, D. M.; Heinecke, J. W., Mass spectrometric quantification of 3-chlorotyrosine in human tissues with attomole sensitivity: a sensitive and specific marker for myeloperoxidase-catalyzed chlorination at sites of inflammation. Free Radic Biol Med **1997,** 23, (6), 909-16.

53. Davies, S. M.; Poljak, A.; Duncan, M. W.; Smythe, G. A.; Murphy, M. P., Measurements of protein carbonyls, ortho- and meta-tyrosine and oxidative phosphorylation complex activity in mitochondria from young and old rats. Free Radic Biol Med **2001,** 31, (2), 181-90.

54. Jacob, J. S.; Cistola, D. P.; Hsu, F. F.; Muzaffar, S.; Mueller, D. M.; Hazen, S. L.; Heinecke, J. W., Human phagocytes employ the myeloperoxidase-hydrogen peroxide system to synthesize dityrosine, trityrosine, pulcherosine, and isodityrosine by a tyrosyl radical-dependent pathway. J Biol Chem **1996,** 271, (33), 19950-6.

55. Frost, M. T.; Halliwell, B.; Moore, K. P., Analysis of free and protein-bound nitrotyrosine in human plasma by a gas chromatography/mass spectrometry method that avoids nitration artifacts. Biochem J **2000,** 345 Pt 3, 453-8.

56. Pitt-Rivers, R., The oxidation of diiodotyrosine derivatives. Biochem J **1948,** 43, (2), 223-31.

57. Hunt, S., Halogenated tyrosine derivatives in invertebrate scleroproteins: isolation and identification. Methods Enzymol **1984,** 107, 413-38.

58. van Oss, C. J., On the mechanism of the cold ethanol precipitation method of plasma protein fractionation. J Protein Chem **1989,** 8, (5), 661-8.

59. Abdelrahim, M.; Morris, E.; Carver, J.; Facchina, S.; White, A.; Verma, A., Liquid chromatographic assay of dityrosine in human cerebrospinal fluid. J Chromatogr B Biomed Sci Appl **1997,** 696, (2), 175-82.

60. MacPherson, J. C.; Comhair, S. A.; Erzurum, S. C.; Klein, D. F.; Lipscomb, M. F.; Kavuru, M. S.; Samoszuk, M. K.; Hazen, S. L., Eosinophils are a major source of

nitric oxide-derived oxidants in severe asthma: characterization of pathways available to eosinophils for generating reactive nitrogen species. J Immunol **2001,** 166, (9), 5763-72.

61. Pennathur, S.; Bergt, C.; Shao, B.; Byun, J.; Kassim, S. Y.; Singh, P.; Green, P. S.; McDonald, T. O.; Brunzell, J.; Chait, A.; Oram, J. F.; O'Brien, K.; Geary, R. L.; Heinecke, J. W., Human atherosclerotic intima and blood of patients with established coronary artery disease contain high density lipoprotein damaged by reactive nitrogen species. J Biol Chem **2004,** 279, (41), 42977-83.

62. Crowley, J. R.; Yarasheski, K.; Leeuwenburgh, C.; Turk, J.; Heinecke, J. W., Isotope dilution mass spectrometric quantification of 3-nitrotyrosine in proteins and tissues is facilitated by reduction to 3-aminotyrosine. Anal Biochem **1998,** 259, (1), 127-35.

63. Delatour, T.; Richoz, J.; Vouros, P.; Turesky, R. J., Simultaneous determination of 3-nitrotyrosine and tyrosine in plasma proteins of rats and assessment of artifactual tyrosine nitration. J Chromatogr B Analyt Technol Biomed Life Sci **2002,** 779, (2), 189-99.

64. Marvin, L. F.; Delatour, T.; Tavazzi, I.; Fay, L. B.; Cupp, C.; Guy, P. A., Quantification of o,o'-dityrosine, o-nitrotyrosine, and o-tyrosine in cat urine samples by LC/ electrospray ionization-MS/MS using isotope dilution. Anal Chem **2003,** 75, (2), 261-7.

65. Knapp, D. R., Chemical derivatization for mass spectrometry. Methods Enzymol **1990,** 193, 314-29.

66. Kaur, H.; Halliwell, B., Evidence for nitric oxide-mediated oxidative damage in chronic inflammation. Nitrotyrosine in serum and synovial fluid from rheumatoid patients. FEBS Lett **1994,** 350, (1), 9-12.

67. Fukuyama, N.; Takebayashi, Y.; Hida, M.; Ishida, H.; Ichimori, K.; Nakazawa, H., Clinical evidence of peroxynitrite formation in chronic renal failure patients with septic shock. Free Radic Biol Med **1997,** 22, (5), 771-4.

68. Francescutti, D.; Baldwin, J.; Lee, L.; Mutus, B., Peroxynitrite modification of glutathione reductase: modeling studies and kinetic evidence suggest the modification of tyrosines at the glutathione disulfide binding site. Protein Eng **1996,** 9, (2), 189-94.

69. Kamisaki, Y.; Wada, K.; Nakamoto, K.; Kishimoto, Y.; Kitano, M.; Itoh, T., Sensitive determination of nitrotyrosine in human plasma by isocratic high-performance liquid chromatography. J Chromatogr B Biomed Appl **1996,** 685, (2), 343-7.

70. Malencik, D. A.; Zhao, Z. Z.; Anderson, S. R., Determination of dityrosine, phosphotyrosine, phosphothreonine, and phosphoserine by high-performance liquid chromatography. Anal Biochem **1990,** 184, (2), 353-9.

71. Ishida, N.; Hasegawa, T.; Mukai, K.; Watanabe, M.; Nishino, H., Determination of nitrotyrosine by HPLC-ECD and its application. J Vet Med Sci **2002,** 64, (5), 401-4.

72. Hensley, K.; Maidt, M. L.; Yu, Z.; Sang, H.; Markesbery, W. R.; Floyd, R. A., Electrochemical analysis of protein nitrotyrosine and dityrosine in the Alzheimer brain indicates region-specific accumulation. J Neurosci **1998,** 18, (20), 8126-32.

73. Crow, J. P., Measurement and significance of free and protein-bound 3-nitrotyrosine, 3-chlorotyrosine, and free 3-nitro-4-hydroxyphenylacetic acid in biologic samples: a high-performance liquid chromatography method using electrochemical detection. Methods Enzymol **1999,** 301, 151-60.

74. Sawa, T.; Akaike, T.; Maeda, H., Tyrosine nitration by peroxynitrite formed from nitric oxide and superoxide generated by xanthine oxidase. J Biol Chem **2000,** 275, (42), 32467-74.

75. Kaur, H.; Fagerheim, I.; Grootveld, M.; Puppo, A.; Halliwell, B., Aromatic hydroxylation of phenylalanine as an assay for hydroxyl radicals: application to activated human neutrophils and to the heme protein leghemoglobin. Anal Biochem **1988,** 172, (2), 360-7.

76. Edwards, D. J.; Sorisio, D.; Knopf, S.; Mujumdar, S., Assay for L-p-tyrosine in plasma and brain by column liquid chromatography with electrochemical detection using m-tyrosine as the internal standard. J Chromatogr **1986,** 383, (1), 142-7.

77. Hensley, K.; Maidt, M. L.; Pye, Q. N.; Stewart, C. A.; Wack, M.; Tabatabaie, T.; Floyd, R. A., Quantitation of protein-bound 3-nitrotyrosine and 3,4-dihydroxyphenylalanine by high-performance liquid chromatography with electrochemical array detection. Anal Biochem **1997,** 251, (2), 187-95.

78. Korfmacher, W. A., Principles and applications of LC-MS in new drug discovery. Drug Discov Today **2005,** 10, (20), 1357-67.

79. Gaut, J. P.; Byun, J.; Tran, H. D.; Heinecke, J. W., Artifact-free quantification of free 3-chlorotyrosine, 3-bromotyrosine, and 3-nitrotyrosine in human plasma by electron capture-negative chemical ionization gas chromatography mass

spectrometry and liquid chromatography-electrospray ionization tandem mass spectrometry. Anal Biochem **2002,** 300, (2), 252-9.

80. Delatour, T.; Guy, P. A.; Stadler, R. H.; Turesky, R. J., 3-Nitrotyrosine butyl ester: a novel derivative to assess tyrosine nitration in rat plasma by liquid chromatography-tandem mass spectrometry detection. Anal Biochem **2002,** 302, (1), 10-8.

81. Althaus, J. S.; Schmidt, K. R.; Fountain, S. T.; Tseng, M. T.; Carroll, R. T.; Galatsis, P.; Hall, E. D., LC-MS/MS detection of peroxynitrite-derived 3-nitrotyrosine in rat microvessels. Free Radic Biol Med **2000,** 29, (11), 1085-95.

82. Orhan, H.; Vermeulen, N. P.; Tump, C.; Zappey, H.; Meerman, J. H., Simultaneous determination of tyrosine, phenylalanine and deoxyguanosine oxidation products by liquid chromatography-tandem mass spectrometry as non-invasive biomarkers for oxidative damage. J Chromatogr B Analyt Technol Biomed Life Sci **2004,** 799, (2), 245-54.

83. Vlasova, II; Arnhold, J.; Osipov, A. N.; Panasenko, O. M., pH-Dependent Regulation of Myeloperoxidase Activity. Biochemistry (Mosc) **2006,** 71, (6), 667-77.

84. Duncan, M. W., A review of approaches to the analysis of 3-nitrotyrosine. Amino Acids **2003,** 25, (3-4), 351-61.

85. Stafford, G., Jr., Ion trap mass spectrometry: a personal perspective. J Am Soc Mass Spectrom **2002,** 13, (6), 589-96.

86. Badman, E. R.; Graham Cooks, R., Miniature mass analyzers. J Mass Spectrom **2000,** 35, (6), 659-71.

87. Noble, C. A.; Prather, K. A., Real-time single particle mass spectrometry: a historical review of a quarter century of the chemical analysis of aerosols. Mass Spectrom Rev **2000,** 19, (4), 248-74.

88. Tsikas, D.; Caidahl, K., Recent methodological advances in the mass spectrometric analysis of free and protein-associated 3-nitrotyrosine in human plasma. J Chromatogr B Analyt Technol Biomed Life Sci **2005,** 814, (1), 1-9.

89. Schwedhelm, E.; Tsikas, D.; Gutzki, F. M.; Frolich, J. C., Gas chromatographic-tandem mass spectrometric quantification of free 3-nitrotyrosine in human plasma at the basal state. Anal Biochem **1999,** 276, (2), 195-203.

90. Herce-Pagliai, C.; Kotecha, S.; Shuker, D. E., Analytical methods for 3-nitrotyrosine as a marker of exposure to reactive nitrogen species: a review. Nitric Oxide **1998,** 2, (5), 324-36.

91. Yi, D.; Smythe, G. A.; Blount, B. C.; Duncan, M. W., Peroxynitrite-mediated nitration of peptides: characterization of the products by electrospray and combined gas chromatography-mass spectrometry. Arch Biochem Biophys **1997,** 344, (2), 253-9.

92. Fenaille, F.; Parisod, V.; Vuichoud, J.; Tabet, J. C.; Guy, P. A., Quantitative determination of dityrosine in milk powders by liquid chromatography coupled to tandem mass spectrometry using isotope dilution. J Chromatogr A **2004,** 1052, (1-2), 77-84.

93. Lorch, S. A.; Banks, B. A.; Christie, J.; Merrill, J. D.; Althaus, J.; Schmidt, K.; Ballard, P. L.; Ischiropoulos, H.; Ballard, R. A., Plasma 3-nitrotyrosine and

outcome in neonates with severe bronchopulmonary dysplasia after inhaled nitric oxide. Free Radic Biol Med **2003,** 34, (9), 1146-52.

94. Aldridge, R. E.; Chan, T.; van Dalen, C. J.; Senthilmohan, R.; Winn, M.; Venge, P.; Town, G. I.; Kettle, A. J., Eosinophil peroxidase produces hypobromous acid in the airways of stable asthmatics. Free Radic Biol Med **2002,** 33, (6), 847-56.

95. Buss, I. H.; Senthilmohan, R.; Darlow, B. A.; Mogridge, N.; Kettle, A. J.; Winterbourn, C. C., 3-Chlorotyrosine as a marker of protein damage by myeloperoxidase in tracheal aspirates from preterm infants: association with adverse respiratory outcome. Pediatr Res **2003,** 53, (3), 455-62.

96. Bergt, C.; Pennathur, S.; Fu, X.; Byun, J.; O'Brien, K.; McDonald, T. O.; Singh, P.; Anantharamaiah, G. M.; Chait, A.; Brunzell, J.; Geary, R. L.; Oram, J. F.; Heinecke, J. W., The myeloperoxidase product hypochlorous acid oxidizes HDL in the human artery wall and impairs ABCA1-dependent cholesterol transport. Proc Natl Acad Sci U S A **2004,** 101, (35), 13032-7.

97. Atwood, C. S.; Perry, G.; Zeng, H.; Kato, Y.; Jones, W. D.; Ling, K. Q.; Huang, X.; Moir, R. D.; Wang, D.; Sayre, L. M.; Smith, M. A.; Chen, S. G.; Bush, A. I., Copper mediates dityrosine cross-linking of Alzheimer's amyloid-beta. Biochemistry **2004,** 43, (2), 560-8.

# CHAPTER III

# PEROXIDASE PROMOTE PROTEIN BROMINATION IN MULTIPLE MOUSE ACUTE IMFLAMMATION MODELS

## 3.1 Introduction

Asthma is an increasing health problem in the developed countries. In the United States, over 17 million individuals, many of them are children, suffer form this chronic pulmonary disease [1, 2]. The major symptoms of this airway obstruction include chronic airway inflammation, recurrent recruitment and activation of leukocytes including eosinophils and T cells into airway [3, 4]. Eosinophil is one of the terminal effectors of the innate immune system and specifically recruited to the inflammation sites. Over decades, numerous studies support that eosinophil activation plays a vital role in airway obstruction and lung dysfunction. Significantly increased eosinophils and their unique granule proteins, including eosinophil peroxidase (EPO) and eosinophil cationic protein (ECP), have been detected in peripheral blood, bronchoalveolar lavage (BAL), induced sputum and bronchial mucosa specimens recovered from asthma patients [5-7].

The activated eosinophil participates host defense by generating reactive oxygen species, including superoxide ($O_2^{\bullet -}$) and hydrogen peroxide ($H_2O_2$), and simultaneously releasing its unique granule proteins in response to the antigen stimulation [8, 9]. EPO is account for nearly 25% of the total protein mass of the secondary granule [10]. Elevated EPO activity was also observed in specimen recovered from patients with acute severe asthma [11]. In addition, EPO activities was associated with prompting mast cell degranulation, activating platelets, and increasing the phagocytic capabilities of macrophages [12, 13].

*In vitro* studies indicate that EPO utilizes hydrogen peroxide to oxidize numerous substrates including halide and pseudohalide thiocyanate [4, 14]. EPO selectively utilizes physiological level of $Br^-$ (20-150 μM) over $Cl^-$ (100 mM) to generate hypobromous acid (HOBr). Further, HOBr and its conjugate base ($OBr^-$) react with amine and further oxidize α- or β- amino acid. However, both oxidation products are labile and easily decomposed to aldehyde [15, 16]. N- dibromoamine ($RNBr_2$) and N-bromoamine species are easily reduced to non-informative products [17, 18]. Due to the evanescence character of these reactive brominating species (RBS), it is impossible to use the RBS as a probe to study the mechanism of EPO catalyzed oxidation *in vivo*. Direct evidence of EPO induced protein modification *in vivo* has not been reported yet.

As an alternative way, stable oxidation products may serve as molecular fingerprints to record peroxidase catalyzed oxidation *in vivo*. Our previous study indicated that EPO utilized $H_2O_2$ and physiological concentrations of $Br^-$ (20-150 μM) to oxidize free or protein-bound L- tyrosine [19]. Two major products were detected by ultraviolet-visible (UV) detector with distinct retention time on the reverse phase HPLC. The two major products were further identified as 3-bromotyrosine (3-BrY) and 3,5-

dibromotyrosine (3,5-diBrY) by electrospray ionization mass spectrometry and multinuclear ($^{1}H$ and $^{15}N$) NMR spectroscopy. The stability of 3-BrY was demonstrated by over 95% recovery even after treated by HCl (6N, 1% phenol) or methane sulfonic acid (MSA, 4N, 1%phenol) at 110 °C for 24 hours (data not shown). The distinct structure and relative stability of 3-BrY suggest that 3-BrY may be used as a specific marker of peroxidase-catalyzed oxidation pathways *in vivo*. Recent studies indicate that significantly elevated protein-bound 3-BrY is recovered in sputum in asthmatic patients compared to that in controls. The levels of this bromination product highly positively correlates with eosinophil peroxidase protein mass ($r = 0.79$, $p < 0.0001$) [20]. We also found that protein-bound 3-BrY level increased 10-fold in bronchoalveolar lavage (BAL) fluid recovered from asthmatic patients but only 2, 3-fold increased in that from healthy controls after segmental allergen challenge[21]. Both *in vitro* and *in vivo* studies suggest that 3-BrY can be used as a chemical probe to study eosinophil peroxidase catalyzed protein bromination *in vivo*.

In current study, we monitored the generation of 3-BrY during allergen challenge to evaluate the relative contribution of EPO in promoting protein bromination *in vivo*. Multiple distinct inflammation models were used to generate robust eosinophil-rich infiltration into airways or peritoneum in EPO knockout ($EPO^{-/-}$) and wild-type ($EPO^{+/+}$) mice. The unique universally labeled tyrosine ($^{13}C_9$, $^{15}N_1$ Tyr) was added prior to protein hydrolysis to quantify natural abundance tyrosine and monitor the potential preparative bromination generation during sample processing. Using this highly sensitive, self-quality control assay, the *in vivo* protein bromination is evaluated. Significantly elevated 3-BrY generation was observed in $EPO^{+/+}$ mice in both models after allergen challenge.

In addition, in helminth protein induced peritonitis model, significantly elevated 3-BrY formation was observed after *M.Corti.* challenge (7-fold increases). Further, dramatic 3-BrY generation (50-fold increases) was observed after zymosan triggered eosinophil activation and degranulation in $EPO^{+/+}$ mice. In contrast, no detectable 3-BrY was recovered in specimen from $EPO^{-/-}$ regardless the treatments. These results support the EPO as the major pathway for generating protein-bound 3-BrY *in vivo*.

## 3.2 Experimental Procedures

### Reagents

Reagents including $H_3PO_4$, $NaH_2PO_4$, and $Na_2HPO_4$ were purchased from Fisher Chemical Co. Chelex 100 resin (200-400 mesh, sodium form) was purchased from BioRad. Methane sulfonic acid and bromide were from Fluka Chemical Co. (Ronkonkoma, NY). L-[$^{13}C_6$] tyrosine, [$^{13}C_9{}^{15}N_1$] tyrosine, and L-[$^{2}H_4$] tyrosine were purchased from Cambridge Isotopes, Inc. (Andover, MA). All other reagents were purchased from Sigma unless otherwise indicated. All gases were of the highest quality available (Praxair, Cleveland, OH).

### Animals

The animal studies described here were all performed using approved protocols from the Animal Research Committees of the Cleveland Clinic Foundation and Mayo Clinic Foundation. 129/SvJ age- and sex-matched EPO knockout (KO) and wild-type (WT) mice were used for the allergen lung challenge and helminth antigen-induced peritonitis studies.

**Aeroallergen Lung Challenge Model**

EPO-KO and WT mice were sensitized by intraperitoneal injection with either normal saline as control or 20 μg of ovalbumin (OVA, grade IV, Sigma) and 2.25 mg of Imject® Alum (Pierce) on days 0 and 14. On days 24, 25, and 26, animals were challenged with 20-min inhalations of a 1% OVA or normal saline aerosol. On day 28, bronchoalveolar lavage (BAL) fluid was obtained by normal saline lavage. The recovered BAL was centrifuged at 1000 rpm at 4 °C for 10 mins to remove cells. The supernatant was frozen and stored under nitrogen at approximately –80 °C until analysis. Lung tissue specimens of wild-type ($EPO^{+/+}$) and $EPO^{-/-}$ mice were harvested 48 hours following the last OVA aerosol challenge (i.e., the maxima of post challenge eosinophilia). Lung tissue was immediately rinsed with an ice-cold anti-oxidant cocktail buffer (50 mM phosphate buffer (pH=7.4), 100 μM diethylenetriaminepentaacetic acid (DTPA), 100 μM butylated hydroxytoluene (BHT)) and stored under argon at approximately –80 °C until analysis.

**Helminth Protein-induced Peritonitis Model**

EPO-KO and WT mice were sensitized by subcutaneous injection with 250 μg of whole protein extract from helminth Mesocestoides corti and $8 \times 10^9$ heat-killed pertussis organisms (Michigan Department of Public Health, Lansing, MI). Animals were challenged with normal saline or 200 μg of *M. corti*. on day 21 by intraperitoneal injection. Peritoneal cavity cells were harvested 72 hours later by lavage with 1x PBS containing 100 μM BHT and 100 μM DTPA, 5% FCS and 20 U/mL heparin. For some animals, the elicited peritoneal leukocytes (typically $>2 \times 10^6$ cells, ~ 25% eosinophils) were activated by intraperitoneal injection with zymosan (250 mg/kg of body weight). Peritoneal lavage was performed 4 h after zymosan injection. Recovered leukocytes

were washed three times with centrifugation/resuspension in 1x PBS before used. Differential counts of cytospin preparations of these cells revealed that neutrophils composed < 1% of all sample examined. The cell-free lavage fluid was overlaid with argon and immediately stored at ~ –80 °C until analysis. Superoxide production was measured as the superoxide dismutase-inhibitable reduction of cytochrome C [22] using eosinophils isolated from EPO-KO and WT mice.

**Immunocytochemical Detection of Eosinophils**

Sections of lung tissue (4 μm) were assessed for the infiltration of eosinophils using a rat mAb (14.7.4) specific for murine MBP-1 [23]. Immunocytochemical staining was performed with DAB-peroxidase detection reagents (Vector Laboratories, Burlingame, CA) as described previously [24].

**Cytochemical Detection of EPO**

Cytospin preparations of peritoneal cavity cells harvested from MCA-sensitized/challenged mice were prepared using a Cytospin3 (Shandon Scientific, Cheshire, U.K.). The slides were subsequently fixed for 30 seconds at 4°C in a formalin-acetone buffer (0.75 mM $Na_2HPO_4$, 7.5 mM $KH_2PO_4$ (pH 7.5), 45% (v/v) acetone, and 10% (w/v) formaldehyde), washed in tap water for several minutes, and stained (10 min at room temperature) for EPO activity using a diaminobenzidine (DAB)-$H_2O_2$ phosphate buffer (6 mM $Na_2HPO_4$, 286 mM $KH_2PO_4$ (pH 7.4), 2 mM (3',3')-DAB tetrahydrochloride (Sigma, St. Louis, MO), 0.01% $H_2O_2$ (Sigma), and 8 mM NaCN (Aldrich, Milwaukee, WI)) as described earlier [25]. The concentration of $CN^-$ (8mM) was used to selectively inhibit the activity of myeloperoxidase that may be present in the sample. The staining reactions were terminated by washing under tap water, and the

slides were counterstained with Harris hematoxylin (Sigma) before dehydration through an ascending series of ethanol washes, incubation in xylene, and mounting with Permount (Fisher Scientific, Pittsburgh, PA).

**Endpoint Colorimetric Assessment of EPO Activity**

The amount of EPO activity was determined by an endpoint colorimetric assay, as described previously [26]. To determine the amount of EPO activity within cells, peritoneal cavity cells and/or leukocytes recovered from BAL fluid were washed in Kreb's buffer (118 mM NaCl, 25 mM $NaHCO_3$, 11 mM glucose, 1 mM $NaH_2PO_4 \cdot H_2O$, 5 mM KCl, 0.5 mM $MgCl_2 \cdot 6H_2O$, and 2.5 mM $CaCl_2 \cdot 6H_2O$ (pH 7.4)) and counted on a hemocytometer. The number of eosinophils in a given leukocyte population was determined by differential cell counts of cytospin preparations. Dilutions ranging from $10^2$ to $10^4$ eosinophils were seeded in 50-µl volumes in a 96-well microtiter plate, and EPO activity was measured in each lysate through the addition 75 µl of o-phenylenediamine-$H_2O_2$ buffer (50 mM Tris-HCl (pH 8), 0.1% Triton X-100, 4 mM $H_2O_2$, and 10 mM of the EPO (vs myeloperoxidase)-specific substrate o-phenylenediamine). The reactions were allowed to proceed at room temperature for 30 minutes before adding 50 µl of stop buffer (2N $H_2SO_4$). Absorbance of each sample was measured at 490 nm using a Vmax Kinetic Microplate Reader (Molecular Devices, Sunnyvale, CA). EPO activity present in BAL fluid was assessed by incubating undiluted cell-free BAL fluid with o-phenylenediamine-$H_2O_2$ buffer at 37°C for 30 minutes [27]. Colorimetric readings due to EPO activity were calculated as the difference in absorbance measurement of each reaction with a duplicate reaction conducted in the presence (30 mM) of the peroxidase inhibitor 3-amino-1,2,4-triazole. The fraction of

EPO released from airway eosinophils was estimated by measuring the amount of EPO activity in cell-free BAL fluid as a function of total EPO activity in the BAL (i.e., the sum of EPO in the BAL fluid and EPO in airway eosinophils). EPO activity was calculated from a standard curve established using 1 x $10^2$–5 x $10^5$ eosinophils purified as a homogeneous population (99% pure) from an IL-5-transgenic mouse line [28]. The reading at 490 nm of each sample (i.e., the BAL fluid and BAL cell pellet derived from each mouse) was used to obtain the equivalent amount of EPO contained in a known number of eosinophils as determined from this standing curve.

**Preparation of Isotope Labeled Internal Standard**

3-Bromo [$^{13}C_6$] tyrosine ($^{13}C_6$ 3-BrY) was prepared by adding freshly made NaOBr (final conc. of 1.5 mM) into a constantly stirring solution containing L-[$^{13}C_6$] ring labeled tyrosine (final conc. 1 mM) and phosphate buffer (Final conc. 20 mM, pH= 7.4). The resulting solution was incubated at 37°C for 2 hours before the addition of trifluoroacetic acid (TFA) to terminate the reaction. The acidified solution was concentrated and isolated by a reverse-phase high performance liquid chromatography (HPLC) [29]. Isotopically labeled tyrosine ($^{13}C_6$ Y) and 3-bromotyrosine ($^{13}C_6$ BrY) was eluted with a linear gradient generated with solvent B (0.1% TFA in methanol, pH=2.0) as follows: 0–5mins, 0% solvent B; 5–25mins, 0–100% solvent B; 25–28mins, 100 % solvent B, 28–33 mins, 100%–0% solvent B. The isotopically labeled 3-BrY was then dried in speed vacuum and kept in –20°C freezer until use. Ring labeled 3-Bromotyrosine was reconstituted with chelex-treated water. The identity and purity of isotopically labeled 3-BrY was confirmed by LC/ESI/MS/MS.

**Tissue Collection and Preparation**

On the day of analysis, tissues were thawed in sealed plastic vials under cool running water. All tissue processing steps were performed at approximately 4°C. Samples were homogenized in PB buffer containing 100 μM BHT and 100 μM DTPA using a Potter-Elvehjem tissue homogenizer with a PTFE pestle. Protein concentration of lung tissue homogenate or extracellular lavage was determined using a Bradford-based Bio-Rad protein assay with IgG as the protein standard. Protein (500 μg) was delipidated and desalted using three sequential extractions with a single phase mixture of $H_2O$/methanol/$H_2O$-saturated diethyl ether (1:3:8 v/v/v). For each extraction, single phase mixture was vortexed, stored at approximately –20 °C for 40 minutes. The protein was precipitated by centrifuging at 4000 rpm for 20 mins at ~ 4°C. After discard supernatant, protein pellet was dried under nitrogen steam. For each sample, known amount $^{13}C$ ring-label 3-Bromotyrosine ($^{13}C_6$ BrY, 1.0 pmol) and universally labeled tyrosine ($^{13}C_9$, $^{15}N_1$ Y, 10 nmol), were added prior to protein hydrolysis.

**Protein Hydrolysis and Derivatization**

Preliminary studies demonstrated in acidic conditions, like methanesulfonic acid (MSA, 4N, 1% phenol) or hydrochloric acid (HCl, 6N, 1% phenol) solution, free tyrosine was stable at 110 °C for 24 hours. Artificial halogenation was eliminated by substituting MSA (4N) for HCl (6N) and washing protein with single phase mixture prior to acidic hydrolysis. Tubes were capped with gas-tight valves and alternately degassed and purged with argon for 3 times. Protein pellet were hydrolyzed by 4N methanesulfonic acid supplemented with 1% phenol at 110 °C for 24 hrs under argon atmosphere. The potential debris generated during protein hydrolysis was removed by passing a mini

solid-phase C18 column (Supelclean LC-C18 SPE mini-column, 3 ml; Supelco, Inc., Bellefone, PA). Briefly, protein hydrolysates (0.5 mL) were diluted with 1.5 mL Chelex-treated water and load on pre-conditioned SPE columns. Following sequential washes with 2 ml of water (0.1% TFA), 3-bromotyrosine and tyrosine were eluted with 2 ml of 30% methanol (0.1% TFA). The resulting amino acid solutions were then dried under vacuum.

Before loading on a GC column, alkylation and acylation reactions were accomplished to improve the gas chromatographic properties and enhance the sensitivity of analytes. n-Propyl esters of tyrosine or 3- bromotyrosine were generated by adding a mixture of 100 µl of n-propanol: concentrated HCl (3:1, v: v), and heating at 65°C for 75 minutes (Eq 1.). Reaction products were dried under vacuum and reconstituted with 100 µL of pentafluoropropionic anhydride: ethyl acetate (1:3, v: v) solution and incubated at 65°C for 15 minutes to generate its n- propyl, per pentafluorylproprionyl derivatives (Eq 2). After evaporation under vacuum, derivatized amino acids were reconstituted in 100 µL of ethyl acetate. An aliquot of resulting solution (1 µL) was loaded on GC/MS for 3-BrY analysis.

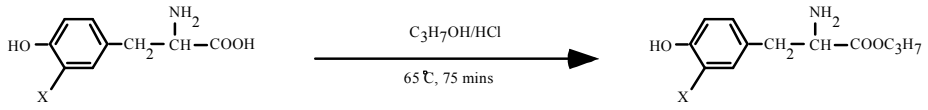


Eq 1.

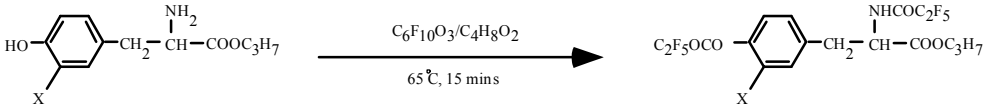


Eq 2.

X= H, Br

**Gas Chromatography-Mass Spectrometry**

The amino acid derivatives were separated and analyzed on Trace GC-2000 gas chromatography with online Voyager Mass Spectrometer (ThermoFinigann, San Jose, CA). The separations were achieved on a 15m long, low bleeding RTX-200 MS column (Restek, 0.25mm i.d., 0.25μm film thickness). Helium was used as carrier gas at a constant flow rate of 1 mL/min. The initial oven temperature was maintained at 40°C for 1 minute, and then the temperature was increased to 150°C at 30°C/min, held at 150°C for 0.5 minute, and then increased to 280°C at 15°C/minute. Tyrosine was analyzed by split mode (split ratio, 50:1) and 3-Bromotyrosine was analyzed by splitless mode respectively. Consistent septum purge was set on to keep septum clean. The injector, transfer line and source temperature were set at 250°C, 250°C and 200°C respectively.

Derivatized tyrosine and 3-Bromotyrosine were detected and quantified by the Voyager mass spectrometer via negative-ion chemical ionization (NICI) with selected ion monitoring (SIM) mode. The emission current, electron energy and detector voltage was set at 350 μA, 70Ev and 500 volts, respectively. n- propyl- per pentafluoroproprionyl derivative of natural abundance 3-Bromotyrosine ($^{12}C_9$ BrY) was monitor at mass charge ratio (m/z) of 445 (for $^{79}Br$), 447 (for $^{81}Br$), and their corresponding isotopically labeled internal standard ($^{13}C_6$ BrY) at m/z ratio of 451 (for $^{79}Br$), 453(for $^{81}Br$). To detect the artificial generation during the hydrolysis and derivatization step, universally labeled 3-Bromotyrosine ($^{13}C_9$, $^{15}N_1$BrY) was routinely monitored at m/z of 455 (for $^{79}Br$), 457 (for $^{81}Br$). n- propyl- per pentafluoroproprionyl derivative of tyrosine ($^{12}C_9$ Y) and the corresponding isotopically labeled internal standard ($^{13}C_9$ $^{15}N_1$ Y) were monitored at m/z ratio of 367 and 377, respectively. Both tyrosine and 3-bromotyrosine were base line

resolved under current GC condition with at least 9-10 scans per chromatographic peak. The 3-bromotyrosine content was normalized to the content of its precursor, tyrosine.

**Statistical Analyses**

Unless otherwise indicated, data were analyzed using an unpaired Student's t tests. The threshold for significance was set at $p \leq 0.05$. The values for all measurements are expressed as the mean ± S.D.

## 3.3 Results

**OVA Challenge Induce eosinophilia in Both Wild Type and Knockout Mice**

The localization of eosinophils within compartments of the lung after allergen challenge was initially determined by an anti-mouse MBP rat mAb that was previously demonstrated to be specific for eosinophils [24]. Figure 3.1 shows that although small numbers of eosinophils are homeostatic resident cells in the lungs of both $EPO^{+/+}$ and $EPO^{-/-}$ mice, OVA challenge resulted in an influx of eosinophils into the peribronchial/perivascular regions of $EPO^{+/+}$ and $EPO^{-/-}$ mice. The localization and number of eosinophils (150–200 eosinophils per millimeter squared) in the lungs after OVA challenge were indistinguishable between $EPO^{+/+}$ and $EPO^{-/-}$ mice.

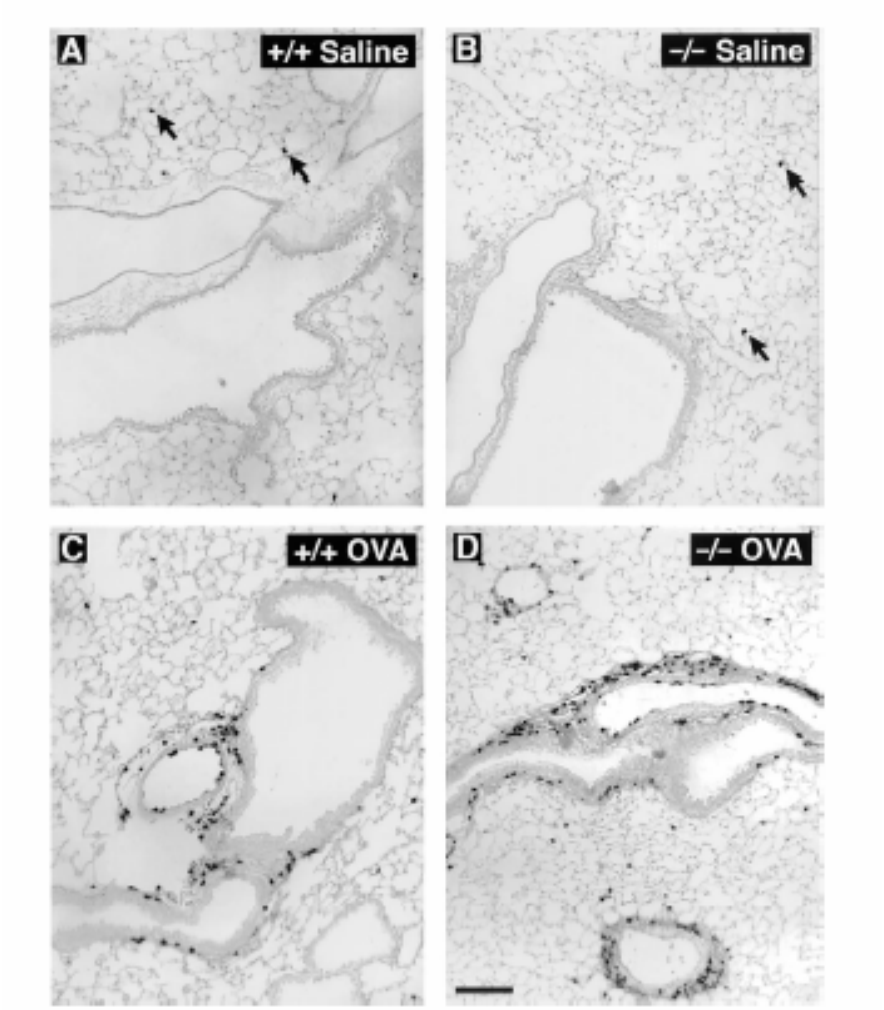


**Figure 3. 1 OVA-Sensitized/Challenged Induced Eosinophilia in $EPO^{-/-}$ and $EPO^{+/+}$ Mice**

Trafficking of eosinophils to the perivascular and peribronchial regions of Wild type ($EPO^{+/+}$) and Knockout ($EPO^{-/-}$) lungs was assessed by immunocytochemistry using a rat mAb (14.7.4) specificially for mouse MBP-1. Saline control groups: A, $EPO^{+/+}$ and B, $EPO^{-/-}$. OVA–challenged groups: C, $EPO^{+/+}$; and D $EPO^{-/-}$. Arrows indicate eosinophils localized in the parenchyma of saline control $EPO^{+/+}$ and $EPO^{-/-}$ mice. No differences in the number or specific location of eosinophils recruited to the lung were observed between similarly treated mice of either genotype. Scale bar = 100 μm.

**Eosinophils from Knockout Mice Are Peroxidase Deficient**

The loss of EPO activity in knockout mice was demonstrated by cytochemical staining of peritoneal cavity exudate cells recovered following sensitization/challenge of mice with a whole-protein extract from the helminth *M. corti*. Figure 3.2 A shows that eosinophils from $EPO^{-/-}$ mice were devoid of peroxidase activity (i.e., $CN^-$–resistant peroxidase activity (DAB staining) was demonstrated only in eosinophils from $EPO^{+/+}$ and $EPO^{+/-}$ mice). The loss of eosinophil peroxidase activity in cells from $EPO^{-/-}$ mice was further demonstrated using an endpoint colorimetric assay detecting EPO in lysate of the peritoneal cavity exudates (Figure 3.2B). The peroxidase activity of $EPO^{+/-}$ eosinophils was roughly 50% of that found in $EPO^{+/+}$ eosinophils, suggesting that EPO levels in eosinophils are proportional to the number of wild-type EPO alleles present. Eosinophils recovered from homozygous knockout mice derived from ES cell clone 6 or 57 were shown to be EPO activity deficient using both the peroxidase cytochemical detection and the endpoint colorimetric assay. Thus, mice derived from either ES clone were considered equivalent. Subsequent studies were performed on animals derived from clone 57.

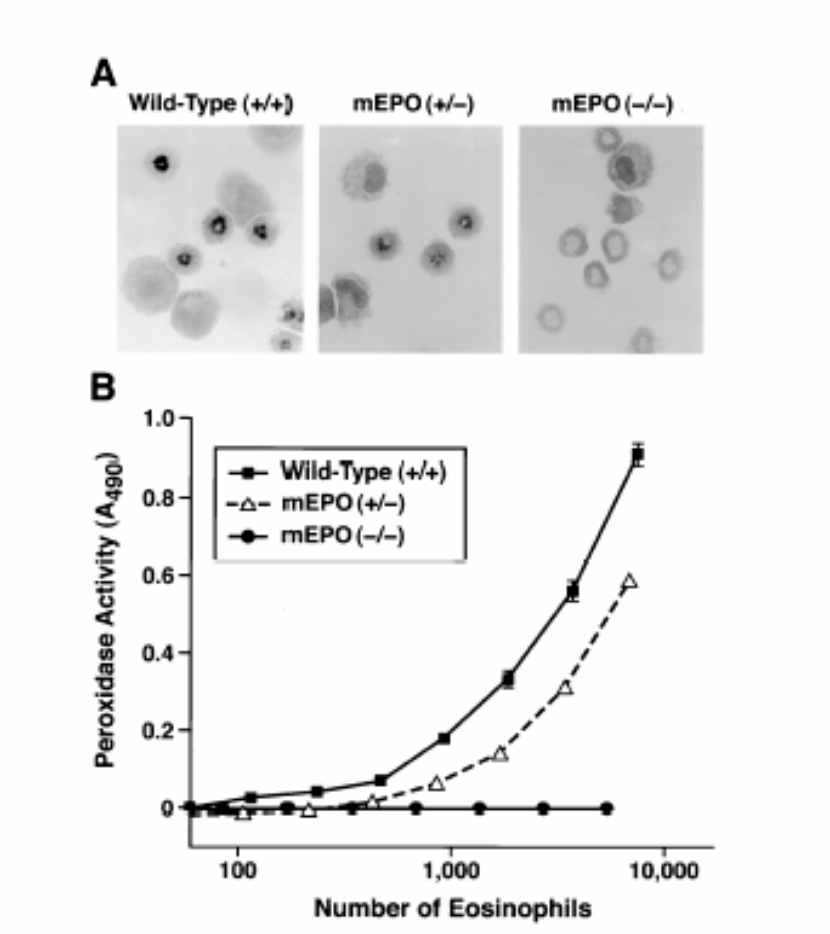


**Figure 3. 2 EPO Activity Is Absent in the Eosinophils of Knockout Mice.**

**A**, EPO activity is detected only in eosinophils recovered from $EPO^{+/+}$ and $EPO^{+/-}$ mice in response to allergen challenge. **B**, EPO activity presented in eosinophils is in proportion to the number of wild-type alleles. Assessments of peroxidase activity (490 nm), the number of eosinophils is plotted as a function of peroxidase activity in the peritoneal cavity exudate. Eosinophils activity of $EPO^{+/-}$ contain half the peroxidase activity as $EPO^{+/+}$ cells. No peroxidase activity was detectable in cell lysate from $EPO^{-/-}$ mice regardless of the input number of eosinophils. The points comprising each curve represent the means of assays performed on exudated cells derived from four different animals within each group. Error bars at each point represent ± SEM.

**GC/MS Analysis of 3-Bromotrysine**

Negative-ion chemical ionization (NICI) mass spectrum of 1-propyl-per pentafluoroproprionyl derivative of 3-Bromotyroisne was illustrated in figure 3.3. Compared with low intensity of molecular ions ($M^{\bullet -}$, 593 for $^{79}Br$ and 595 for $^{81}Br$), the base ion was observed at m/z 261 ($[M^- - CH_2C_5H_4BrOOC_2F_5]$), which was lack of structure information. Other major fragment ions were observed with isotopic character at m/z 573 ($[M^- - HF]$ for $^{79}Br$), m/z 575 ($[M^- - HF]$ for $^{81}Br$), m/z 445 ($[M^- - CF_3CF_2COH]$ for $^{79}Br$) and m/z 447 ($[M^- - CF_3CF_2COH]$ for $^{81}Br$). The isotopic distribution of natural abundance 3-BrY was confirmed by bromine-containing product ions (similar abundance between $^{79}Br$: $^{81}Br$, 573: 575 and 445: 447). Product ions with corresponding isotopic information 445, 447 were used to quantify natural abundance 3-Bromotyrosine because their preserved the structure information and provided a better sensitivity compared to the molecular ions (m/z 573 and 575).

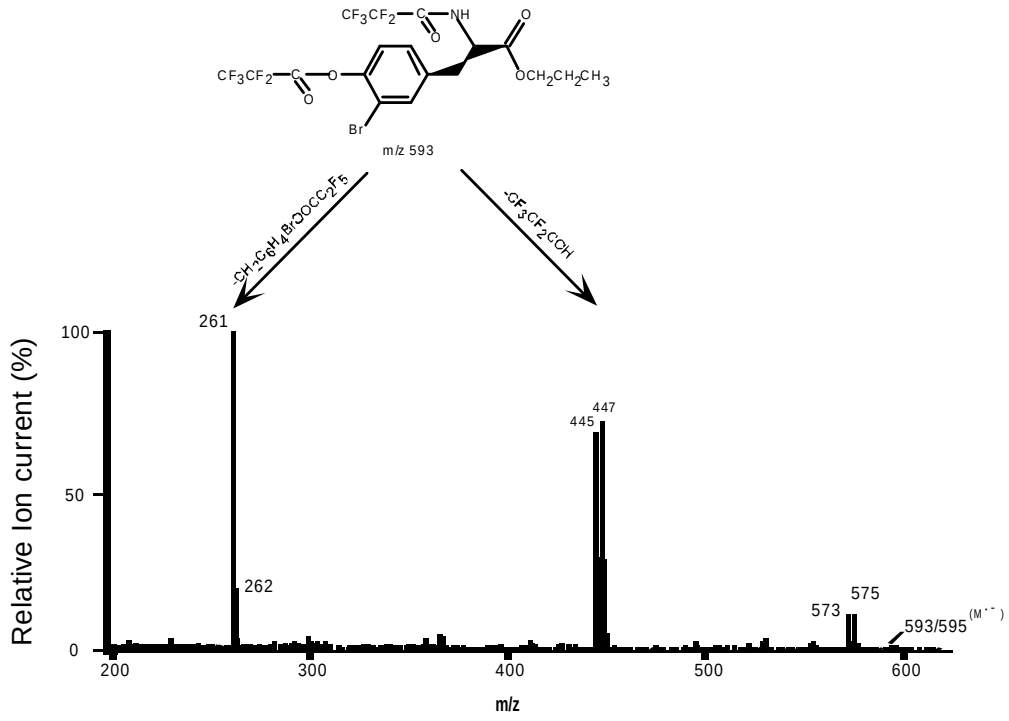


**Figure 3. 3 Negative-ion chemical ionization mass spectrum of 3-bromotyrosine**

1-propyl-per pentafluoroproprionyl derivative of 3-Bromotyroisne was derivatized and analyzed by GC/MS in the NICI mode as described in experimental procedures. The structure of derivatized 3-BrY and its proposed fragmentation is illustrated above. Molecular ions were observed at m/z ratio of 593 (for $^{79}Br$) and 595 (for $^{81}Br$).

**Elevated 3-BrY Generation in EPO$^{+/+}$ Mice after Allergen Challenge**

The levels of protein-bound 3-BrY recovered from lung homogenate and bronchoalveolar lavage (BAL) in an aeroallergen lung challenge model from wild-type (WT, EPO$^{+/+}$) and knockout (KO, EPO$^{-/-}$) mice were quantified by isotope dilution GC/MS assay to evaluate the potential involvement of EPO in the generation of 3-Bromotyrosine *in vivo*. The topical chromatograms of 3-BrY in tissue specimen recovered from an OVA–treat EPO$^{+/+}$ mouse are presented in Figure 3.4. For quantitation purpose, each chromatographic peak contained a minimum 9-10 scans. The natural abundance 3-BrY was identify by the corresponding isotope labeled internal standard ($^{13}C_6$ BrY) and confirmed by the equal isotope abundance of bromine ($^{79}$Br:$^{81}$Br, approximately 50:50). Native tyrosine and universally labeled tyrosine ($^{13}C_9$ $^{15}N_1$ Y) are identical in chemical structure expect that universally labeled tyrosine ($^{13}C_9$ $^{15}N_1$ Y) has ten extra atomic mass unit (10 Da). Therefore identical chemical character and same chromatographic behavior should be observed in sample preparation and GC separation. If trace amount of bromide was left in the system and caused bromination during sample preparation, universally labeled 3-bromotyrosine ($^{13}C_9$ $^{15}N_1$ BrY) will be generated proportionally. As demonstrated in Figure 3.4, there was no detectable universally labeled 3-bromotyrosine ($^{13}C_9$ $^{15}N_1$ BrY) indicating no detectable artifact generation during sample process.

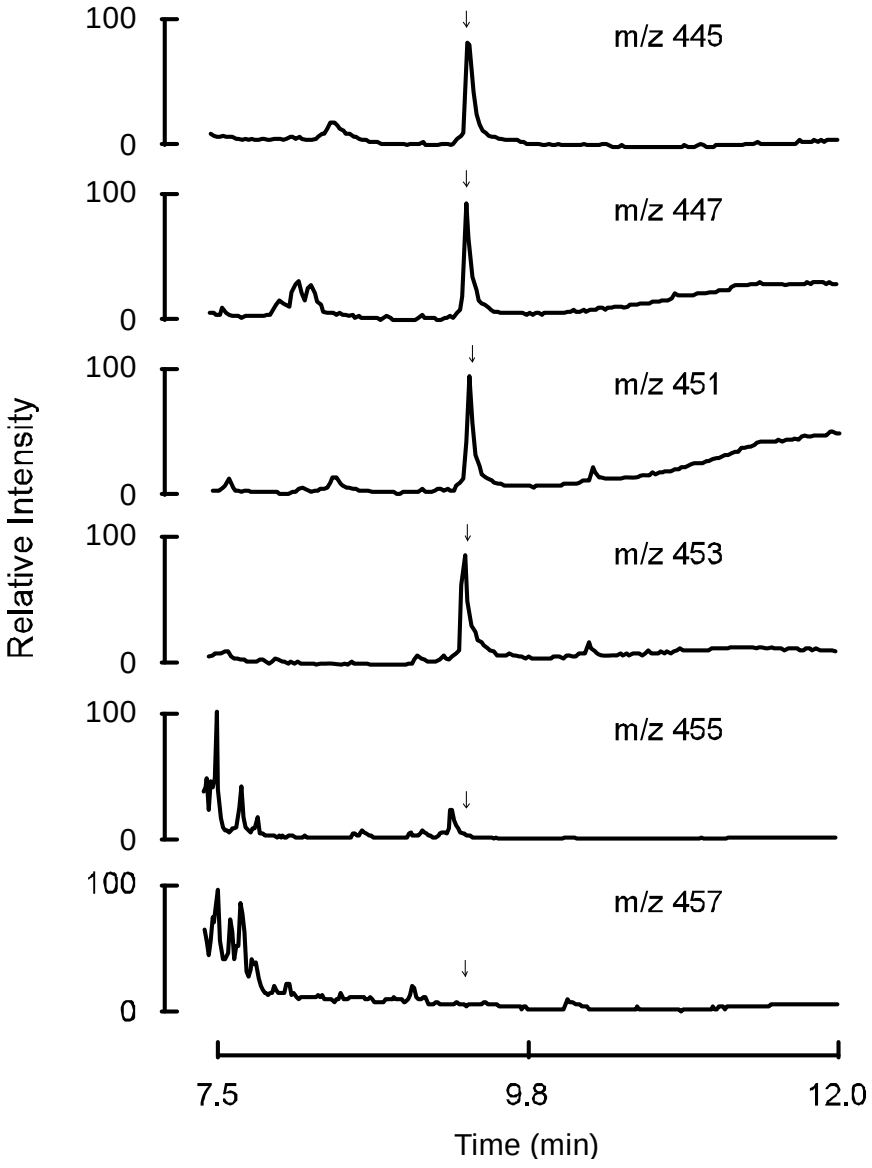


**Figure 3. 4 Detection of 3-bromotyrosine in Mouse Lung Tissue by GC/MS**

Mouse lung tissue specimen from OVA–treated $EPO^{+/+}$ mouse was prepared and analyzed by GC/MS as described in experimental procedures. Native 3-BrY (m/z, 445 and 447) was identified by having the appropriate retention time compared to the corresponding internal standards $^{13}C_6$ BrY (m/z, 451 and 453). No detectable *ex vivo* bromination generation ($^{13}C_9$, $^{15}N_1$ BrY, m/z, 455 and 457) was observed.

The loss of peroxidase activity in knockout animals during allergen challenge was functionally demonstrated by assessing an EPO-specific oxidation product, 3-BrY, in whole-lung homogenates from $EPO^{+/+}$ and $EPO^{-/-}$ mice using multiple allergen challenge models. $EPO^{+/+}$ (WT) and $EPO^{-/-}$ (KO) mice were pre-sensitized to antigen (Ovalbumin, OVA) and then exposed to nebulized antigen. An eosinophil-rich leukocyte infiltration was observed in lung and airway in both genotypes (Figure 3.1.). This similarity of eosinophil infiltration was further confirmed by demonstrating comparable eosinophilia recovered from bronchoalveolar lavage in WT and EPO-KO mice after OVA challenge (BAL eosinophils, $EPO^{+/+-}$, 0.97±0.29, $EPO^{-/-}$, 1.0 ±0.30, $p> 0.6$). Lung specimens and BAL lavage of $EPO^{+/+}$ and $EPO^{-/-}$ mice were harvested 48 hr following the last OVA aerosol challenge. The specimens were prepared following protein precipitation, acid hydrolysis, solid phase extraction and derivatization. The level of 3-BrY in tissue or BAL specimens from OVA–treated $EPO^{+/+}$ and $EPO^{-/-}$ mice was normalized to the content of its precursor, tyrosine, and presented in Figure 3.5. In $EPO^{+/+}$ mice, the contents of 3-BrY were significantly increased in whole-lung homogenates and BAL after OVA challenge compared to saline-challenged controls (3-BrY/Y (μmol/mol), lung tissue, OVA, 215, NS, 0, $p< 0.05$; BAL, OVA, 96, NS, 0, $p< 0.05$). No detectable 3-BrY was observed in $EPO^{-/-}$ mice regardless treatments. The mouse Ovalbumin challenge model did elicit a robust eosinophil-rich leukocyte infiltration into the lung and airway (Figure. 3.1.). However, assessments of free EPO activity from BAL fluids from OVA–treated WT mice only account about 9% of total activity. This limited degranulation may contribute that only nominal protein bromination (3-BrY/Y, 96 μmol/mol) was observed

in WT mice lavage after OVA challenge compared to that recovered in mild asthmatics after segmental allergen challenge (3-BrY/Y, 1085 μmol/mol) [21, 31].

To further investigate EPO catalyzed protein bromination *in vivo*, an alternative inflammation model, *M. Corti/Zymosan* peritonitis model, were applied and protein-bound 3-BrY was monitored. $EPO^{+/+}$ and $EPO^{-/-}$ mice were sensitized to induce peritonitis and peritoneal lavage was harvested 72 hr after challenge. Pilot study indicated that sensitization/challenge helminth protein from *M. Corti* elicited a more robust eosinophil-rich leukocyte infiltration into the peritoneum 72hr after the challenge (topically > $2x10^6$ cells, 25-30% eosinophils). In addition, yeast cell wall zymosan was injected into the peritoneum to trigger extensive leukocyte activation and degranulation. For some animals, as indicated, peritoneal lavage was recovered 72 hours after *M. Corti* challenge and/or 4 hours after subsequent to intraperitoneal injection of zymosan (4hr). Stable isotope dilution GC/NICI/MS quantification of protein-bound 3-BrY was performed (Figure 3.6). Basal level 3-BrY levels were only observed in $EPO^{+/+}$ mice (BrY/Y, 10 ± 23 μmol/mol). 3-BrY levels were significantly increased in $EPO^{+/+}$ mice following *M. Corti* challenge compared with normal saline (7-fold increase, *M. Corti*, 71 ± 58 μmol/mol; normal saline, 10 ± 23 μmol/mol, $p < 0.001$). After *M. Corti* and zymosan treatment, there was 50-fold increases over basal level 3-BrY generation (*M. Corti*/zymosan, 499 ± 390μmol/mol; normal saline, 10 ± 23 μmol/mol, $p < 0.001$). These results confirm that elevated protein bromination consistent with helminth protein induced peritoneal eosinophilia. Zymosan induced leukocytes activation and degranulation results in extensive EPO-catalyzed protein bromination in $EPO^{+/+}$ mice. However, 3- BrY was undetectable in the peritoneal lavage recovered from $EPO^{-/-}$ mice

regardless the treatments. Parasite antigen induced extensive eosinophilia and zymosan treatment stimulated eosinophil activation and degranulation failed to generate detectable 3-BrY in EPO $^{-/-}$ mice. This evidence strongly supports that loss of EPO activity links the absence of protein bromination in vivo. Significantly elevated protein bromination in EPO$^{+/+}$ mice after allergen challenge supports the hypothesis that activated eosinophils associate with protein bromination *in vivo*. 3-BrY serves as a specific molecular fingerprint for EPO catalyzed bromination *in vivo*.

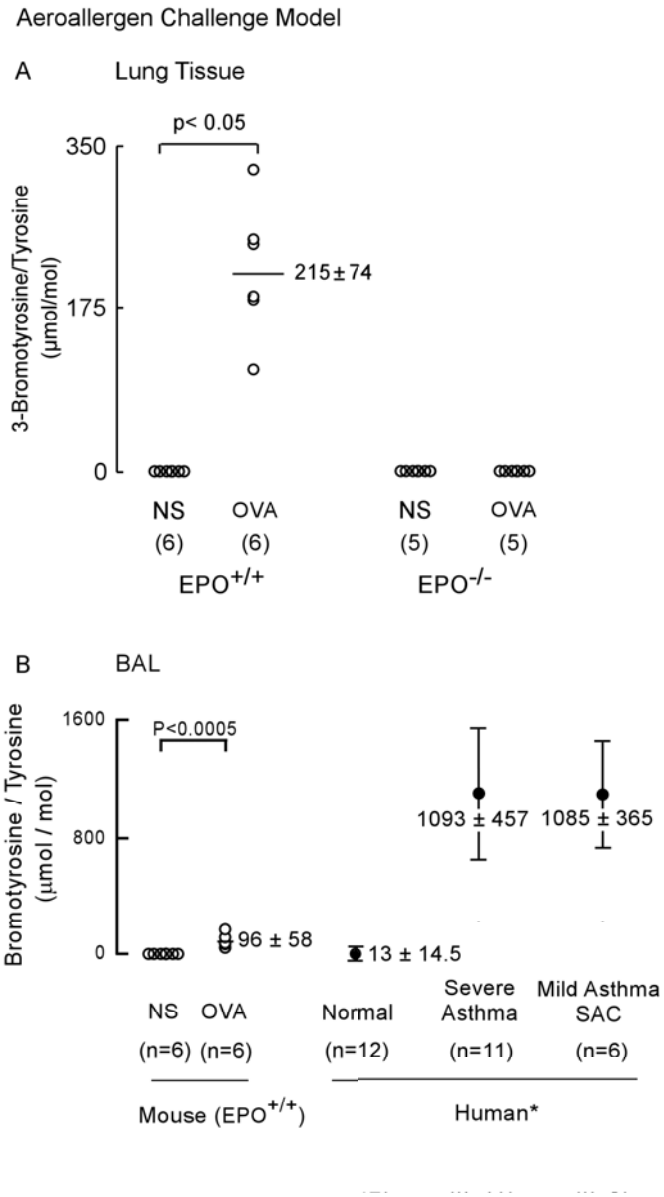


**Figure 3. 5 Elevated 3-BrY Generation in EPO$^{+/+}$ Mice after Allergen Challenge**

The lung/BAL specimens of EPO$^{+/+}$ and EPO$^{-/-}$ mice were harvested 48 hr after ovalbumin (OVA) or normal saline (NS) aerosol challenge. Isotope dilution GC/MS analysis of 3-BrY/Y content: (A) in lung homogenates and (B) in extracelluar lavage protein. The 3-BrY level was normalized to its precursor, tyrosine. Numbers in the parentheses represent the sample size of each group. Data represent the mean ± SD.

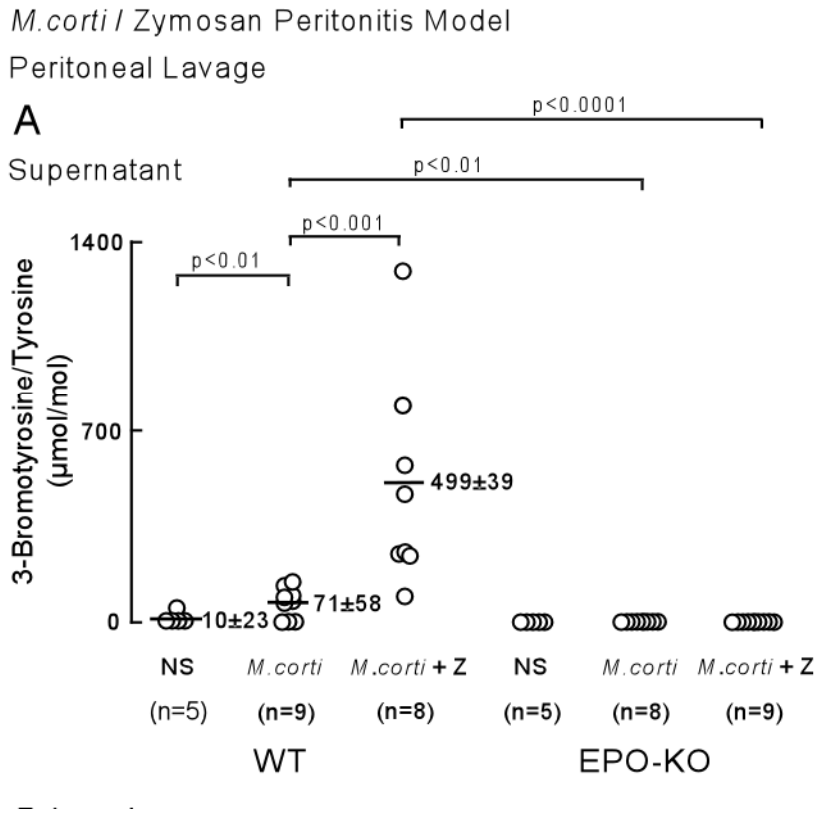


**Figure 3. 6 Detection of 3-BrY in Lavage in Helminth-induced Peritonitis Model**

$EPO^{+/+}$ and $EPO^{-/-}$ mice were sensitized by subcutaneous injection with whole protein extract from the helminth *M. corti.* Animals were challenged on day 21 by intraperitoneal injection with either normal saline (NS) or *M. corti* to elicit an eosinophil-rich peritoneal infiltrate. Where indicated, for some animals, peritoneal lavage was recovered 72 hours after *M. Corti* challenge or 4 hours after subsequent to intraperitoneal injection of zymosan. The content of bromotyrosine in lavage supernatant was subsequently measured by GC/MS. The level of 3-BrY was normalized to the protein content of tyrosine, the precursor amino acid. Numbers in the parentheses represent the sample size of each group. Values represent mean ± S.D.

## 3.4 Discussion

Peroxidase catalyzed protein modification may be implicated in respiratory disorders including asthma, rhinosinusitis [3, 4, 14, 32]. *In vitro* studies support reactive intermediates generated by MPO/EPO react with variety of targets including protein, lipid and genetic materials. Detection and quantitation protein-bound of stable oxidation product has been used as a powerful tool to investigate peroxidase-catalyzed oxidative pathways both *in vitro* and *in vivo* [14, 33-36]. In present studies, we showed significantly elevated protein bromination in specimens recovered from $EPO^{+/+}$ mice after allergen challenge in multiple distinct inflammation models. Both OVA and *M. Corti* challenges elicited a remarkable eosinophil-rich leukocytes infiltration into inflammation sites. Only nominal levels of 3-BrY were observed in lung tissue specimens recovered from $EPO^{+/+}$ mice. Zymosan, a potent trigger of leukocyte activation and degranulation, injected after *M. Corti* challenges resulted a dramatic elevation in protein bromination *in vivo*. No detectable protein-bound 3-BrY was observed in specimens recovered from $EPO^{-/-}$ mice regardless the allergen challenge treatments. Our results support the EPO as the major pathway for generating protein-bound 3-bromotyrosine *in vivo*.

To examine the potential role of EPO in 3-bromotyrosine generation *in vivo*, it was fundamentally important to ascertain the genetic background of KO ($EPO^{-/-}$) and the loss of EPO activity. EPO knockout mouse was generated from 129/SvJ background by replacing 3 target exons [37]. Southern blot and RT-PCR were used to confirm the genetic background of in $EPO^{-/-}$ mouse[37]. Electron Microscopy of eosinophils from $EPO^{-/-}$ mice revealed the ultra structural changes of eosinophil secondary granules (detail in Ref [37]). Cytochemical staining of eosinophils, which were recovered $EPO^{-/-}$ mice, demonstrated

the loss of EPO activity (Figure. 3.2A). The loss of peroxidase activity in cells from $EPO^{-/-}$ mice was further evaluated by using an endpoint colorimetric assay. No detectable EPO activity in cell lysate from $EPO^{-/-}$ mice peritoneal cavity exudates (Figure. 3.2B).

The loss of EPO had no significant impact on the recruitment of leukocytes in $EPO^{-/-}$ mice after allergen challenge. 48 hours after aerosol challenge, the similar eosinophil infiltrations were observed in the lungs and airways recovered from $EPO^{+/+}$ and $EPO^{-/-}$ mice. The localization and number of eosinophils (150–200 eosinophils per millimeter squared) in the lungs after OVA challenge were indistinguishable between $EPO^{+/+}$ and $EPO^{-/-}$ mice (Figure. 3.1). This similarity was also confirmed by comparable total cell counts in bronchoalveolar lavage recovered from $EPO^{+/+}$ and $EPO^{-/-}$ mice (eosinophils, $EPO^{+/+}$ *vs.* $EPO^{-/-}$, $0.97x10^4$ *vs.* $1.0x10^4$). Using helminth protein-induced peritonitis model, a dramatic eosinophil-rich infiltration of leukocytes in peritoneum was observed 72 hours after re-challenge regardless genotype. Comparable total cell count (>2x $10^6$ cells) and differentials (~25-30% eosinophils) were recovered in the peritoneal lavage from $EPO^{+/+}$ and $EPO^{-/-}$ mice.

The loss of EPO was associated with significantly elevated superoxide generation in OVA challenge model. *In vitro* studies demonstrate that EPO-catalyzed free tyrosine or protein-bound tyrosine bromination can be inhibited by eliminated the presence of $H_2O_2$ or $O_2^{\bullet-}$ in the system [38]. To access EPO-catalyzed oxidation *in vivo*, the $O_2^{\bullet-}$ generation of eosinophils recovered from $EPO^{+/+}$ vs. $EPO^{-/-}$ mice was compared. Superoxide production was consistently enhanced ~1.6 fold in eosinophils isolated from $EPO^{-/-}$ mice compared to $EPO^{+/+}$ mice of homogeneous genetic background ($26 \pm 4.8$ vs. $41.5 \pm 7.3$ nmol/$10^6$ cells over one hr for WT vs. EPO-KO; $p < 0.001$).

In the current study, the sample preparation procedures were optimized to prevent artificial 3-BrY generation during sample preparation. *In vitro* studies indicate trace amount of oxidized tyrosine can be generated at acidic condition in the present of corresponding substrates [39, 40]. Preliminary studies found that trace amount of 3-BrY was detected by LC/MS after tyrosine incubated with HCl (6N, ACS certified) at elevated temperature (data not shown). To prevent *ex vivo* 3-BrY generation, tissue specimens were subjected to three sequential extractions with a single phase mixture of $H_2O$/methanol/$H_2O$-saturated diethyl ether (1:3:8 v/v/v) to remove trace amount of bromide. Traditional protein hydrolysis protocol is carried out in 6 N HCl for 24 hrs at 110 °C. Our preliminary studies found HCl (6N, ACS certified) might bring trace amount of bromide into the system. To eliminate the artificial bromination generation during protein hydrolysis, HCl (6N, 1% phenol) was substituted by methanesulfonic acid (MSA, 4N, 1% phenol). The protein hydrolysis efficiency was examined by comparing 500 μg bovine serum albumin (BSA) in HCl (6N, 1% phenol) with that in MSA (4N, 1% phenol) for 24 hrs at 110 °C (Table 3.1). The resulting free amino acids solution (10 μL) was loaded on a C-18 ultrasphere column (Beckman, 5μm resin, 4.6mmx250mm) and detected by UV detector at 280 nm (HPLC gradient listed in experimental procedures). Similar hydrolysis efficiency was achieved by using MSA (4N, 1% phenol) for 24 hrs at 110 °C (Table 3.1). Constant boiling HCl (6N, ultra pure grade, 1 mL ampoule) was used in derivatization to eliminate potential contamination.

**Table 3. 1 Protein Hydrolysis Efficiency**

| | *MSA (4N, 1% Phenol)* | *HCl (6N, 1% Phenol)* |
|---|---|---|
| **Area** | 23565 | 25123 |
| | 24766 | 23294 |
| | 25194 | 20148 |
| | 23443 | 20892 |
| **Mean** | 24242 | 22364 |
| **Std** | 871 | 2277 |
| **t test** | 0.201 | |

500 μg bovine serum albumin (BSA) was incubated with hydrochloric acid (6N, 1% phenol) or methanesulfonic acid (MSA, 4N, 1% phenol) for 24 hrs at 110 °C. The resulting free amino acids solution (10 μL) was loaded on a C-18 ultrasphere column and detected by UV detector at 280 nm.

It is necessary to monitor the *ex vivo* protein bromination due to the complexity of biological matrices. Mass spectrometry is superior to other techniques because of its better sensitivity and specificity. Immunohistochemical approaches have been widely used to detect and localize post translational modification of protein within the tissue both *in vitro* and *in vivo* [41-43]. Immunochemical assay does not require extensive sample preparation [43]. However, cross-reaction and semi-quantitative character dramatically limit the utilization of this technique for quantitation purposes. The creditability of the data is questionable due to lack of direct structural information of the analyte(s) [44, 45]. High performance liquid chromatography (HPLC) and gas chromatography (GC) based approaches are developed to detect oxidized tyrosine species using ultraviolet-visible (UV), fluorescence, electrochemical detection (ECD) and mass spectrometer (MS) detector [46 40, 47, 48]. Both UV and ECD detector are limited by providing adequate sensitivity [49]. In addition, neither of them is able to identify any *ex vivo* oxidation generation [50]. Mass spectrometer and unique isotope labeled internal standard addition provided a powerful tool to detect the potential artifacts generation during sample processing. Universally labeled tyrosine is added prior to protein hydrolysis to serve as a chemical detector of preparative oxidation. Universally labeled tyrosine is structurally identical to the natural abundance tyrosine except the difference in molecular weight. During the sample preparation, if trace amount of anion ions are left in the acidic system, natural abundance tyrosine ($^{12}C_9$, $^{14}N_1$ Tyr) and universally labeled tyrosine ($^{13}C_9$, $^{15}N_1$ Tyr) will be oxidized at the same reaction rate to generate distinct oxidation products which can be only distinguished by the mass spectrometer [39, 51]. In deed, universally labeled tyrosine ($^{13}C_9$, $^{15}N_1$ Tyr) is served as an internal quality controller for the

potential *ex vivo* oxidized tyrosine generation to insure the final result only represent oxidation stress *in vivo*.

Finally, using stable isotope dilution GC/MS and multiple inflammation models in $EPO^{+/+}$ and $EPO^{-/-}$ mice, we explore the mechanism of EPO-catalyzed bromination pathway in response allergen challenge *in vivo*. Aerosolized saline challenge alone had no effect on the homeostatic level of eosinophils in the airways from $EPO^{-/-}$ and $EPO^{+/+}$ mice. After OVA challenge, significantly elevated eosinophils were recruited in both $EPO^{-/-}$ and $EPO^{+/+}$ mice. Eosinophil recruitments were indistinguishable in either genotype. The loss of EPO in $EPO^{-/-}$ mice had no significant effect on eosinophil recruitment in response to allergen challenge compared to $EPO^{+/+}$ mice. Superoxide, one of the reactive oxygen species (ROS), may serve as the fuel for the leukocyte implicated oxidation. Even though the enhanced superoxide generation of eosinophils was found in $EPO^{-/-}$ mice, protein bromination product was absent after OVA challenge. One explanation for the enhance superoxide generation by eosinophil from $EPO^{-/-}$ mice might associate with the loss of EPO activity, which significantly decreased reactive oxygen consumption by EPO-dependent oxidation *in vivo*. In helminth protein induced peritonitis model, the more eosinophil infiltration the higher bromination product was observed in $EPO^{+/+}$ mice (M. Corti, 71±58 μmol/mol vs. Normal saline, 3-BrY/Y 10±23 μmol/mol, $p<0.01$). In addition, zymosan stimulation triggered eosinophil activation and degranulation results a 50-fold increase in 3-BrY content compared to the baseline challenged by normal saline (*M. Corti* + zymosan , 499±39 μmol/mol vs. Normal saline, 3-BrY/Y 10±23 μmol/mol, $p<0.001$). On the other hand, no detectable 3-BrY was observed in $EPO^{-/-}$ mice regardless treatments. This strongly supports that protein-bound

3-Bromotyrosine serves a "molecular fingerprint" of EPO activation and induced modification *in vivo*. Collectively, these results suggest that EPO is the major pathway for the generating protein-bound 3-BrY in these allergen challenge models in $EPO^{+/+}$ and $EPO^{-/-}$ mice.

## 3.5 Reference:


1. Ryu, J. H.; Scanlon, P. D., Obstructive lung diseases: COPD, asthma, and many imitators. Mayo Clin Proc 2001, 76, (11), 1144-53.
2. Massanari, M. J., Asthma management: curtailing costs and improving patient outcomes. J Asthma 2000, 37, (8), 641-51.
3. Fujisawa, T., Role of oxygen radicals on bronchial asthma. Curr Drug Targets Inflamm Allergy 2005, 4, (4), 505-9.
4. Andreadis, A. A.; Hazen, S. L.; Comhair, S. A.; Erzurum, S. C., Oxidative and nitrosative events in asthma. Free Radic Biol Med 2003, 35, (3), 213-25.
5. Nong, G. M.; Li, S. Q.; Yao, L.; Liu, J.; Jiang, M.; Liang, X. A., [Eosinophils apoptosis in asthmatic children]. Zhonghua Er Ke Za Zhi 2003, 41, (4), 278-81.
6. Romagnoli, M.; Vachier, I.; Tarodo de la Fuente, P.; Meziane, H.; Chavis, C.; Bousquet, J.; Godard, P.; Chanez, P., Eosinophilic inflammation in sputum of poorly controlled asthmatics. Eur Respir J 2002, 20, (6), 1370-7.
7. Wardlaw, A. J.; Dunnette, S.; Gleich, G. J.; Collins, J. V.; Kay, A. B., Eosinophils and mast cells in bronchoalveolar lavage in subjects with mild asthma. Relationship to bronchial hyperreactivity. Am Rev Respir Dis 1988, 137, (1), 62-9.

8. Ohshima, H.; Tatemichi, M.; Sawa, T., Chemical basis of inflammation-induced carcinogenesis. Arch Biochem Biophys 2003, 417, (1), 3-11.

9. Kiehl, P.; Kapp, A., [Tissue eosinophilia and local deposition of eosinophil-specific granule proteins. Regulation and significance for inflammatory response in atopic dermatitis and other inflammatory dermatoses]. Hautarzt 1998, 49, (3), 176-83.

10. Carlson, M. G.; Peterson, C. G.; Venge, P., Human eosinophil peroxidase: purification and characterization. J Immunol 1985, 134, (3), 1875-9.

11. Nagy, L.; Sutto, Z.; Tolnay, E.; Terek, K.; Orosz, M.; Szentpaly, O., [Eosinophil activation markers in status asthmaticus]. Orv Hetil 1996, 137, (3), 121-4.

12. Henderson, W. R.; Chi, E. Y.; Jong, E. C.; Klebanoff, S. J., Mast cell-mediated tumor-cell cytotoxicity. Role of the peroxidase system. J Exp Med 1981, 153, (3), 520-33.

13. Lukacs, N. W.; Strieter, R. M.; Shaklee, C. L.; Chensue, S. W.; Kunkel, S. L., Macrophage inflammatory protein-1 alpha influences eosinophil recruitment in antigen-specific airway inflammation. Eur J Immunol 1995, 25, (1), 245-51.

14. Agosti, J. M.; Altman, L. C.; Ayars, G. H.; Loegering, D. A.; Gleich, G. J.; Klebanoff, S. J., The injurious effect of eosinophil peroxidase, hydrogen peroxide, and halides on pneumocytes in vitro. J Allergy Clin Immunol 1987, 79, (3), 496-504.

15. Weiss, S. J.; Test, S. T.; Eckmann, C. M.; Roos, D.; Regiani, S., Brominating oxidants generated by human eosinophils. Science 1986, 234, (4773), 200-3.

16. Thomas, E. L.; Bozeman, P. M.; Jefferson, M. M.; King, C. C., Oxidation of bromide by the human leukocyte enzymes myeloperoxidase and eosinophil peroxidase. Formation of bromamines. J Biol Chem 1995, 270, (7), 2906-13.

17. Kanofsky, J. R., Bromine derivatives of amino acids as intermediates in the peroxidase-catalyzed formation of singlet oxygen. Arch Biochem Biophys 1989, 274, (1), 229-34.

18. Kanofsky, J. R., Singlet oxygen production from the peroxidase-catalyzed oxidation of indole-3-acetic acid. J Biol Chem 1988, 263, (28), 14171-5.

19. Wu, W.; Chen, Y.; d'Avignon, A.; Hazen, S. L., 3-Bromotyrosine and 3,5-dibromotyrosine are major products of protein oxidation by eosinophil peroxidase: potential markers for eosinophil-dependent tissue injury in vivo. Biochemistry 1999, 38, (12), 3538-48.

20. Aldridge, R. E.; Chan, T.; van Dalen, C. J.; Senthilmohan, R.; Winn, M.; Venge, P.; Town, G. I.; Kettle, A. J., Eosinophil peroxidase produces hypobromous acid in the airways of stable asthmatics. Free Radic Biol Med 2002, 33, (6), 847-56.

21. Wu, W.; Samoszuk, M. K.; Comhair, S. A.; Thomassen, M. J.; Farver, C. F.; Dweik, R. A.; Kavuru, M. S.; Erzurum, S. C.; Hazen, S. L., Eosinophils generate brominating oxidants in allergen-induced asthma. J Clin Invest 2000, 105, (10), 1455-63.

22. Mayo, L. A.; Curnutte, J. T., Kinetic microplate assay for superoxide production by neutrophils and other phagocytic cells. Methods Enzymol 1990, 186, 567-75.

23. Ohmori, J.; Tokunaga, H.; Ezaki, T.; Maruyama, H.; Nawa, Y., Eosinophil peroxidase deficiency in New Zealand white mice. Int Arch Allergy Immunol 1996, 111, (1), 30-5.

24. Denzler, K. L.; Farmer, S. C.; Crosby, J. R.; Borchers, M.; Cieslewicz, G.; Larson, K. A.; Cormier-Regard, S.; Lee, N. A.; Lee, J. J., Eosinophil major basic protein-1 does not contribute to allergen-induced airway pathologies in mouse models of asthma. J Immunol 2000, 165, (10), 5509-17.

25. Horton, M. A.; Larson, K. A.; Lee, J. J.; Lee, N. A., Cloning of the murine eosinophil peroxidase gene (mEPO): characterization of a conserved subgroup of mammalian hematopoietic peroxidases. J Leukoc Biol 1996, 60, (2), 285-94.

26. Strath, M.; Warren, D. J.; Sanderson, C. J., Detection of eosinophils using an eosinophil peroxidase assay. Its use as an assay for eosinophil differentiation factors. J Immunol Methods 1985, 83, (2), 209-15.

27. White, S. R.; Kulp, G. V.; Spaethe, S. M.; Van Alstyne, E.; Leff, A. R., A kinetic assay for eosinophil peroxidase activity in eosinophils and eosinophil conditioned media. J Immunol Methods 1991, 144, (2), 257-63.

28. Lee, N. A.; McGarry, M. P.; Larson, K. A.; Horton, M. A.; Kristensen, A. B.; Lee, J. J., Expression of IL-5 in thymocytes/T cells leads to the development of a massive eosinophilia, extramedullary eosinophilopoiesis, and unique histopathologies. J Immunol 1997, 158, (3), 1332-44.

29. Hunt, S., Halogenated tyrosine derivatives in invertebrate scleroproteins: isolation and identification. Methods Enzymol 1984, 107, 413-38.

30. Larson, K. A.; Horton, M. A.; Madden, B. J.; Gleich, G. J.; Lee, N. A.; Lee, J. J., The identification and cloning of a murine major basic protein gene expressed in eosinophils. J Immunol 1995, 155, (6), 3002-12.

31. MacPherson, J. C.; Comhair, S. A.; Erzurum, S. C.; Klein, D. F.; Lipscomb, M. F.; Kavuru, M. S.; Samoszuk, M. K.; Hazen, S. L., Eosinophils are a major source of nitric oxide-derived oxidants in severe asthma: characterization of pathways available to eosinophils for generating reactive nitrogen species. J Immunol 2001, 166, (9), 5763-72.

32. Bernardes, J. F.; Shan, J.; Tewfik, M.; Hamid, Q.; Frenkiel, S.; Eidelman, D. H., Protein nitration in chronic sinusitis and nasal polyposis: role of eosinophils. Otolaryngol Head Neck Surg 2004, 131, (5), 696-703.

33. Zhang, R.; Brennan, M. L.; Shen, Z.; MacPherson, J. C.; Schmitt, D.; Molenda, C. E.; Hazen, S. L., Myeloperoxidase functions as a major enzymatic catalyst for initiation of lipid peroxidation at sites of inflammation. J Biol Chem 2002, 277, (48), 46116-22.

34. Persson, T.; Andersson, P.; Bodelsson, M.; Laurell, M.; Malm, J.; Egesten, A., Bactericidal activity of human eosinophilic granulocytes against Escherichia coli. Infect Immun 2001, 69, (6), 3591-6.

35. Shen, Z.; Mitra, S. N.; Wu, W.; Chen, Y.; Yang, Y.; Qin, J.; Hazen, S. L., Eosinophil peroxidase catalyzes bromination of free nucleosides and double-stranded DNA. Biochemistry 2001, 40, (7), 2041-51.

36. Shen, Z.; Wu, W.; Hazen, S. L., Activated leukocytes oxidatively damage DNA, RNA, and the nucleotide pool through halide-dependent formation of hydroxyl radical. Biochemistry 2000, 39, (18), 5474-82.

37. Denzler, K. L.; Borchers, M. T.; Crosby, J. R.; Cieslewicz, G.; Hines, E. M.; Justice, J. P.; Cormier, S. A.; Lindenberger, K. A.; Song, W.; Wu, W.; Hazen, S. L.; Gleich, G. J.; Lee, J. J.; Lee, N. A., Extensive eosinophil degranulation and peroxidase-mediated oxidation of airway proteins do not occur in a mouse ovalbumin-challenge model of pulmonary inflammation. J Immunol 2001, 167, (3), 1672-82.

38. Wu, W.; Chen, Y.; Hazen, S. L., Eosinophil peroxidase nitrates protein tyrosyl residues. Implications for oxidative damage by nitrating intermediates in eosinophilic inflammatory disorders. J Biol Chem 1999, 274, (36), 25933-44.

39. Frost, M. T.; Halliwell, B.; Moore, K. P., Analysis of free and protein-bound nitrotyrosine in human plasma by a gas chromatography/mass spectrometry method that avoids nitration artifacts. Biochem J 2000, 345 Pt 3, 453-8.

40. Shigenaga, M. K., Quantitation of protein-bound 3-nitrotyrosine by high-performance liquid chromatography with electrochemical detection. Methods Enzymol 1999, 301, 27-40.

41. Kooy, N. W.; Lewis, S. J.; Royall, J. A.; Ye, Y. Z.; Kelly, D. R.; Beckman, J. S., Extensive tyrosine nitration in human myocardial inflammation: evidence for the presence of peroxynitrite. Crit Care Med 1997, 25, (5), 812-9.

42. Hill, K. E.; Zollinger, L. V.; Watt, H. E.; Carlson, N. G.; Rose, J. W., Inducible nitric oxide synthase in chronic active multiple sclerosis plaques: distribution,

cellular expression and association with myelin damage. J Neuroimmunol 2004, 151, (1-2), 171-9.

43. Haddad, I. Y.; Pataki, G.; Hu, P.; Galliani, C.; Beckman, J. S.; Matalon, S., Quantitation of nitrotyrosine levels in lung sections of patients and animals with acute lung injury. J Clin Invest 1994, 94, (6), 2407-13.

44. Khan, J.; Brennand, D. M.; Bradley, N.; Gao, B.; Bruckdorfer, R.; Jacobs, M., 3-Nitrotyrosine in the proteins of human plasma determined by an ELISA method. Biochem J 1998, 330 (Pt 2), 795-801.

45. Khan, J.; Brennand, D. M.; Bradley, N.; Gao, B.; Bruckdorfer, R.; Jacobs, M., 3-Nitrotyrosine in the proteins of human plasma determined by an ELISA method. Biochem J 1998, 332 (Pt 3), 807-8.

46. Kaur, H.; Halliwell, B., Evidence for nitric oxide-mediated oxidative damage in chronic inflammation. Nitrotyrosine in serum and synovial fluid from rheumatoid patients. FEBS Lett 1994, 350, (1), 9-12.

47. Hensley, K.; Maidt, M. L.; Pye, Q. N.; Stewart, C. A.; Wack, M.; Tabatabaie, T.; Floyd, R. A., Quantitation of protein-bound 3-nitrotyrosine and 3,4-dihydroxyphenylalanine by high-performance liquid chromatography with electrochemical array detection. Anal Biochem 1997, 251, (2), 187-95.

48. Herce-Pagliai, C.; Kotecha, S.; Shuker, D. E., Analytical methods for 3-nitrotyrosine as a marker of exposure to reactive nitrogen species: a review. Nitric Oxide 1998, 2, (5), 324-36.

49. Kaur, H.; Lyras, L.; Jenner, P.; Halliwell, B., Artefacts in HPLC detection of 3-nitrotyrosine in human brain tissue. J Neurochem 1998, 70, (5), 2220-3.

50. Tsikas, D.; Caidahl, K., Recent methodological advances in the mass spectrometric analysis of free and protein-associated 3-nitrotyrosine in human plasma. J Chromatogr B Analyt Technol Biomed Life Sci 2005, 814, (1), 1-9.

51. Yi, D.; Ingelse, B. A.; Duncan, M. W.; Smythe, G. A., Quantification of 3-nitrotyrosine in biological tissues and fluids: generating valid results by eliminating artifactual formation. J Am Soc Mass Spectrom 2000, 11, (6), 578-86.

# CHAPTER IV

# HIGH THROUGHPUT LC-MS/MS ASSAY FOR QUANTITATION OF PROTEIN OXIDATION BY DISTINCT PATHWAYS IN BIOLOGICAL MATRICES

## 4.1 Introduction

The failure of potential antioxidant strategies to influence the propensity to develop a number of disease processes has raised considerable debate over the significance of oxidative stress in disease pathogenesis. For example, α-tocopherol supplementation in human clinical trials of cancer chemoprevention[1-3] and cardiovascular disease[4-6] has for the most part failed to demonstrate clinical benefit. However, in virtually all large-scale human clinical "anti-oxidant" studies there was no convincing evidence that the interventions employed had any impact on oxidative events. This is because concomitant systemic markers of oxidative stress were never performed, due in large part to limitations in current methodology that permits performance of such measures in a practical fashion on large numbers of clinical specimens.

Of interest, where molecular markers of oxidant stress have been performed on subjects supplemented with large doses of α-tocopherol, reductions in levels have not always been observed[7], whereas drugs with proven clinical benefit, such as statins for cardiovascular risks, have shown potent systemic anti-oxidant effects as reflected by multiple distinct oxidant stress markers[8, 9].

Numerous lines of evidence support a mechanistic role for oxidative processes in disease pathogenesis[10-13]. Increasingly, it is recognized that oxidative modification of a number of proteins participates in the pathogenesis of aging and a number of disease states including atherosclerosis, asthma and neurodegenerative disorders[14-18]. Protein modification by reactive nitrogen species and halogenating oxidants (both brominating and chlorinating species) lead to the generation of a number of stable products that can be identified in a wide range of biological samples[8, 19-27]. As a result, the pathways that promote protein modification have become potential targets for therapeutic intervention. In addition, the detection of these products, which can act as molecular fingerprints of disease processes (Figure 4.1), can potentially stratify patients according to their disease risk, as well as potentially indicate which patients are most likely to benefit from potential antioxidant promoting interventions[8, 9, 23, 28].

The leukocyte derived enzymes, eosinophil peroxidase (EPO) and myeloperoxidase (MPO), have proven roles in the promotion of oxidative modification of proteins *in vivo*. EPO, a granule protein secreted by activated eosinophils, preferentially utilizes hydrogen peroxide and bromide as co-substrates to form reactive brominating species including hypobromous acid (HOBr)[29]. MPO, secreted by activated neutrophils, monocytes and certain tissue macrophages, can catalyze the formation of reactive

chlorinating species such as hypochlorous acid (HOCl) and molecular chlorine ($Cl_2$) by utilizing hydrogen peroxide and chloride[30]. Nitric oxide (NO)-derived oxidants may also be generated by EPO and MPO catalyzed pathways[31-34], in addition to interactions with peroxynitrite ($ONOO^-$), a potent oxidant formed by the reaction of nitric oxide and superoxide[35]. Aromatic amino acid residues serve as prime targets for oxidative modification. The side chain of tyrosine is preferentially modified by these reactive species to form a number of oxidative products that are chemically stable and can be detected in a wide variety of biological samples (Figure 4.1).

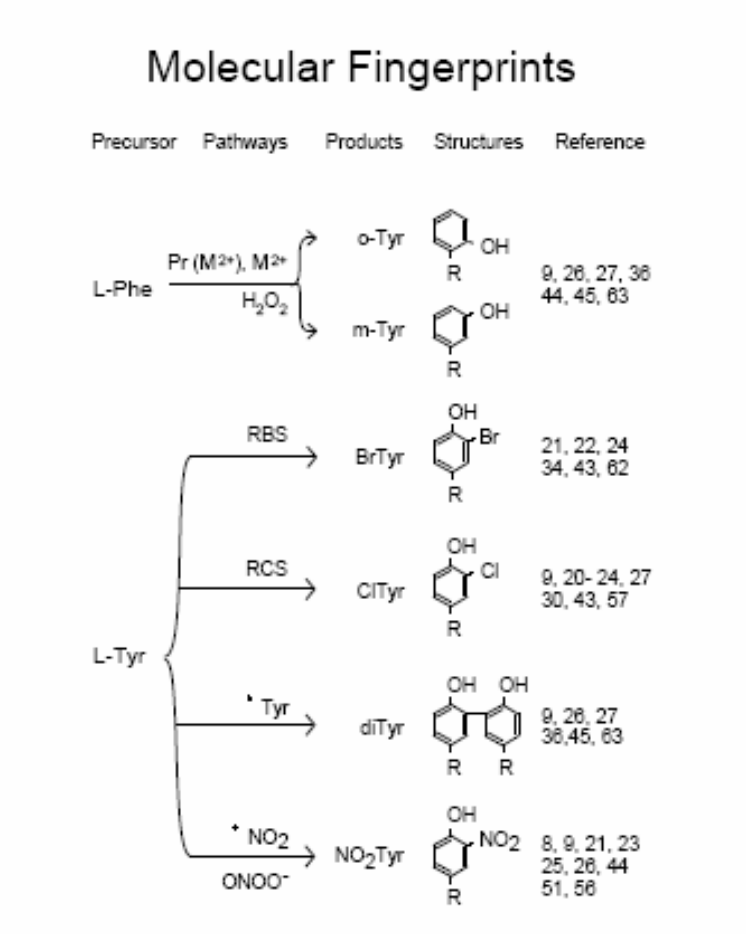


**Figure 4. 1 Chemical Structures of Molecular Fingerprints of Protein Oxidation *In Vivo***

Hydroxyl radical can be generated by a redox-active metal ion ($M^{2+}$) or a protein-bound redox-active metal ion [Pr ($M^{2+}$)] and reacts with phenylalanine to form meta-tyrosine (*m*-Tyr) and ortho-tyrosine (*o*-Tyr). EPO and MPO generate reactive brominating species (RBS) and reactive chlorinating species (RCS) which oxidize tyrosine to form 3-bromotyrosine (BrTyr) and 3-chlorotyrosine (ClTyr). Tyrosyl radical ($^{\cdot}$Tyr) cross reacts with tyrosine to form di-tyrosine (diTyr). Nitrogen dioxide ($\cdot NO_2$) can be generated by enzymatic pathways working with peroxynitrite ($ONOO^{-}$) to oxidize tyrosine and form 3-nitrotyrosine.

Increasing evidence has emerged to highlight the role that oxidative protein modification plays in the promotion of a number of diseases[18, 36, 37]. Reactive nitrogen species have been implicated in the initiation of lipid peroxidation, protein nitration and subsequent conversion of low density lipoprotein (LDL) into an atherogenic form[38-41]. It has been demonstrated that systemic levels of protein-bound nitrotyrosine predicts a risk of atherosclerotic disease in clinical studies and that levels decline following administration of statin therapy, independent of the degree of LDL lowering[8, 9]. Further, breast cancer samples with a high microvascular density are associated with elevated tissue levels of nitrotyrosine[42]. Similarly, the content of apolipoprotein A-I chlorotyrosine in subjects is strongly associated with cardiovascular risk[23]. Moreover, levels of bromotyrosine in bronchoalveolar lavage (BAL) samples increase significantly following allergen challenge in asthmatic subjects[22]. Bromotyrosine levels are significantly elevated in BAL recovered from subjects with severe asthma[21], and are elevated in both induced sputum[24] and urine[43] of asthmatic subjects. It has also been reported that meta-tyrosine and ortho-tyrosine, markers of protein oxidation by hydroxyl radical-like oxidants, can be detected *in vivo* in a range of inflammatory settings[9, 44, 45].

Because of the potential utility of protein oxidative modifications in determining mechanisms of disease pathogenesis and oxidative processes *in vivo*, a number of methods have been reported to quantify the levels of oxidized protein products in various biological samples. The presence of oxidized protein products in tissue samples and identification of their cellular origin have been demonstrated through several immunochemical techniques using antibodies that are specific for protein oxidative modifications [46-49]. However, many molecular markers of protein oxidation that are of

interest do not yet have commercially available specific antibodies for their detection. Moreover, antibody-based methods in general may be limited in their ability to accurately quantify levels of individual specific oxidative products in varying sequence and protein conformational contexts[50]. This is because antibodies typically display some degree of cross-reactivity with other antigens and differing affinities for small haptens depending upon the structural/sequence context in where the antigen resides. Finally, until multiple specific antibodies and quantitative methods are developed, no current immunochemical assays can simultaneously quantify multiple structurally distinct oxidized amino acids and their precursors.

Alternative analytical approaches for oxidized amino acid quantification typically involve in chromatographic separation of the components of protein hydrosylates by high performance liquid chromatography (HPLC) or gas chromatography (GC), followed by detection and quantification of oxidized aromatic amino acid species and their precursors (tyrosine and phenylalanine) by ultraviolet detector (UV), electrochemical detection detector (ECD), electron capture-negative chemical ionization mass spectrometry (EC-NCI/MS) and electrospray ionization mass spectrometry (ESI/MS)[25, 36, 51-56]. Mass spectrometry is currently the only method that provides direct structural information of the analyte as well as permits simultaneous monitoring for intra-preparative generation of oxidative products during sample handling. The high sensitivity of mass spectrometry allows for the detection of trace amounts of analytes in biological samples[10, 25, 32, 57, 58]. Early mass spectrometry studies of oxidized amino acids employing isotopically labeled precursor amino acids for the first time revealed the generation of artifactual intra-preparative oxidized amino acids such as 3-bromotyrosine (BrTyr), 3,5-

dibrbromotyrosine ($Br_2Tyr$)[22, 59], 3-chlorotyrosine (ClTyr)[22, 59], 3-nitrotyrosine ($NO_2Tyr$)[59-61], and o,o'-dityrosine (diTyr)[59]. Use of isotopically labeled precursors has subsequently been adopted by many others because of the power of the technique in fine-tuning sample preparation methods that exclude intra-preparative oxidation[25, 32].

With accumulating evidence supporting a pivotal role for protein oxidation in a wide range of disease processes, substantial interest has focused on the development of analytical methods that can measure molecular markers of protein oxidation *in vivo*. However, the labor- and time-intensive proposition of analyzing clinical specimens for the presence of individual oxidation products in large scale human clinical studies presents a daunting challenge. The development of a mass spectrometry-based approach that permits simultaneous monitoring of an array of molecular markers of protein oxidation while monitoring for the presence of artifactual intra-preparative oxidation would appear to be a major advance in this field. Here we describe a highly sensitive and specific assay for simultaneous quantification of 3-chlorotyrosine, 3,5-dichlorotyrosine, 3-bromotyrosine, 3,5-dibromotyrosine, *o*-tyrosine, *m*-tyrosine, o,o'-dityrosine, nitrotyrosine, and their respective precursor amino acids in biological tissues and fluids. The method involves use of high performance liquid chromatography (HPLC) with on-line electrospray ionization tandem mass spectrometry (LC-ESI/MS/MS). The incorporation of synthetic $^{13}C_6$-labled synthetic internal standards permits accurate quantification of each natural abundance analyte. Inclusion of $^{13}C_9$, $^{15}N$-labeled precursor amino acids, tyrosine and phenylalanine, permits quantification of precursors and monitoring for artifactual generation of oxidative products during sample processing simultaneously. Use of column switching technique further enhances sample analysis

throughput, resulting in a robust overall method with practical utility for both larger scale clinical and animal model studies. The high sensitivity, specificity and detection of multiple oxidized tyrosine species of this analytical method provides a unique opportunity to both further delineate oxidative mechanisms in disease processes. It also will enable exploration of the potential clinical utility of specific protein oxidative modifications as diagnostic and prognostic indicators in human health and disease.

## 4.2 Experimental Procedures

Hydrochloric acid (optima), $H_3PO_4$, $NaH_2PO_4$, $Na_2HPO_4$ and all organic solvents were from Fisher Chemical Co. (Pittsburgh, PA). Methanesulfonic acid and liquid bromine were from Acros organics (New Jersey). Chelex 100 resin (200-400 mesh, sodium from) was from BioRad (Hercules, CA). L-[$^{13}C_6$] tyrosine, L-[$^{13}C_6$] phenylalanine and L-[$^{13}C_9$, $^{15}N_1$] universally labeled tyrosine and phenylalanine were from Cambridge Isotopes (Andover, MA). All other reagents were purchased from Sigma (St. Louis, MO) unless otherwise indicated. All gasses were of highest quality available and were from Praxair (Cleveland, OH).

### Human Studies

Normal levels of protein oxidation products in plasma were evaluated in samples obtained from sequential healthy subjects who responded to local advertisements or were participating in health care screenings following informed consent. Subjects who were at least 25 years old with no history or clinical evidence of coronary artery disease were eligible to enroll into study. These subjects had a mean (±SD) age of 52.0 (±11.9) years, 25.7% were current smokers, 27.1% had a history of hypertension and 10% had a history

of diabetes. All participants provided written informed consents. The study protocol was approved by the Institutional Review Board of the Cleveland Clinic Foundation.

Whole blood was collected into purple (EDTA) top vacutainer tubes and samples were spun at 4 °C for 10 min at 2500 rpm. Plasma was removed and spiked with a 100X stock solution of anti-oxidant cocktail comprised of diethylenetriaminepentaacetic acid (DTPA) and butylated hydroxytoluene (BHT), resulting in a plasma final concentration of 100 μM each. Specimens were snap frozen under Argon atmosphere in liquid nitrogen and stored at approximately –80 °C until analyses.

**Aeroallergen Lung Challenge Model**

The animal studies were performed using approved protocols from the Animal Research Committees of the Cleveland Clinic Foundation and University of Minnesota. Three groups of adult age- and sex- matched Hartley guinea pigs were sensitized by intraperitoneal injections of 500 μg of ovalbumin (OVA, grade IV, Sigma) with 50 mg aluminum hydroxide adjuvant on days 0 and 14. One group of animals (Group 1, n= 5) consumed a normal chow diet with drinking water throughout the study. On day 21 these animals were challenged with aerosolized normal saline to serve as controls. Group 2 (n=6) received a normal chow diet with drinking water, while Group 3 (n= 6) received drinking water supplemented with 0.2% sodium thiocyanate (NaSCN). On day 21, animals in Groups 2 and 3 were both challenged by aerosolized normal saline supplemented with 0.1% OVA solution. The challenge was performed for one minute on five successive occasions, each separated by a minute of recovery. Two days later, the animals were sacrificed. Lung tissue was harvested, immediately rinsed in ice-cold normal saline and placed in 20 mM phosphate buffer saline (pH 7.4), supplemented with

100 μM BHT and 100 μM DTPA, and overlaid with argon prior to storage at approximately –80 °C until analyzed.

**Tissue Homogenization**

Samples were processed on the day of analysis. Tissue specimens were thawed and immediately homogenized in ice-cold 20 mM PBS (pH = 7.4), containing 100 μM DTPA and 100 μM BHT, using a Potter-Elvehjem Tissue Homogenizer with PTFE pestle. The protein concentration of the tissue homogenate was determined using a Bradford-based Biorad Protein Assay (Hercules, CA) with BSA as the standard.

**Synthesis and Purification of Isotope Labeled Internal Standards**

Isotope labeled precursors, [$^{13}C_6$] tyrosine and phenylalanine, were purchased from Cambridge Isotopes. The purity and isotope composition of each isotope-labeled amino acid was confirmed by mass spectrometry analyses to be > 99% pure before use in syntheses. Isotope labeled 3-[$^{13}C_6$] bromotyrosine, 3-[$^{13}C_6$] chlorotyrosine, 3,5-[$^{13}C_6$] di-bromotyrosine, 3,5-[$^{13}C_6$] di-chlorotyrosine, *o,o'*-[$^{13}C_{12}$]dityrosine and 3-[$^{13}C_6$] nitrotyrosine were synthesized as previously described[20, 59, 62]. *m*-[$^{13}C_6$] tyrosine and *o*-[$^{13}C_6$] tyrosine were prepared from [$^{13}C_6$] phenylalanine[63]. Briefly, 3-Bromo [$^{13}C_6$] tyrosine and 3,5-[$^{13}C_6$]di-bromotyrosine were prepared by adding fresh made NaOBr to an equimolar concentration of L-[$^{13}C_6$] tyrosine solution in 20 mM PBS (pH 7.4) as described previously[59]. The concentration of the NaOBr solution was determined on the day of synthesis by UV spectrophotometer ($\varepsilon_{331}$ = 315 $M^{-1}$ $CM^{-1}$, 0.1N sodium hydroxide). The tyrosine/NaOBr solutions were incubated at 37°C for 2 hours, and reactions stopped by the addition of large molar excess of methionine. Prior to HPLC

purification, reaction mixtures were treated with trifluoroacetic acid (TFA) to adjust the pH to 2. 3-[$^{13}C_6$] chlorotyrosine, 3,5-[$^{13}C_6$] di-bromotyrosine and 3-[$^{13}C_6$] nitrotyrosine were synthesized from L-[$^{13}C_6$] tyrosine using an equimolar concentration HOCl, a 2.0 molar excess of HOCl and equimolar concentration of sodium peroxynitrite, respectively. *o,o'*-[$^{12}C_{12}$]dityrosine and *o,o'*-[$^{13}C_{12}$]dityrosine were prepared by the oxidation reaction of L-[$^{12}C_6$] tyrosine and L-[$^{13}C_6$] tyrosine, respectively, with hydrogen peroxide ($H_2O_2$), catalyzed by horseradish peroxidase. *m*-[$^{13}C_6$] tyrosine and *o*-[$^{13}C_6$] tyrosine were prepared from [$^{13}C_6$] phenylalanine. $H_2O_2$ and $CuSO_4$ (ratio, 100:1) were used to generate the hydroxyl radical used in reactions to oxidize phenylalanine.

Each synthetic reaction mixture containing isotopically labeled amino acids were first partially resolved and desalted using disposable mini solid-phase extraction (SPE) columns. Samples were reconstituted with water containing 0.1% TFA and eluted with 30% methanol and dried under anhydrous nitrogen. The eluted material was individually resuspended in chelex 100 (Bio-Rad, Hercules, CA) resin treated water and DTPA (final concentration 100 μM) was added before loading material onto a reversed-phase Ultrasphere ODS column (Beckman Instruments, Fullerton, CA, 10 mm x 250 mm, 5 μm particle) for further purification. L-[$^{13}C_6$] ring labeled tyrosine and its oxidized products were separated using reverse-phase HPLC using a diode array detector with dual wavelength detection capability at 254 and 280 nm. Amino acids were eluted with a linear gradient generated with solvent B (methanol). Universally labeled [$^{13}C_9$, $^{15}N_1$] phenylalanine as commercially supplied was noted to typically require purification by reverse-phase HPLC prior to use to eliminate trace amounts of contaminating universally labeled ortho- and meta- tyrosine species.

Before isolating isotopically labeled amino acids, the corresponding non-labeled amino acids were used to optimize HPLC chromatographic condition, identify elution times and develop calibration curve. After thorough rinsing of the HPLC system to avoid isotope contamination from carry-over, individual internal standards were subsequently purified by HPLC. The identity and purity of isotopically labeled standards were individually confirmed by HPLC with on-line high-resolution mass spectrometry. The isotope labeled internal standards were dried in a speed vacuum and stored at –20 °C.

**General Procedures**

Samples were maintained under argon to prevent artificial oxidation during sample handling. In the event that samples could not be analyzed immediately, they were purged with argon in gas-tight Cryovials (Corning Inc., Acton, MA), snap-frozen in liquid nitrogen and stored at –80 °C. All buffers were treated with chelex-100 resin to remove traces of residual transition metal ions. All glassware was treated with DTPA, rinsed with chelex-100 resin treated water, and baked at 500 $^{o}$C overnight prior to use. The HPLC columns, filters, and solid phase extraction columns were also rinsed with DTPA at neutral pH, and then cleaned with chelex-100 resin treated water. These procedures were found necessary to preclude intrapreparative formation of *o*-tyrosine and *m*-tyrosine during sample hydrolysis and analysis.

**Desalting and Delipidation**

Typically, samples are processed in batches of 50 or less. Samples (20 μL plasma or 600 μg tissue homogenate) were diluted to 500 μL with $H_2O$ and spiked with DTPA to achieve a final concentration of 100 μM. Ice-cold methanol (1.5 mL) and water saturated ether (4 mL) were then added sequentially. The mixture was vortexed and maintained in

a slush ice-bath for 20 minutes and then centrifuged at 2500 g for 20 min. The supernatant was discarded and the protein pellet was briefly dried under a nitrogen stream in an N-EVAP nitrogen evaporator (Organomation Associates Inc., Berlin, MA). Desalting and delipidation was repeated one more time in the absence of DTPA supplementation. The resulting protein pellet was dried under nitrogen prior to protein hydrolysis.

**Protein Hydrolysis**

Known amounts of universally labeled [$^{13}C_9$,$^{15}N_1$] tyrosine (4 nmol) and [$^{13}C_9$,$^{15}N_1$] phenylalanine (4 nmol) and $^{13}C_6$-ring labeled internal standards (20 pmol each) were added to the protein pellet, followed by the addition of 0.5 mL 4 M methanesulfonic acid containing 1% phenol and 0.3% benzoic acid. Hydrolysis of the desalted protein pellet was carried out under argon at 110 °C overnight (~18 hours).

**Solid Phase Extraction**

Protein hydrolysates were subjected to solid-phase extraction (SPE) to remove acid and concentrate the analytes prior to LC/ESI/MS/MS analysis. Hydrolysates (0.5 mL) were adjusted to 2 mL with Chelex-treated water and passed over a C18 solid phase extraction column (Supelco Inc., Bellefonte, PA). The column was preconditioned with 6 mL methanol, rinsed with 6 mL 50 mM PB buffer containing 100 μM DTPA (pH 7.0), followed by 6 mL Chelex-treated water and equilibrated with 0.1% TFA water. Following sequential washes with 2 mL of 0.1% TFA water, the oxidized amino acids and their precursors were eluted with 2 mL 30% methanol solution supplemented with 0.1% TFA. Samples were dried under vacuum (Speed Vac) and resuspended with 120 μL Chelex resin-treated water prior to analysis by mass spectrometry.

**Instrumentation**

LC/ESI/MS/MS analysis of oxidized amino acids and their precursors was performed using a triple quadruple mass spectrometer (ABI/Sciex 365, Applied Biosystems, Foster city, CA) equipped with Ionics (Concord, Ontario, Canada) EP 10+, EP XP, and HSID upgrades with electrospray ionization (ESI) needle connected to an Aria LX4 series multiplexed HPLC system with Flux pumps (Cohesive Technologies, Franklin, MA). The amino acid standards were separated over four matched Prodigy C18 columns (Phenomenex, 150 x 2.0 mm ID, 5 μm particle), each at a flow rate of 0.2 ml/min (Figure 4.2). Six oxidized tyrosine and phenylalanine species and the corresponding precursors were separated within a 16 minute time-frame (2- 18 minutes). The mobile phases used were 0.2% formic acid in water (solvent A) and 0.2% formic acid in acetonitrile (solvent B). The elution conditions were as follows: the column was first equilibrated with 100% A (0% B), held for 2 min at 100% A (0% B) immediately after the injection, then a linear gradient was run from 100% A (0% B) to 82% A (18% B) over 18 min, the linear gradient was then run from 82% A (18% B) to 20% A (80% B) over the next 2 min. The gradient was held at 80% B for 4 min and immediately cycled back to 100% A (0% B) for 12 minutes.

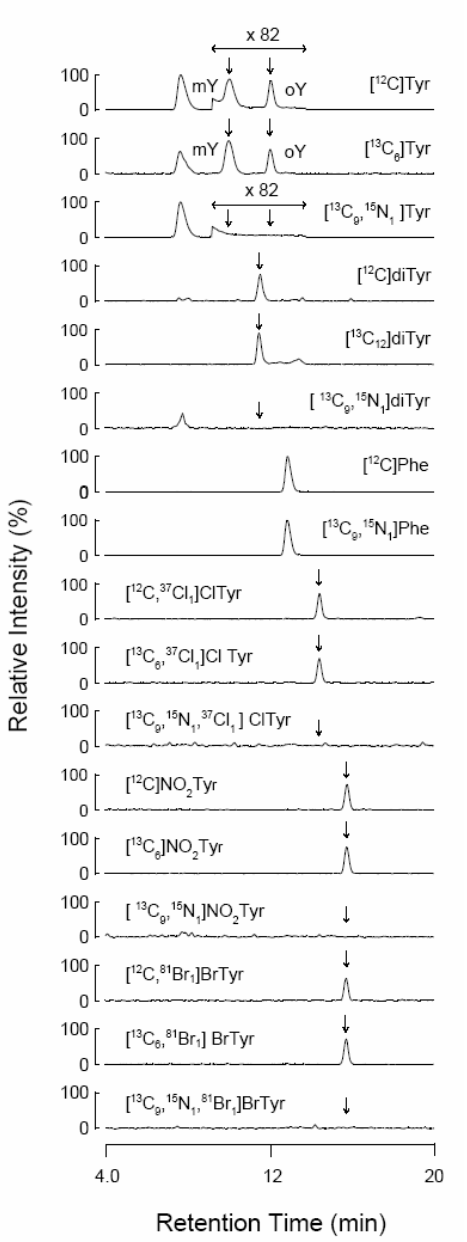


**Figure 4. 2 Topical Chromatograms of Oxidized Tyrosine Species Obtained with Pure Standard Solutions by LC-MS/MS**

Six oxidized tyrosine species and two precursors, the corresponding [$^{13}C_6$] labeled internal standard and the universally labeled precursors (i.e. all carbons $^{13}C$, all nitrogen $^{15}N$), were spiked into 20 µl HPLC grade water and processed as described in the methods. Natural abundance oxidized tyrosine species and the precursors were identified

by reverse phase HPLC coupled to tandem mass spectrometry in positive mode. The retention times of Tyr, *m*-Tyr, diTyr, *o*-Tyr, Phe, ClTyr, $NO_2$Tyr and BrTyr were 7.5, 9.8, 11.2, 11.7, 12.7, 14.2, 15.6 and 16.2 minutes respectively. Each natural abundance oxidized tyrosine (arrow), the universally labeled artifact indicator (arrow) were identified by the corresponding [$^{13}C_6$] labeled internal standard which posing exact retention time and unique parent-daughter transition. As shown in the figure, no universally labeled artifacts were detected in hydrolysated standard solution.

The mass spectrometer was operated in positive ionization mode. The positively charged molecules were selected by mass, and focused in the collision chamber containing nitrogen gas. Each distinct parent-daughter ion transition was detected by an on-line triple quadruple analyzer. The multiple-reaction monitoring (MRM) transitions, the mass-charge ratio (m/z) for the molecular cation $[MH]^+$ precursor and the corresponding product ions, used to detect the amino acid standards and their corresponding isotopomers were listed in Table 4.1.

Instrument parameters were programmed for the ABI/Sciex API 365 with Ionics EP 10+, EP XT collision cell upgrade and Hot Source-Induced Desolvation (HSID) interface operated in the positive ionization mode. The ion spray needle was maintained at 4000 volts. The turbo gas temperature was set at 500 °C. Ultra pure nitrogen was used as the nebulizer gas (NEB, 15), curtain gas (CUR, 12) and collisionally activated dissociation gas (CAD, 3). The Hot Source-Induced Desolvation (HSID) module was set to 300$^{o}$C. The peak width at the half-height (mass resolution) was set to one mass unit for both Q1 and Q3. Other parameters were set as follows: declustering potential (DP), 13 V; focusing potential (FP) 20; prefilter (ST) –18; focusing lens 1 (IQ1) –10.6; collision energy (CE), 20; entrance potential (EP), 10; collision cell exit potential (CXP), 15. The dwell time of each MRM pair was set at 0.1 sec with a 5 msec pause. The electronic multiplier detector was set at 2500 volts with the repeller at –250 volts.

**Table 4. 1 Parent →Daughter Transition of Analytes**

**(Positive Ionization Mode)**

| Natural Abundance | Parent Ion (m/z) | Daughter Ion (m/z) |
|---|---|---|
| [$^{12}$C] Phe | 166.0 | 120.0 |
| m-[$^{12}$C] Tyr | 182.1 | 136.1 |
| o-[$^{12}$C] Tyr | 182.1 | 136.1 |
| [$^{12}$C] Tyr | 182.1 | 136.1 |
| [$^{12}$C] BrTyr | 260.1 [$^{79}$Br]; 262.0 [$^{81}$Br] | 214.0 [$^{79}$Br]; 216.0 [$^{81}$Br] |
| [$^{12}$C] ClTyr | 216.0 [$^{35}$Cl]; 218.0 [$^{37}$Cl] | 170.1 [$^{35}$Cl]; 172.0 [$^{37}$Cl] |
| [$^{12}$C] $NO_2$Tyr | 227.1 | 181.1 |
| [$^{12}$C] diTyr | 361.1 | 315.1 |
| Internal Standard | Parent Ion (m/z) | Daughter Ion (m/z) |
| [$^{13}C_9$,$^{15}N_1$] Phe | 176.0 | 129.0 |
| m-[$^{13}C_6$] Tyr | 188.0 | 142.0 |
| o-[$^{13}C_6$] Tyr | 188.0 | 142.0 |
| [$^{13}C_9$,$^{15}N_1$] Tyr | 192.0 | 145.0 |
| [$^{13}C_6$] BrTyr | 266.1 [$^{79}$Br]; 268.0 [$^{81}$Br] | 220.0 [$^{79}$Br]; 222.0 [$^{81}$Br] |
| [$^{13}C_6$] ClTyr | 222.0 [$^{35}$Cl]; 224.0 [$^{37}$Cl] | 176.0 [$^{35}$Cl]; 178.0 [$^{37}$Cl] |
| [$^{13}C_6$] $NO_2$Tyr | 233.0 | 187.0 |
| [$^{13}C_{12}$] diTyr | 373.0 | 327.0 |
| Artifact Indicator | Parent Ion (m/z) | Daughter Ion (m/z) |
| m-[$^{13}C_9$,$^{15}N_1$] Tyr | 192.0 | 145.0 |
| o-[$^{13}C_9$,$^{15}N_1$] Tyr | 192.0 | 145.0 |
| [$^{13}C_9$,$^{15}N_1$] BrTyr | 270.1 [$^{79}$Br]; 272.0 [$^{81}$Br] | 223.0 [$^{79}$Br]; 225.0 [$^{81}$Br] |
| [$^{13}C_9$,$^{15}N_1$] ClTyr | 226.0 [$^{35}$Cl]; 228.0 [$^{37}$Cl] | 179.0 [$^{35}$Cl]; 181.0 [$^{37}$Cl] |
| [$^{13}C_9$,$^{15}N_1$] $NO_2$Tyr | 237.0 | 190.0 |
| [$^{13}C_9$,$^{15}N_1$] diTyr | 371.0 | 324.0 |

### Statistical Analysis

Statistical analyses were performed using SPSS version 11.0. Data are presented as mean ± SD. Comparisons between groups were performed using two-tailed unpaired Student's t tests with significance determined by $p < 0.05$. Spearmen-rank correlation coefficients were used to assess associations between oxidized amino acid species.

## 4.3 Results

### MS-MS Spectral Analysis of Tyrosine Species

The Q1 scan ESI/ MS analysis of all natural abundance oxidized tyrosine species and their corresponding isotopomers was performed to confirm the purity and isotopic pattern of the sample. Two approximately equally abundant ions with mass-charge ratios at 260 and 262 were detected in the 3-Bromotyrosine spectrum. The mass-charge ratio represents the protonated molecular ion $[M+H]^+$. This isotopic pattern confirms the presence of bromine ($^{79}Br$: $^{81}Br$; 49:51). Similarly, the presence of chlorine ($^{35}Cl$: $^{37}Cl$; 3:1) in 3-Chlorotyrosine was validated by the presence of two ions at m/z 216 and 218 with the relative intensity of 3 to 1 respectively (data not shown). Multiple reaction monitoring (MRM) mode was used to increase specificity. The MRM transitions were monitored for each natural abundance analyte, the corresponding isotopic internal standard and universally labeled artifact. The loss of ammonia ($NH_3$) from molecular ion yields a product ion with m/z at [M +H-17]. The m/z ratios of parent-daughter transitions of natural abundance analytes, isotope internal standards and artifact indicators are summarized in Table 4.1. Naturally abundant dihalogenated tyrosine species (3, 5-di-Bromotryosine and 3, 5-di-Chlorotryosine) and their corresponding heavy isotope labeled isotopomers were synthesized. The corresponding parent-daughter transition of each

dihalogenated tyrosine is summarized in table 4.2. Using current HPLC condition, all of the dihalogenated tyrosine species have distinct retention times and do not interfere with the detection of mono-halogenated tyrosine and other oxidized tyrosine species.

**Solid-Phase Extraction (SPE) Efficiency**

The SPE extraction efficiencies of oxidized tyrosine species including Bromotyrosine, Chlorotyrosine, dityrosine, meta-tyrosine, ortho-tyrosine and nitrotyrosine, were evaluated by comparing peak areas of extracted analytes to those of neat standards. The SPE recovery of each analyte was calculated from three independence experiments. As shown in Table 4.3 A, the extraction efficiency of most of oxidized tyrosine was larger than 85% except meta-tyrosine and ortho-tyrosine. The low recovery of ortho-tyrosine and meta-tyrosine was compensated by the loss of corresponding isotope internal standard. Thus, the low recovery of meta-tyrosine and ortho-tyrosine had no impact on the linearity of the corresponding standard curve.

**Linear Calibration Range and Limits of Detection**

The seven-point standard curve was sequentially diluted from a primary cocktail solution that contains natural abundance oxidized tyrosine species and their precursors, tyrosine and phenylalaine. All natural abundance oxidized tyrosine species were identified and quantified by the corresponding [$^{13}C_6$] ring labeled isotopomer by LC/MS/MS. The isotope internal standard cocktail which contained known amounts of L-[$^{13}C_{9,}$ $^{15}N_1$] labeled tyrosine (4 nmol), phenylalanine (4 nmol) and of [$^{13}C_6$] ring labeled oxidized tyrosine species (20 pmol) was added into solutions containing varying amounts of natural abundance tyrosine, phenylalanine and oxidized tyrosine species. The analytes and corresponding internal standards were processed and purified as unknown samples.

Peak areas of analyte and the corresponding internal standard were integrated by using the Analyst Software (Version 1.4) provided by PE Sciex. The calibration curve was determined from peak area ratio vs. concentration ratio using linear regression. The calibration curves for the amino acids are shown in figure 3. The correlation coefficient (r) of each oxidized tyrosine species ranged from 0.995 to 0.999.

The limit of detection (LOD) of each oxidized tyrosine was achieved by injecting a known amount of standard solution with a signal to noise ratio larger than 5. For each analyte, the limit of detection (LOD) and limit of quantitation (LOQ) was listed in Table 4.3 A.

**Reproducibility and Accuracy**

To determine the accuracy and precision of this assay, known amount of natural abundance tyrosine, phenylalanine and oxidized tyrosine species at three concentrations (low, medium and high) in triplicates were spiked with isotope internal standard cocktail and processed with calibration curves. Back-calculated concentrations of these samples were used for determine of accuracy and precision. The accuracy of the method was measured by relative error (RE%=100x Mean/Nominal) and precision was determined by the coefficient of variation (CV%=100x standard deviation/ Mean). The precision values of six oxidized tyrosine species were range from 0.0 to 8.48%. The accuracy values of all analytes were range from -13.8 to 6.73% (detail in Table 4.3A). The ratio of oxidized tyrosine and its corresponding precursors were also calculated. The precision values of oxidized tyrosine/precursor were range from 0.986% to 10.7% and the accuracy values from -4.79 to 10.2% (details in Table 4.3 B).

**Table 4. 2 Parent →Daughter Transition of Dihalogenated Tyrosines**

**(Positive Ionization Mode)**

| Natural Abundance | Parent Ion (m/z) | Daughter Ion (m/z) |
|---|---|---|
| [$^{12}$C] $Br_2$Tyr | 337.5 [$^{79}$Br, $^{79}$Br] | 291.9 [$^{79}$Br, $^{79}$Br] |
| | 339.7 [$^{79}$Br, $^{81}$Br] | 294.2 [$^{79}$Br, $^{81}$Br] |
| | 341.7 [$^{81}$Br, $^{81}$Br] | 295.8 [$^{81}$Br, $^{81}$Br] |
| [$^{12}$C] $Cl_2$Tyr | 249.9 [$^{35}$Cl, $^{35}$Cl] | 203.8 [$^{35}$Cl, $^{35}$Cl] |
| | 251.8 [$^{35}$Cl, $^{37}$Cl] | 205.8 [$^{35}$Cl, $^{37}$Cl] |
| **Internal Standard** | **Parent Ion (m/z)** | **Daughter Ion (m/z)** |
| [$^{13}C_6$] $Br_2$Tyr | 343.7 [$^{79}$Br, $^{79}$Br] | 297.8 [$^{79}$Br, $^{79}$Br] |
| | 345.7 [$^{79}$Br, $^{81}$Br] | 299.8 [$^{79}$Br, $^{81}$Br] |
| | 347.6 [$^{81}$Br, $^{81}$Br] | 301.7 [$^{81}$Br, $^{81}$Br] |
| [$^{13}C_6$] $Cl_2$Tyr | 255.8 [$^{35}$Cl, $^{35}$Cl] | 209.9 [$^{35}$Cl, $^{35}$Cl] |
| | 257.9 [$^{35}$Cl, $^{37}$Cl] | 211.8 [$^{35}$Cl, $^{37}$Cl] |
| **Artifact Indicator** | **Parent Ion (m/z)** | **Daughter Ion (m/z)** |
| [$^{13}C_9$,$^{15}N_1$] $Br_2$Tyr | 348.0 [$^{79}$Br, $^{79}$Br] | 301.1 [$^{79}$Br, $^{79}$Br] |
| | 350.0 [$^{79}$Br, $^{81}$Br] | 303.3 [$^{79}$Br, $^{81}$Br] |
| | 351.6 [$^{81}$Br, $^{81}$Br] | 305.0 [$^{81}$Br, $^{81}$Br] |
| [$^{13}C_9$,$^{15}N_1$] $Cl_2$ Tyr | 260.4 [$^{35}$Cl, $^{35}$Cl] | 212.9 [$^{35}$Cl, $^{35}$Cl] |
| | 262.0 [$^{35}$Cl, $^{37}$Cl] | 215.1 [$^{35}$Cl, $^{37}$Cl] |

**Table 4. 3 Summary of Method Development**

A

| | | BrY | ClY | *di*Y | m-Y | o-Y | $NO_2$Y |
|---|---|---|---|---|---|---|---|
| LOD (pg) | | 2.46 | 8.62 | 14.4 | 3.62 | 1.81 | 1.13 |
| LOQ (pg) | | 416 | 345 | 576 | 290 | 290 | 362 |
| Recovery | | 92.5 | 85.7 | 91.2 | 35.5 | 34.0 | 86.1 |
| Precision (CV%) | Low | 2.94 | 5.33 | 6.77 | 2.10 | 2.62 | 0.00 |
| | Med | 3.28 | 5.74 | 8.48 | 1.97 | 1.15 | 6.62 |
| | High | 1.68 | 5.12 | 2.98 | 3.02 | 5.90 | 1.95 |
| Accuracy (RE%) | Low | 89.5 | 95.7 | 94.5 | 92.8 | 94.7 | 90.1 |
| | Med | 100 | 107 | 107 | 101 | 102 | 98.5 |
| | High | 97.7 | 104 | 91.5 | 99.7 | 101 | 96.8 |

B

| | | BrY/Y | ClY/Y | *di*Y/Y | m-Y/F | o-Y/F | $NO_2$Y/Y |
|---|---|---|---|---|---|---|---|
| Precision (CV%) | Low | 2.90 | 3.23 | 4.95 | 4.81 | 4.43 | 4.92 |
| | Med | 4.03 | 5.18 | 10.7 | 1.54 | 0.986 | 9.10 |
| | High | 6.16 | 2.24 | 1.77 | 2.88 | 10.2 | 6.12 |
| Accuracy (RE%) | Low | 97.1 | 104 | 102 | 108 | 110 | 97.9 |
| | Med | 97.8 | 104 | 104 | 102 | 103 | 96.4 |
| | High | 102 | 108 | 95.2 | 98.6 | 100 | 101 |

LOD: Limit of Detection, LOQ Limit of Quantitation The SPE recovery of each analyte was calculated from three independence experiments.

CV (%) = (Standard deviation/mean) x 100

RE (%) = (Mean/Nominal Concentration) x 100

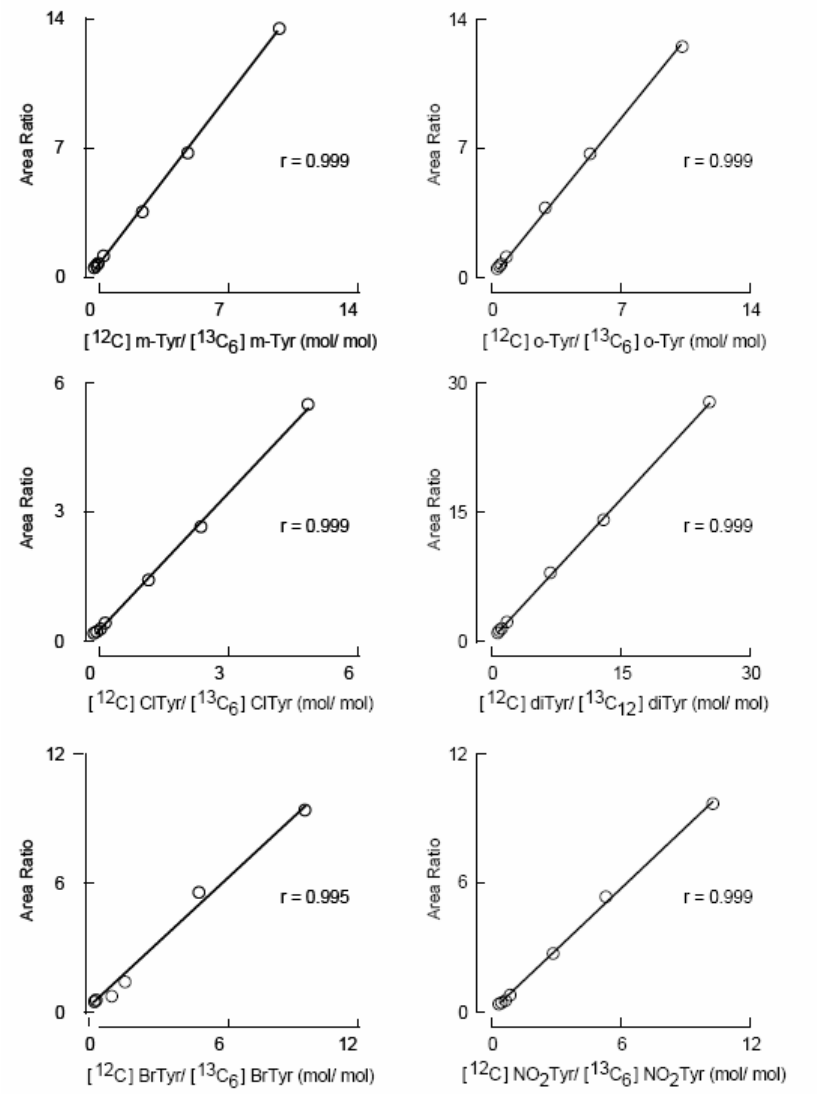


**Figure 4. 3 Calibration Curves of Oxidized Tyrosine Species.**

The standard curve of each oxidized tyrosine was generated by incorporation of the fixed amount of internal standard and varying levels of the corresponding analyte. The resulting standard solutions were processed and analyzed by LC-MS/MS. Each standard curve was plotted as peak area ratio versus mol ratio for each analyte. The linear regression analysis of graphs revealed r values of 0.999, 0.999, 0.999, 0.999, 0.995, and 0.999 for *m*-Tyr, *o*-Tyr, Cl Tyr, diTyr, Br Tyr and $NO_2$ Tyr respectively. Data points represent the mean of triplicate determinations.

**Quantification of Protein-bound Oxidized Tyrosine Species in Human Serum**

The normal ranges of each oxidized tyrosine species in human serum was determined by analysis of blood collected from 140 healthy volunteers. The typical chromatograms of a serum sample are depicted in figure 4.4. The natural abundance tyrosine species were identified and quantified in relation to their corresponding ring-labeled isotope internal standard. As demonstrated in figure 4.4, there were no detectable artifacts, which possess the anticipated m/z transitions for the corresponding universally labeled oxidized amino acid. The amount of protein-bound oxidized tyrosine species was normalized to its corresponding precursor, tyrosine and phenylalanine respectively. The level of each species in healthy subjects is presented in figure 4.5. A strong correlation was found between the *m*-Tyr/Phe and *o*-Tyr/Phe ratios ($R= 0.57$, $p<0.001$). Moderate correlations were found between levels of chlorotyrosine with nitrotyrosine ($R=0.366$, $p<0.001$), bromotyrosine ($R= 0.207$, $p< 0.05$), *o*-tyrosine ($R=0.203$, $p<0.05$) and *m*-tyrosine ($R=0.262$, $p<0.005$) and between levels of bromotyrosine and nitrotyrosine ($R= 0.219$, $p< 0.01$). (Table 4.4)

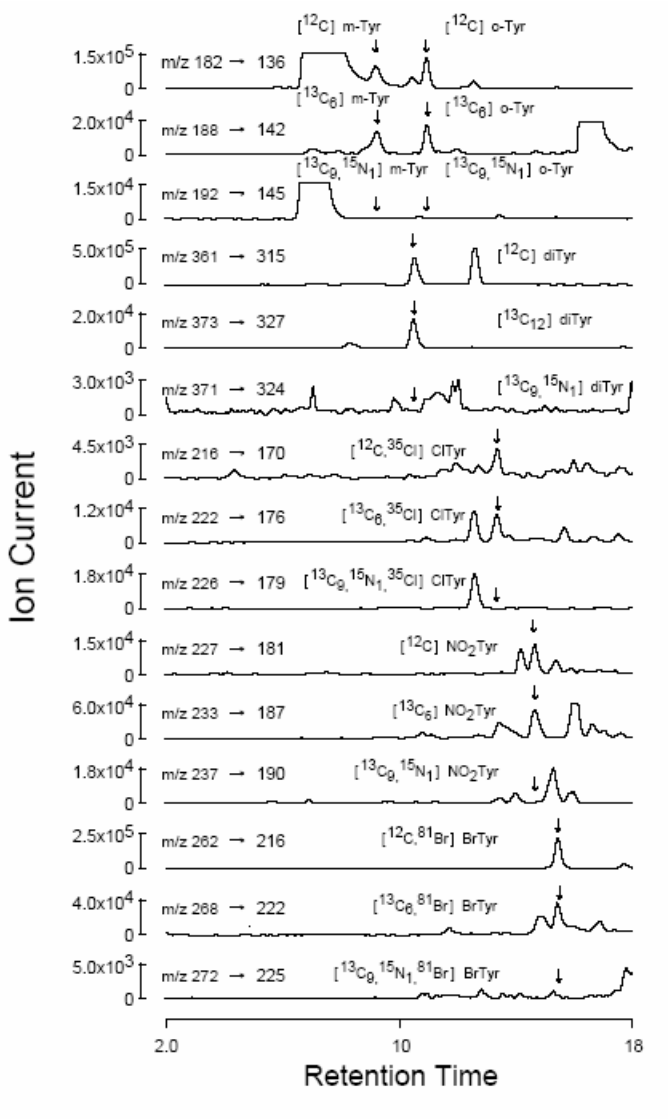


**Figure 4. 4 LC- MS/MS Detection of Oxidized Tyrosine Species in Human Serum**

Human serum (20 μL) was processed as described in the methods. Each natural abundance oxidized tyrosine was detected and quantified by the corresponding stable isotope labeled internal standard. The typical chromatograph of each analyte and the corresponding characteristic MRM transitions was listed above. The retention time of Tyr, m-Tyr, o-Tyr, diTyr, ClTyr, $NO_2$Tyr and BrTyr were 6.1, 9.1, 11.4, 10.5, 13.2, 14.5 and 15.2 minutes respectively.

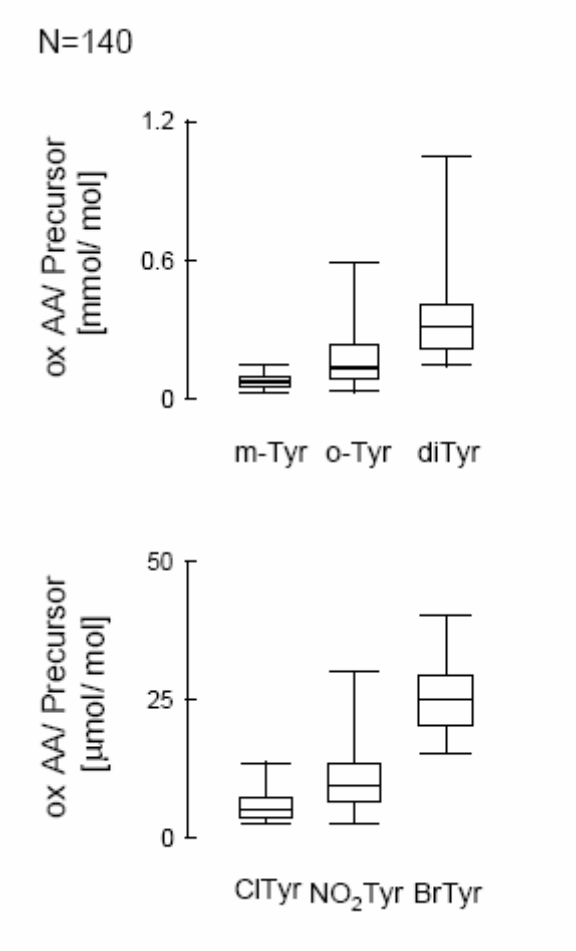


**Figure 4. 5 Serum Levels of Oxidized Tyrosine in Healthy Volunteers.**

140 serum samples from healthy volunteers were analyzed by LC-MS/MS. The result of each oxidized amino acid was normalized to the amount of its corresponding precursor. In the box plots, the lower boundary indicates the 25$^{th}$ percentile, the line within the box marks the median, and upper boundary of the box indicates the 75$^{th}$ percentile. Error bars above and below the box indicate 95$^{th}$ and 5$^{th}$ percentile.

**Table 4. 4 Spearman Correlations Among Oxidized Tyrosine Species**

| N=140 | o-Tyr/ Phe | m-Tyr/ Phe | $NO_2$Tyr/ Tyr | BrTyr/ Tyr | ClTyr/ Tyr | diTyr/ Tyr |
|---|---|---|---|---|---|---|
| o-Tyr/ Phe | 1.000 | 0.570 **** | 0.097 | 0.002 | 0.203 * | 0.047 |
| m-Tyr/ Phe | | 1.000 | 0.016 | -0.003 | 0.262 ** | 0.061 |
| $NO_2$Tyr/ Tyr | | | 1.000 | 0.219 ** | 0.366 **** | 0.031 |
| BrTyr/ Tyr | | | | 1.000 | 0.207 * | 0.140 |
| ClTyr/ Tyr | | | | | 1.000 | 0.049 |
| diTyr/ Tyr | | | | | | 1.000 |

In 140 healthy volunteer, the serum level of oxidation markers was studied to further explore the underlining mechanism of oxidation in vivo. * $p<0.05$, ** $p<0.01$, *** $p<0.005$ and **** $p<0.001$.

**Quantification of Oxidized Tyrosine Species in Guinea Pig Lung Tissue**

As thiocyanate ($SCN^-$) is a preferred substrate for EPO, it is possible that increased systemic level of $SCN^-$ following dietary supplementation may result in preferential oxidation of $SCN^-$ in comparison with halide species including $Br^-$ and $Cl^-$. To test this hypothesis, the effect of dietary $SCN^-$ supplementation on an aeroallergen challenge model of asthma in age- and sex- matched Hartley guinea pigs was determined. In animals fed normal chow, lung levels of 3-BrTyr increased following challenge with OVA, in comparison with normal saline. This further supports the notion that aerosol exposure with OVA is associated with enhanced bromination in lung tissue. However, the allergen induced increment of bromination was completely abrogated by dietary supplementation with $SCN^-$ prior to OVA challenge. This result suggests that dietary supplementation with $SCN^-$ enriched food may afford relief from oxidative injury of lung and airway proteins during the asthmatic response. (Figure 4.6)

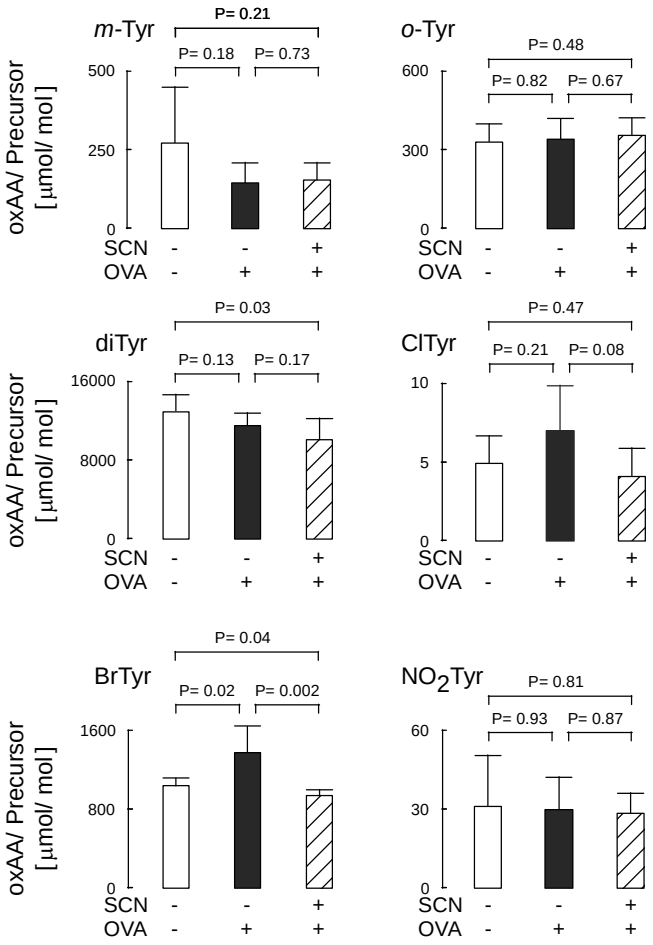


**Figure 4. 6 Comparison of the Levels of Oxidized Tyrosine Species in OVA Challenged Model**

Hartley guinea pigs were fed a normal diet ($SCN^-$, n=11) or thiocyanate enriched diet ($SCN^-$, n=6). The animals on normal diet were sensitized with ovalbumin ($SCN^-$, OVA+, n=6) or normal saline ($SCN^-$, OVA-, n=5) on days 0 and 14, then challenged later on day 21 with aerosolized either OVA or normal saline. OVA challenge were also performed on the animal with thiocyanate enriched diet ($SCN^-$, OVA+, n=6). 48 hours after the challenge, lungs were harvested and preserved. The oxidized tyrosine species and their precursors were quantified by LC/MS/MS. The result of each oxidized amino acid was normalized to the amount of the corresponding precursor. Values represent mean ± SD.

## 4.4 Discussion

As evidence accumulates supporting a pivotal role for oxidized tyrosine species in the pathogenesis of a wide range of disease processes, it has become important to develop accurate analytical methods to quantify the levels of these products *in vivo*. The generation of oxidized tyrosine species has been implicated in the development of atherosclerotic plaque, asthma and breast cancer. In addition, it has been demonstrated that protein-bound levels of nitrotyrosine decline in response to statin therapy. These molecular fingerprints have the potential to be developed as a marker of disease risk and activity. In order to be a useful clinical biomarker it is necessary to develop accurate analytical methods that can rapidly and reproducibly quantify levels in a range of biological matrices. The use of the bench top triple quadrupole LC/MS/MS method described in this report fulfills these criteria.

The method can be subject to modification depending on the clinical scenario. Biological matrices containing high levels of endogenous nitrite/nitrate, such as salivary fluid and endobronchial aspirates, often require additional desalting steps. In addition, different methods for protein hydrolysis can be used, depending on the oxidized species of interest. As the described method aims to measure levels of multiple oxidized species simultaneously, methanesulfonic acid is typically used. In contrast, when it is unnecessary to measure chlorotyrosine levels, acid hydrolysis is often performed using hydrochloric acid. Similarly, the total monitored precursor-product transitions can be adjusted to fulfill the requirement of sensitivity and specificity. When using different biological matrices, protein concentration and extraction procedure should be re-evaluated to eliminate *ex vivo* artifacts generation prior to proceeding with sample assays.

The CVs of QC samples (oxidized tyrosine/precursor, three concentrations in triplicates) were ranged from 0.986 to 10.7%. To determine the coefficient of variations of real samples, five replicates of two human serum samples were also processed and the CV of protein-bound of bromotyrosine, chlorotyrosine, dityrosine, meta-tyrosine, ortho-tyrosine and nitrotyrosine were range from 11 to 22%, 25 to 30%, 22 to 33%, 13 to 18%, 14 to 18%, and 29 to 30%. The high variations of protein-bound of oxidized tyrosine species may reflect the complex of oxidized tyrosine residue in sample and the variation of protein recovery during desalting and delipidation step.

This analytical method can be particularly useful because it can be applied to a large number of samples simultaneously. Furthermore, it demonstrates a high sensitivity and specificity for the detection and quantification of a number of oxidized species at the same time. The low limit of detection of standard samples is consistent with previous reports of assays using triple quadrupole systems. Incorporation of heavy isotope labeled internal standards that assist in the detection of artifactual generation of oxidized products *ex vivo* during sample preparation is a key component of this assay. Using these standards, we have found that the degree of artifactual oxidation is minimal. In the rare event that the level of artifactual species exceeded 5% of the total level detected, we repeated the sample preparative step with a more exhaustive desalting step. In certain circumstances it is necessary to modify the sample preparation to eliminate intra-preparative artifacts generation. In patients receiving nitrate therapy in the setting of acute coronary syndromes, an extra desalting step is often required to remove the excess nitrate when assaying nitrotyrosine levels.

The ability to determine levels of multiple oxidized markers in biological samples expands our understanding of the role of particular oxidative pathways in the pathogenesis of a range of disease processes. The correlations between individual oxidized species, demonstrated in the serum of healthy volunteers, provides insight into the pathways that generate these species *in vivo*. The strong correlation between levels of m-tyrosine and o-tyrosine highlights the role of phenylalanine hydroxylation. Similarly, correlations between the level of 3-ChloroTyrosine with both 3-NitroTyrosine and 3-BromoTyrosine, and between levels of 3-BromoTyrosine and 3-NitroTyrosine, are consistent with *in vivo* activity of myeloperoxidase and eosinophil peroxidase respectively. These relationships provide chemical evidence that pathways induced by leukocyte activation contribute to the generation of oxidative stress *in vivo*. The current study adds further support for the notion that bromination, catalyzed by the leukocyte derived enzyme eosinophil peroxidase, is enhanced in an animal model of aeroallergen challenged asthma. In addition, elevated peripheral $SCN^-$ from dietary supplement partially inhibits EPO catalyzed protein bromination *in vivo*. Increase systemic level of $SCN^-$ may become a potential strategy for therapeutic intervention of EPO induced oxidative modification.

In summary, the current report describes the development of an analytical method using a bench top triple quadrupole LC/MS/MS system that reliably detects and quantifies oxidized tyrosine species and their precursors in a wide range of biological matrices. This method avoids the need for chemical derivatization of samples and minimizes the possibility that artifactual generation of oxidation products may interfere with the detection of native levels. The evolution of bench top mass spectrometric systems allows for the ability to analyze multiple samples simultaneously. As a result, the

detection of levels of oxidized products in biological samples has provided further insights into the specific oxidative pathways that promote the pathogenesis of a wide variety of disease processes.

## 4.5 References:


1. The effect of vitamin E and beta carotene on the incidence of lung cancer and other cancers in male smokers. The Alpha-Tocopherol, Beta Carotene Cancer Prevention Study Group. N Engl J Med **1994,** 330, (15), 1029-35.
2. Greenberg, E. R.; Baron, J. A.; Tosteson, T. D.; Freeman, D. H., Jr.; Beck, G. J.; Bond, J. H.; Colacchio, T. A.; Coller, J. A.; Frankl, H. D.; Haile, R. W.; et al., A clinical trial of antioxidant vitamins to prevent colorectal adenoma. Polyp Prevention Study Group. N Engl J Med **1994,** 331, (3), 141-7.
3. Hunter, D. J.; Manson, J. E.; Colditz, G. A.; Stampfer, M. J.; Rosner, B.; Hennekens, C. H.; Speizer, F. E.; Willett, W. C., A prospective study of the intake of vitamins C, E, and A and the risk of breast cancer. N Engl J Med **1993,** 329, (4), 234-40.
4. MRC/BHF Heart Protection Study of antioxidant vitamin supplementation in 20,536 high-risk individuals: a randomised placebo-controlled trial. Lancet **2002,** 360, (9326), 23-33.
5. Brown, B. G.; Zhao, X. Q.; Chait, A.; Fisher, L. D.; Cheung, M. C.; Morse, J. S.; Dowdy, A. A.; Marino, E. K.; Bolson, E. L.; Alaupovic, P.; Frohlich, J.; Albers, J. J., Simvastatin and niacin, antioxidant vitamins, or the combination for the prevention of coronary disease. N Engl J Med **2001,** 345, (22), 1583-92.

6. Yusuf, S.; Dagenais, G.; Pogue, J.; Bosch, J.; Sleight, P., Vitamin E supplementation and cardiovascular events in high-risk patients. The Heart Outcomes Prevention Evaluation Study Investigators. N Engl J Med **2000,** 342, (3), 154-60.

7. Meagher, E. A.; Barry, O. P.; Lawson, J. A.; Rokach, J.; FitzGerald, G. A., Effects of vitamin E on lipid peroxidation in healthy persons. Jama **2001,** 285, (9), 1178-82.

8. Shishehbor, M. H.; Aviles, R. J.; Brennan, M. L.; Fu, X.; Goormastic, M.; Pearce, G. L.; Gokce, N.; Keaney, J. F., Jr.; Penn, M. S.; Sprecher, D. L.; Vita, J. A.; Hazen, S. L., Association of nitrotyrosine levels with cardiovascular disease and modulation by statin therapy. Jama **2003,** 289, (13), 1675-80.

9. Shishehbor, M. H.; Brennan, M. L.; Aviles, R. J.; Fu, X.; Penn, M. S.; Sprecher, D. L.; Hazen, S. L., Statins promote potent systemic antioxidant effects through specific inflammatory pathways. Circulation **2003,** 108, (4), 426-31.

10. Andreadis, A. A.; Hazen, S. L.; Comhair, S. A.; Erzurum, S. C., Oxidative and nitrosative events in asthma. Free Radic Biol Med **2003,** 35, (3), 213-25.

11. Moriel, P.; Abdalla, D. S., Nitrotyrosine bound to beta-VLDL-apoproteins: a biomarker of peroxynitrite formation in experimental atherosclerosis. Biochem Biophys Res Commun **1997,** 232, (2), 332-5.

12. Smith, M. A.; Richey Harris, P. L.; Sayre, L. M.; Beckman, J. S.; Perry, G., Widespread peroxynitrite-mediated damage in Alzheimer's disease. J Neurosci **1997,** 17, (8), 2653-7.

13. Tanaka, K.; Shirai, T.; Nagata, E.; Dembo, T.; Fukuuchi, Y., Immunohistochemical detection of nitrotyrosine in postischemic cerebral cortex in gerbil. Neurosci Lett **1997,** 235, (1-2), 85-8.

14. Beal, M. F., Oxidatively modified proteins in aging and disease. Free Radic Biol Med **2002,** 32, (9), 797-803.

15. Brennan, M. L.; Hazen, S. L., Amino acid and protein oxidation in cardiovascular disease. Amino Acids **2003,** 25, (3-4), 365-74.

16. Christen, Y., Oxidative stress and Alzheimer disease. Am J Clin Nutr **2000,** 71, (2), 621S-629S.

17. Drew, B.; Leeuwenburgh, C., Aging and the role of reactive nitrogen species. Ann N Y Acad Sci **2002,** 959, 66-81.

18. Stadtman, E. R., Protein oxidation in aging and age-related diseases. Ann N Y Acad Sci **2001,** 928, 22-38.

19. Comhair, S. A.; Ricci, K. S.; Arroliga, M.; Lara, A. R.; Dweik, R. A.; Song, W.; Hazen, S. L.; Bleecker, E. R.; Busse, W. W.; Chung, K. F.; Gaston, B.; Hastie, A.; Hew, M.; Jarjour, N.; Moore, W.; Peters, S.; Teague, W. G.; Wenzel, S. E.; Erzurum, S. C., Correlation of systemic superoxide dismutase deficiency to airflow obstruction in asthma. Am J Respir Crit Care Med **2005,** 172, (3), 306-13.

20. Hazen, S. L.; Heinecke, J. W., 3-Chlorotyrosine, a specific marker of myeloperoxidase-catalyzed oxidation, is markedly elevated in low density lipoprotein isolated from human atherosclerotic intima. J Clin Invest **1997,** 99, (9), 2075-81.

21. MacPherson, J. C.; Comhair, S. A.; Erzurum, S. C.; Klein, D. F.; Lipscomb, M. F.; Kavuru, M. S.; Samoszuk, M. K.; Hazen, S. L., Eosinophils are a major source of nitric oxide-derived oxidants in severe asthma: characterization of pathways available to eosinophils for generating reactive nitrogen species. J Immunol **2001,** 166, (9), 5763-72.

22. Wu, W.; Samoszuk, M. K.; Comhair, S. A.; Thomassen, M. J.; Farver, C. F.; Dweik, R. A.; Kavuru, M. S.; Erzurum, S. C.; Hazen, S. L., Eosinophils generate brominating oxidants in allergen-induced asthma. J Clin Invest **2000,** 105, (10), 1455-63.

23. Zheng, L.; Nukuna, B.; Brennan, M. L.; Sun, M.; Goormastic, M.; Settle, M.; Schmitt, D.; Fu, X.; Thomson, L.; Fox, P. L.; Ischiropoulos, H.; Smith, J. D.; Kinter, M.; Hazen, S. L., Apolipoprotein A-I is a selective target for myeloperoxidase-catalyzed oxidation and functional impairment in subjects with cardiovascular disease. J Clin Invest **2004,** 114, (4), 529-41.

24. Aldridge, R. E.; Chan, T.; van Dalen, C. J.; Senthilmohan, R.; Winn, M.; Venge, P.; Town, G. I.; Kettle, A. J., Eosinophil peroxidase produces hypobromous acid in the airways of stable asthmatics. Free Radic Biol Med **2002,** 33, (6), 847-56.

25. Frost, M. T.; Halliwell, B.; Moore, K. P., Analysis of free and protein-bound nitrotyrosine in human plasma by a gas chromatography/mass spectrometry method that avoids nitration artifacts. Biochem J **2000,** 345 Pt 3, 453-8.

26. Pennathur, S.; Jackson-Lewis, V.; Przedborski, S.; Heinecke, J. W., Mass spectrometric quantification of 3-nitrotyrosine, ortho-tyrosine, and o,o'-dityrosine in brain tissue of 1-methyl-4-phenyl-1,2,3, 6-tetrahydropyridine-treated mice, a

model of oxidative stress in Parkinson's disease. J Biol Chem **1999,** 274, (49), 34621-8.

27. Woods, A. A.; Linton, S. M.; Davies, M. J., Detection of HOCl-mediated protein oxidation products in the extracellular matrix of human atherosclerotic plaques. Biochem J **2003,** 370, (Pt 2), 729-35.

28. Pennathur, S.; Bergt, C.; Shao, B.; Byun, J.; Kassim, S. Y.; Singh, P.; Green, P. S.; McDonald, T. O.; Brunzell, J.; Chait, A.; Oram, J. F.; O'Brien, K.; Geary, R. L.; Heinecke, J. W., Human atherosclerotic intima and blood of patients with established coronary artery disease contain high density lipoprotein damaged by reactive nitrogen species. J Biol Chem **2004,** 279, (41), 42977-83.

29. Weiss, S. J.; Test, S. T.; Eckmann, C. M.; Roos, D.; Regiani, S., Brominating oxidants generated by human eosinophils. Science **1986,** 234, (4773), 200-3.

30. Hazen, S. L.; Hsu, F. F.; Mueller, D. M.; Crowley, J. R.; Heinecke, J. W., Human neutrophils employ chlorine gas as an oxidant during phagocytosis. J Clin Invest **1996,** 98, (6), 1283-9.

31. Brennan, M. L.; Wu, W.; Fu, X.; Shen, Z.; Song, W.; Frost, H.; Vadseth, C.; Narine, L.; Lenkiewicz, E.; Borchers, M. T.; Lusis, A. J.; Lee, J. J.; Lee, N. A.; Abu-Soud, H. M.; Ischiropoulos, H.; Hazen, S. L., A tale of two controversies: defining both the role of peroxidases in nitrotyrosine formation in vivo using eosinophil peroxidase and myeloperoxidase-deficient mice, and the nature of peroxidase-generated reactive nitrogen species. J Biol Chem **2002,** 277, (20), 17415-27.

32. Gaut, J. P.; Byun, J.; Tran, H. D.; Lauber, W. M.; Carroll, J. A.; Hotchkiss, R. S.; Belaaouaj, A.; Heinecke, J. W., Myeloperoxidase produces nitrating oxidants in vivo. J Clin Invest **2002,** 109, (10), 1311-9.

33. Baldus, S.; Eiserich, J. P.; Mani, A.; Castro, L.; Figueroa, M.; Chumley, P.; Ma, W.; Tousson, A.; White, C. R.; Bullard, D. C.; Brennan, M. L.; Lusis, A. J.; Moore, K. P.; Freeman, B. A., Endothelial transcytosis of myeloperoxidase confers specificity to vascular ECM proteins as targets of tyrosine nitration. J Clin Invest **2001,** 108, (12), 1759-70.

34. Denzler, K. L.; Borchers, M. T.; Crosby, J. R.; Cieslewicz, G.; Hines, E. M.; Justice, J. P.; Cormier, S. A.; Lindenberger, K. A.; Song, W.; Wu, W.; Hazen, S. L.; Gleich, G. J.; Lee, J. J.; Lee, N. A., Extensive eosinophil degranulation and peroxidase-mediated oxidation of airway proteins do not occur in a mouse ovalbumin-challenge model of pulmonary inflammation. J Immunol **2001,** 167, (3), 1672-82.

35. Beckman, J. S.; Beckman, T. W.; Chen, J.; Marshall, P. A.; Freeman, B. A., Apparent hydroxyl radical production by peroxynitrite: implications for endothelial injury from nitric oxide and superoxide. Proc Natl Acad Sci U S A **1990,** 87, (4), 1620-4.

36. Leeuwenburgh, C.; Rasmussen, J. E.; Hsu, F. F.; Mueller, D. M.; Pennathur, S.; Heinecke, J. W., Mass spectrometric quantification of markers for protein oxidation by tyrosyl radical, copper, and hydroxyl radical in low density lipoprotein isolated from human atherosclerotic plaques. J Biol Chem **1997,** 272, (6), 3520-6.

37. Dean, R. T.; Fu, S.; Stocker, R.; Davies, M. J., Biochemistry and pathology of radical-mediated protein oxidation. Biochem J **1997,** 324 (Pt 1), 1-18.

38. Podrez, E. A.; Febbraio, M.; Sheibani, N.; Schmitt, D.; Silverstein, R. L.; Hajjar, D. P.; Cohen, P. A.; Frazier, W. A.; Hoff, H. F.; Hazen, S. L., Macrophage scavenger receptor CD36 is the major receptor for LDL modified by monocyte-generated reactive nitrogen species. J Clin Invest **2000,** 105, (8), 1095-108.

39. Podrez, E. A.; Poliakov, E.; Shen, Z.; Zhang, R.; Deng, Y.; Sun, M.; Finton, P. J.; Shan, L.; Febbraio, M.; Hajjar, D. P.; Silverstein, R. L.; Hoff, H. F.; Salomon, R. G.; Hazen, S. L., A novel family of atherogenic oxidized phospholipids promotes macrophage foam cell formation via the scavenger receptor CD36 and is enriched in atherosclerotic lesions. J Biol Chem **2002,** 277, (41), 38517-23.

40. Podrez, E. A.; Poliakov, E.; Shen, Z.; Zhang, R.; Deng, Y.; Sun, M.; Finton, P. J.; Shan, L.; Gugiu, B.; Fox, P. L.; Hoff, H. F.; Salomon, R. G.; Hazen, S. L., Identification of a novel family of oxidized phospholipids that serve as ligands for the macrophage scavenger receptor CD36. J Biol Chem **2002,** 277, (41), 38503-16.

41. Podrez, E. A.; Schmitt, D.; Hoff, H. F.; Hazen, S. L., Myeloperoxidase-generated reactive nitrogen species convert LDL into an atherogenic form in vitro. J Clin Invest **1999,** 103, (11), 1547-60.

42. Samoszu, M.; Brennan, M. L.; To, V.; Leonor, L.; Zheng, L.; Fu, X.; Hazen, S. L., Association between nitrotyrosine levels and microvascular density in human breast cancer. Breast Cancer Res Treat **2002,** 74, (3), 271-8.

43. Mita, H.; Higashi, N.; Taniguchi, M.; Higashi, A.; Kawagishi, Y.; Akiyama, K., Urinary 3-bromotyrosine and 3-chlorotyrosine concentrations in asthmatic patients:

lack of increase in 3-bromotyrosine concentration in urine and plasma proteins in aspirin-induced asthma after intravenous aspirin challenge. Clin Exp Allergy **2004,** 34, (6), 931-8.

44. Lamb, N. J.; Gutteridge, J. M.; Baker, C.; Evans, T. W.; Quinlan, G. J., Oxidative damage to proteins of bronchoalveolar lavage fluid in patients with acute respiratory distress syndrome: evidence for neutrophil-mediated hydroxylation, nitration, and chlorination. Crit Care Med **1999,** 27, (9), 1738-44.

45. Leeuwenburgh, C.; Hansen, P. A.; Holloszy, J. O.; Heinecke, J. W., Hydroxyl radical generation during exercise increases mitochondrial protein oxidation and levels of urinary dityrosine. Free Radic Biol Med **1999,** 27, (1-2), 186-92.

46. Viera, L.; Ye, Y. Z.; Estevez, A. G.; Beckman, J. S., Immunohistochemical methods to detect nitrotyrosine. Methods Enzymol **1999,** 301, 373-81.

47. Inoue, H.; Hisamatsu, K.; Ando, K.; Ajisaka, R.; Kumagai, N., Determination of nitrotyrosine and related compounds in biological specimens by competitive enzyme immunoassay. Nitric Oxide **2002,** 7, (1), 11-7.

48. Kato, Y.; Wu, X.; Naito, M.; Nomura, H.; Kitamoto, N.; Osawa, T., Immunochemical detection of protein dityrosine in atherosclerotic lesion of apo-E-deficient mice using a novel monoclonal antibody. Biochem Biophys Res Commun **2000,** 275, (1), 11-5.

49. Beckmann, J. S.; Ye, Y. Z.; Anderson, P. G.; Chen, J.; Accavitti, M. A.; Tarpey, M. M.; White, C. R., Extensive nitration of protein tyrosines in human atherosclerosis detected by immunohistochemistry. Biol Chem Hoppe Seyler **1994,** 375, (2), 81-8.

50. Khan, J.; Brennand, D. M.; Bradley, N.; Gao, B.; Bruckdorfer, R.; Jacobs, M.; Brennan, D. M., 3-Nitrotyrosine in the proteins of human plasma determined by an ELISA method. Biochem J **1998,** 330 (Pt 2), 795-801.

51. Schwedhelm, E.; Tsikas, D.; Gutzki, F. M.; Frolich, J. C., Gas chromatographic-tandem mass spectrometric quantification of free 3-nitrotyrosine in human plasma at the basal state. Anal Biochem **1999,** 276, (2), 195-203.

52. Ishida, N.; Hasegawa, T.; Mukai, K.; Watanabe, M.; Nishino, H., Determination of nitrotyrosine by HPLC-ECD and its application. J Vet Med Sci **2002,** 64, (5), 401-4.

53. Ohshima, H.; Gilibert, I.; Bianchini, F., Induction of DNA strand breakage and base oxidation by nitroxyl anion through hydroxyl radical production. Free Radic Biol Med **1999,** 26, (9-10), 1305-13.

54. Crowley, J. R.; Yarasheski, K.; Leeuwenburgh, C.; Turk, J.; Heinecke, J. W., Isotope dilution mass spectrometric quantification of 3-nitrotyrosine in proteins and tissues is facilitated by reduction to 3-aminotyrosine. Anal Biochem **1998,** 259, (1), 127-35.

55. Guo, W.; Adachi, T.; Matsui, R.; Xu, S.; Jiang, B.; Zou, M. H.; Kirber, M.; Lieberthal, W.; Cohen, R. A., Quantitative assessment of tyrosine nitration of manganese superoxide dismutase in angiotensin II-infused rat kidney. Am J Physiol Heart Circ Physiol **2003,** 285, (4), H1396-403.

56. Kaur, H.; Lyras, L.; Jenner, P.; Halliwell, B., Artefacts in HPLC detection of 3-nitrotyrosine in human brain tissue. J Neurochem **1998,** 70, (5), 2220-3.

57. Hazen, S. L.; Crowley, J. R.; Mueller, D. M.; Heinecke, J. W., Mass spectrometric quantification of 3-chlorotyrosine in human tissues with attomole sensitivity: a sensitive and specific marker for myeloperoxidase-catalyzed chlorination at sites of inflammation. Free Radic Biol Med **1997,** 23, (6), 909-16.

58. Shishehbor, M. H.; Hazen, S. L., Inflammatory and oxidative markers in atherosclerosis: relationship to outcome. Curr Atheroscler Rep **2004,** 6, (3), 243-50.

59. Wu, W.; Chen, Y.; Hazen, S. L., Eosinophil peroxidase nitrates protein tyrosyl residues. Implications for oxidative damage by nitrating intermediates in eosinophilic inflammatory disorders. J Biol Chem **1999,** 274, (36), 25933-44.

60. Hazen, S. L.; Zhang, R.; Shen, Z.; Wu, W.; Podrez, E. A.; MacPherson, J. C.; Schmitt, D.; Mitra, S. N.; Mukhopadhyay, C.; Chen, Y.; Cohen, P. A.; Hoff, H. F.; Abu-Soud, H. M., Formation of nitric oxide-derived oxidants by myeloperoxidase in monocytes: pathways for monocyte-mediated protein nitration and lipid peroxidation In vivo. Circ Res **1999,** 85, (10), 950-8.

61. Wu, W.; Chen, Y.; d'Avignon, A.; Hazen, S. L., 3-Bromotyrosine and 3,5-dibromotyrosine are major products of protein oxidation by eosinophil peroxidase: potential markers for eosinophil-dependent tissue injury in vivo. Biochemistry **1999,** 38, (12), 3538-48.

62. Huggins, T. G.; Wells-Knecht, M. C.; Detorie, N. A.; Baynes, J. W.; Thorpe, S. R., Formation of o-tyrosine and dityrosine in proteins during radiolytic and metal-catalyzed oxidation. J Biol Chem **1993,** 268, (17), 12341-7.

# CHAPTER V

# NASAL MUCOSA IS A SANCTUARY SITE FOR ENHANCE OXIDATIVE STRESS AS REVEALED BY MOLECULAR FOOTPRINTS OF MULTIPLE OXIDATIVE PATHWAYS

## 5.1 Introduction

The mucosal lining of the nose and paranasal sinuse serves as an important barrier between the host and the external environment. This barrier function occurs in two principal ways. Firstly, the mucosa provides a physical covering that blocks the entry by potentially pathogenic micro-organisms and non-living substances. Secondly, the immune system performs its surveillance function against non-self antigens within the mucosa and along its surface. The immune system targets specific antigens through the processes of adaptive immunity, which is mediated by both T- and B-cells. Innate immunity provides nonspecific protection against nonself antigens. Mechanisms for innate immunity include phagocytosis (by neutrophils, monocytes and macrophages),

the complement cascade and peroxidases (secreted by neutrophils, monocytes, eosinophils, etc.). Because innate immunity is intrinsically nonspecific, its action may inadvertently damage host tissues. Derangements of immune system function in sinonasal mucosa lead to a wide variety of chronic inflammatory conditions, including allergic rhinitis (AR) and rhinosinusitis (RS, previously termed sinusitis).

Approximately 31 million Americans report suffering from RS [1]. The hallmark of this condition is a chronic inflammatory infiltration [2]. The etiology of RS is unknown bacteria, fungus and immunological dysfunction. Outcome studies have confirmed that RS has a large adverse impact on patient quality of life measures including reductions of patient sense of physical, functional and emotional well-being [3 4].

Once activated, eosinophils and neutrophils are recruited to the sites of inflammation and release unique leukocytes peroxidases and cytotoxic granule proteins, including major basic protein (MBP) [5]. The leukocytes peroxidases, eosinophil peroxidase (EPO) and myeloperoxidase (MPO), are some of the most abundant proteins in these cells [6 7]. In the past several years, studies suggest that EPO and MPO utilize $H_2O_2$ with halides or pseudohalides as co-substrates to generate reactive hypohalous acid (HOX): $H_2O_2 + X^- + H^+ \rightarrow HOX + H_2O$ (X= $Br^-$[8], $Cl^-$[9], $I^-$[10] and $SCN^-$[11] respectively) to fight invading pathogens [12]. Although peroxynitrite ($ONOO^-$), the reactive species formed by nitric oxide radical ($NO^\cdot$) and superoxide ($O2^{\cdot -}$)[13], is believed the major reactive nitrogen species (RNS), recent studies support EPO and MPO may also participate to generation of RNS[14-16]. Using free or protein-bound tyrosyl residues as substrate, EPO/MPO also participates the formation of tyrosyl radical [17]. Further, redox-active metal ions interact with $H_2O_2$ to generate hydroxyl radical ($HO^\cdot$)[18](Fig. 5.1.).

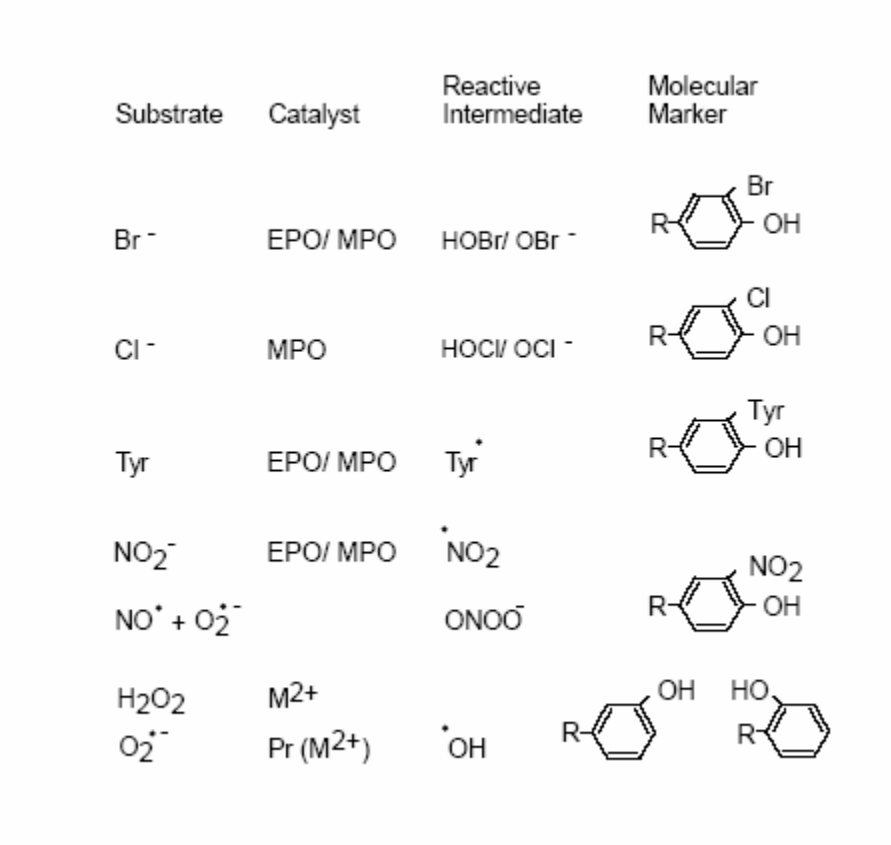


**Figure 5. 1 Reactive Intermediates Generated by Enzymatic Ppathways and Free Metal Ions React with Tyrosine and Phenylalanine**

EPO and MPO utilize hydrogen peroxide and various substrates, including bromide, chloride, tyrosine and nitrite ($NO_2^-$) to generate an array of reactive intermediates: hypobromous acid and hypobromite ion ($HOBr/OBr^-$), hypochlorous acid and hypochlorite ion ($HOCl/OCl^-$), tyrosyl radical and nitrogen dioxide ($NO_2^{\cdot}$). Another reactive nitrogen species, peroxynitrite ($ONOO^-$), is generated by the interaction of nitric oxide radical with superoxide. Redox-active metal ion (free or protein-bound) reacts with hydrogen peroxide to generate hydroxyl radical ($^{\bullet}OH$). These reactive intermediates react with tyrosine or phenylalanine to generate distinct molecular fingerprints of 3-BrTyr, 3- 3-ClTyr, di Tyr, 3-$NO_2$Ty, m-Tyr and o-Tyr, respectively.

These reactive oxidants provide host defense mechanisms against pathogenic organisms through oxidative modifcation. Obviously, the reactions of RBS, RCS, RNS, tyrosyl radical, hydroxyl radical and peroxynitrite are all non-specific, and inevitably host tissues can be modified through these oxidations. Host tissue injury may be assessed through quantifying the amounts of stable end-products, which serve as a molecular footprint of the oxidative modification. Previous studies have demonstrated that RBS, RCS, RNS and tyrosyl radicals oxidize protein-bound tyrosine residues to produce 3-bromotyrosine (3-BrTyr)[19, 20], 3-chlorotyrosine (3-ClTyr) [21, 22], 3-nitrotyrosine (3-$NO_2$Tyr) [15, 23] and o, o'-di-tyrosine (di Tyr) [24], respectively. Similarly, hydroxyl radicals convert protein-bound phenylalanine residues to meta-tyrosine (m-Tyr) and ortho-tyrosine (o-Tyr). [25, 26]

The current study seeks to demonstrate patterns of oxidative metabolism in sinonasal mucosa under normal conditions and in the presence of chronic inflammation. This approach highlights the presence of oxidants produced by both EPO and MPO under normal, healthy conditions. In addition, this method may serve as a powerful tool for the study of mechanisms of RS pathogenesis.

## 5.2 Experimental Procedures

### Subjects

RS patients (n=42) were recruited from the clinical practices of the Section of Nasal and Sinus Disorders in Cleveland Clinic Foundation Head & Neck Institute. A symptom-based history of chronic RS, as defined by the criteria established by the Sinus and Allergy Health Partnership[27], was present in all RS patients. All RS patients reported

symptoms of rhinorrhea and nasal obstruction, and the clinical diagnosis was confirmed through nasal endoscopy and CT scan. Atopy was assessed through a RAST inhalent panel that measured specific IgE for a variety regionally relevant allergens (specific IgE to Timothy grass, June grass, Bermuda grass, short ragweed, English plantain, Lamb's quarters, box elder tree, oak tree, Elm tree, cat dander, dog dander, Penicillium notatum, Cladosporium herbarum, Aspergillus fumigatus, Alternaria tenuis, house dust and Dermatophagoides farinae analyzed by ImmunoCap, Pharmacia & Upjohn, Kalamazoo, MI). RS patients with a positive RAST panel (defined as detectable Class I or greater reaction for one or more antigens) were grouped into the allergic rhinosinusitis (ARS) group, while the remaining patients with a negative RAST panel were grouped into the nonallergic rhinosinusitis (NARS) group.

A total of 16 volunteers were recruited by local advertisements following informed consent. Only ten subjects who were at least 25 years old with normal Ig E and RAST panel were eligible to enroll into study.

The Cleveland Clinic Foundation Institutional Review Board approved the protocol.

**Table 5. 1 Population Characteriistics**

| | **Controls** (n=10) | **Rhinosinusitis (RS)** (n=42) |
|---|---|---|
| **Age (Mean ± SD)** | 28.1 ± 7.7 | 51.4 ± 11.3** |
| **Male gender (%)** | 60 | 60 |
| **IgE (Unit per ml)** | 21.7 ± 20.2 | 263.1 ± 522.5* |
| **Eosinophil differential (%)** | 2.8 ± 1.5 | 5.1 ± 3.4* |
| **Abnormal RAST panel (%)** | 0 | 40** |
| **Asthma (%)** | 0 | 50** |
| **Steroid (%)** | 0 | 70** |

**Comparison RS vs. control: * = p< 0.01, ** = p< 0.01;**

**Sample Collection and Storage**

Sinonasal mucosa was obtained from RS patients under endoscopic visualization, and middle turbinate biopsies were performed in control subjects under endoscopic visualization. Approximate tissue size was 3 mm x 3 mm x 3 mm. Tissue samples were immediately placed in the ice-cold antioxidant phosphate buffer (100 μM DTPA, 100 μM BHT, PB, 20 mM, pH 7.4) and overlaid with argon and saved in approximately –80 °C until analysis.

At the time of biopsy, sera samples were collected from all subjects. Sera samples were then spiked with anti-oxidant cocktail (100 μM DTPA, 100 μM BHT), covered by argon layer and stored frozen at approximately –80 °C freezer.

**Preparation of Tissue**

All samples were processed on the date of analysis. Tissue specimens were thawed and immediately homogenized in ice-cold PBS buffer (100 μM DTPA, 100 μM BHT, PB= 20mM, pH = 7.4) using a Potter-Elvehjem Tissue Homogenizer with a PTFE pestle. A Bradford-based Biorad (Hercules, CA) Protein Assay with human serum albumIn (HSA) as the standard was used for determination of protein concentration.

**Materials**

All solvents were purchased from Fisher Chemical Co. (Pittsburgh, PA,) and were the highest or HPLC grade. All other reagents were purchased from Sigma (St. Louis, MO,) unless otherwise indicated. All gasses were of highest quality available and were from Praxair (Cleveland, OH). Isotopically labeled amino acids were from Cambridge Isotopes (Andover, MA).

**Preparation and Purification of Isotope-labeled Internal Standard**

Isotopically labeled 3-[$^{13}C_6$] bromotyrosine, 3- [$^{13}C_6$] chlorotyrosine, and 3-[$^{13}C_6$] nitrotyrosine and o, o'-di Tyrosine were synthesized as previously described [17, 19, 28, 29]. m-[$^{13}C_6$] tyrosine and o-[$^{13}C_6$] tyrosine were synthesized using [$^{13}C_6$] phenylalanine, copper and $H_2O_2$ [30]. Each isotopically labeled compound solution was purified by reversed-phase HPLC and collected at the exactly same retention time of the corresponding natural abundance oxidized tyrosine. The identity and purifity of isotop internal standard was confirmed by LC/MS.

**General Procedures**

To prevent the artificial oxidation during sample handling, samples were always kept under argon. All buffers were treated with chelex-100 resin (Bio-Rad, Hercules, CA) to remove residual amount of transition metal ions. The glassware was treated with DTPA, rinsed with chelex-100 resin treated water, and baked at 500$^{o}$ C overnight prior to use.

**Desalting and Delipidation**

The quantity of 20 μl serum or 600 μg tissue homogenate was spiked with DTPA (final concentration100 μM) and adjusted to 500 μl with Chelex-resin treated water. Ice-cold methanol (1.5 ml) was added and followed by diethyl ether (4 ml, water saturated). The resulting solution was gently vortexed and incubated in an ice-bath for 20 minutes. The suspension was spun down at ~ 4000 rpm for 20 minutes. The supernatant was discarded and the protein pellet was dried under nitrogen. Desalting and delipidation was repeated again using the procedure above without DTPA supplementation.

**Protein Hydrolysis**

The protein or tissue residue was dried under nitrogen piror to addition of isotopically labeled internal standard cocktail. The sample was then hydrolyzed at 110 °C for 20 hours in 0.5 ml methane sulfonic acid (MSA, 4 N) with 1% phenol and 0.3% benzoic acid supplement.

**Solid Phase Extraction**

Protein hydrolysates were diluted to 2 ml with Chelex-treated water and passed over a C18 SPE column (500 mg, Supelco Inc., Bellefonte, PA). The column was pretreated with 6ml methanol, rinsed with 6ml PB buffer (50 mM, pH 7.0, 100 μM DTPA), followed by 6ml Chelex-treated water and equilibrated with 6 ml 0.1% TFA water. After 2 x 2 ml of 0.1% TFA water wash, the amino acids were eluted with 2 ml 30% methanol in water containing 0.1% TFA. The samples were dried under speed vac and re-dissolved in 120 μl chelex-treated water before analysis by mass spectrometer.

**Instrumentation**

Amino acids were quantified by stable isotope dilution LC-MS/MS. Each 60 μl sample was analyzed on a Quattro Ultima mass spectrometer (Waters, Altrincham, U.K.) interfaced with a Waters 2690 Separation Module HPLC system (Waters, Milford, MA, USA). The source temperature was set at 250 °C. The cone and capillary voltages were optimized at 30 V and 5 KV respectively. The collision energy was set to 15 eV with a dwell time of 100 ms for each analyte.

The positively charged molecules were selected by mass-charge ratios and focused in the collision chamber containing argon gas. The multiple-reaction monitoring (MRM) transitions were used to detect oxidized tyrosine species and their precursors,

tyrosine and phenylalaine, respecitvely. Each distinct parent-daughter transition was detected by triple quadruple analyzer. The molecular ions of 3-BrTyr ($M^+$) in positive mode are m/z 260 [$^{79}$ Br], 262 [$^{81}$Br]. The product ion of 3-BrTyr include m/z 243 ([$^{79}$Br] $M^+$ -$NH_3$), 245 ([$^{81}$Br] $M^+$ -$NH_3$), 214 ([$^{79}$Br] $M^+$ -$CO_2H_2$), and 216 ([$^{81}$Br] $M^+$ -$CO_2H_2$). The parent-daughter transition 260 → 214 was used to quantify 3- Br Tyr. Similarly, the transitions of 218 → 172, 361 → 315, 227 → 181 and 166 → 120 were used to quantify 3-ClTyr, di Tyr, 3-$NO_2$ Tyr and phenylalanine respectively. Tyr, m-Tyr and o-Tyr use same parent-daughter transition 182 → 136, with different retention times.

A Prodigy ODS 18 column (150 x 2 mm, 5 μm resin, Phenomenex, Torrance, CA, USA) was used to separate amino acids at a flow rate of 0.2 ml/min. The column was equilibrated with solvent A (0.2% formic acid in water) first. Then the analytes were separated by a stepped linear gradient with solvent B (0.2% formic acid in acetonitrile) as follow: 0% solvent B was held for 2 min, followed by a linear change from 0% B to 18% B over 18 min, then hold at 80% B in next 2 min. The gradient was then kept at 80% B for 4 min before return to 0% solvent B.

**Statistical Analysis**

Data are presented as mean ± SD. The statistic studies were performed using SPSS version 11.0 (SPSS. Inc. Chicago, IL). The significance level was set at 95%.

## 5.3 Results

**Oxidized Tyrosine Species in Nasal Mucosa in Normal Subjects**

Amino acids isolated from acid hydrolysates of nasal mucosa were analyzed by LC-MS/MS as described in experimental procedures. The identity of each authentic

oxidized tyrosine was confirmed by the corresponding isotopically labeled internal standard possessing identical retention time (Figure. 5.2).

**Elevated o-Tyr, 3-BrTyr, and 3-ClTyr in Healthy Nasal Mucosa**

To explore the mechanisms of leukocyte-catalyzed oxidative damage in healthy sinonasal mucosa, the peripheral serum level of each oxidized tyrosine species and the corresponding sinonasal tissue level were compared. In normal subjects, protein-bound 3-BrTyr level was significantly elevated in sinonasal tissue compared with that in serum (556.9 μmol/mol vs. 40.0 μmol/mol, $p<0.01$). Levels of protein-bound tissue o-Tyr and 3-ClTyr in tissue were also observed (o-Tyr, 394.0 μmol/mol vs. 190.1 μmol/mol, $p<0.05$; 3-ClTyr/Tyr, 10.9 μmol/mol vs 5.3 μmol/mol, $p<0.05$). No other significant differences between systemic and local levels of m-Tyr and diTyr were noted in healthy volunteers, although there were trends toward higher levels in nasal mucosa (Figure. 5.3A).

**Elevated m-Tyr, o-Tyr, di Tyr, 3-BrTyr, and 3-$NO_2$Tyr in Nasal Mucosa from RS Patients**

In RS subjects, levels of m-Tyr, o-Tyr, di Tyr, 3-BrTyr and 3-$NO_2$Tyr were all elevated in sinonasal tissue compared with serum (m-Tyr, 131.4 μmol/mol vs. 88.4 μmol/mol, $p< 0.01$; o-Tyr, 458.0 μmol/mol vs. 213.5 μmol/mol, $p< 0.001$; diTyr, 5449.9 μmol/mol vs. 536.0 μmol/mol, $p< 0.001$; 3-BrTyr, 897.5 μmol/mol vs. 35.1 μmol/mol, $p< 0.001$; 3-$NO_2$Tyr, 43.9 μmol/mol vs. 17.6 μmol/mol, , $p< 0.05$) (Figure 5.3 B).

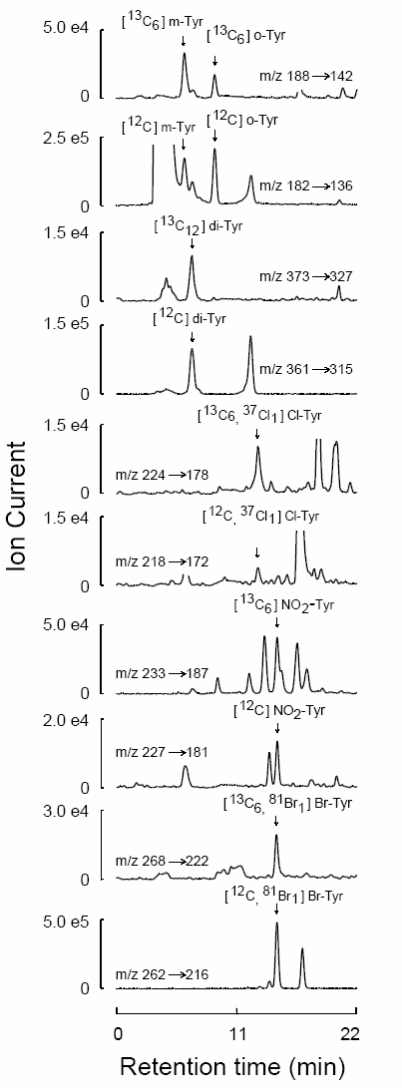


**Figure 5. 2 Chromatograph of Oxidized Tyrosine Species in Nasal Tissue Specimen from a Rhinosinusitis Patient**

Nasal tissue specimen was obtained from a RS patient and prepared as described in Experimental Procedures. m-Tyr, o-Tyr (MRM: 182 → 136), diTyr (361 → 315), ClTyr (218 → 172) and NO2Tyr (227→ 181) were quantified by the corresponding isotope internal standard, [$^{13}C_6$] m-Tyr, o-Tyr (MRM: 188 → 142), [$^{13}C_{12}$] diTyr (373 → 327), [$^{13}C_6$] ClTyr (224 → 178) and [$^{13}C_6$] NO2Tyr (233→ 187) and [$^{13}C_6$] BrTyr (266→ 220).

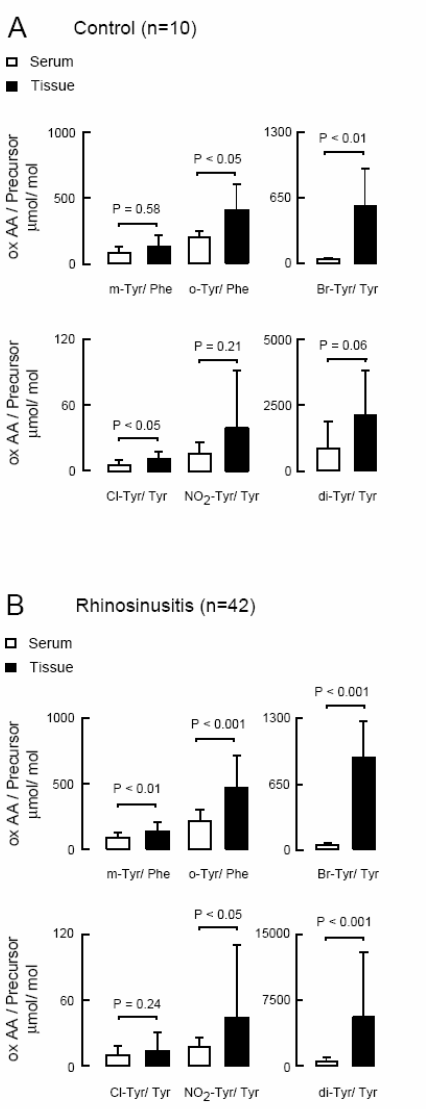


**Figure 5. 3 Sinonasal Tissue and Peripheral Serum Levels of m-Tyr, o-Tyr, 3-BrTyr, 3-ClTyr, 3NO2Tyr and di Tyr**

Panel A, comparisons of tissue and serum levels oxidized tyrosine species from control subjects (n=10). The levels of o-Tyr, 3-BrTyr and3-ClTyr in sinonasal tissue were significantly elevated. Panel B, comparisions of tissue and serum levels oxidized tyrosine species from RS patients (n= 42). Sinonasal levels of m-Tyr, o-Tyr, 3-BrTyr, 3-$NO_2$Tyr and di Tyr were significantly elvelated. Data represent the mean ±SD.

**Sgnificantly Elevated Bromination and Tyrosylation in RS Patients Compare to Those in Healthy Controls**

To understand the mechanism of oxidative modification in nasal mucosa, the tissue/serum ratio (T/S ratio) of each oxidized tyrosine species was calculated to normalize individual differences. T/S ratios greater than one were noted for all analytes indicating an elevated oxidative stress in sinonasal tissue. TheT/S ratios in RS patients were significant greater than corresponding T/S ratios in control subjects (T/S ratio (mean, μmol/mol/ μmol/mol), 3-BrTyr, RS, 27.0, control, 15.5, $p<0.005$; diTyr, RS, 18.4, control, 4.9, $p< 0.05$) (Figure. 5.4.). However, the T/S ratio for m-Tyr, o-Tyr, 3-ClTyr and 3-$NO_2$Tyr was similar in RS patients and controls (T/S ratio (mean, μmol/mol/ μmol/mol), m-Tyr, control, 1.8, RS, 1.7, $p=0.90$; o-Tyr, control, 2.2, RS, 2.3, $p= 0.79$; 3-ClTyr, control, 3.4, RS, 3.0, $p=0.72$; $NO_2$Tyr, Control, 2.9, RS, 2.8, $p= 0.94$.).

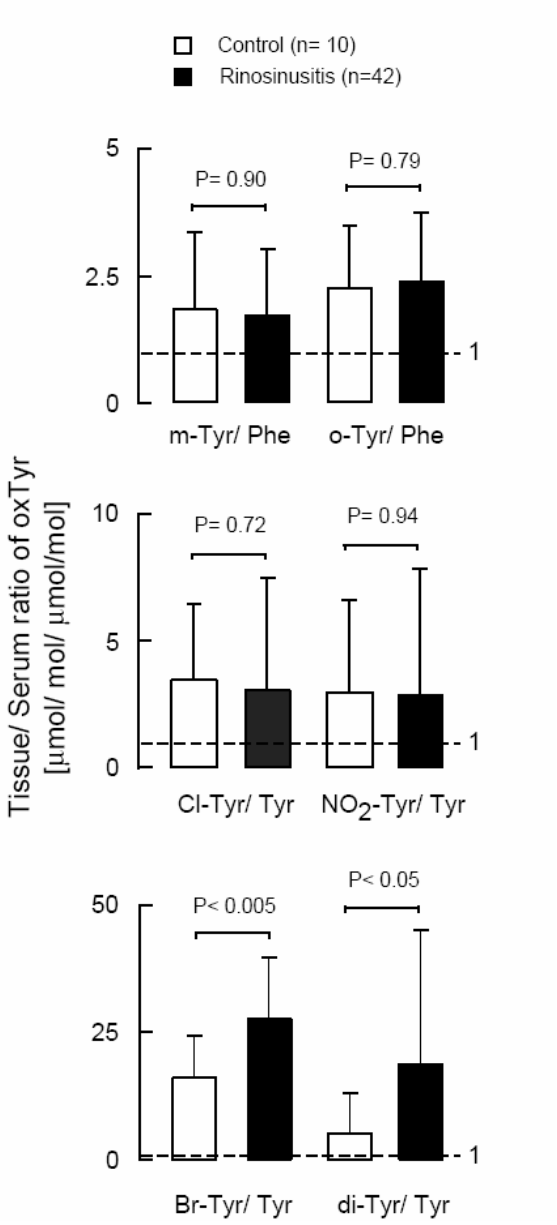


**Figure 5. 4 Bromination and Tyrosylation Were Significantly Increased in RS Patients Compared with Control Subjects**

The tissue/serum ratio of each oxidized tyrosine was calculated to normalize individual differences. Elevated bromination and tyrosylation were significantly increased in RS patients compared to those in controls (3-BrTyr T/S ratio, RS, 27.0± 11.6, control, 15.5± 8.1, $p< 0.005$; di Tyr T/S ratio, RS, 18.4± 25.8, control, 4.9 ± 7.8, $p< 0.05$).

## 5.4 Discussion

Human eosinophils produce reactive brominating species which can serve as oxidants to participate host defense and may also cause host tissue damage [8, 20]. Previous *in vitro* data have demonstrated that peroxidases can utilize physiological levels of halides or pseudohalides as co-substrates to generate reactive hypohalous acid even in the presence of multiple competing co-substrates [17]. Eosinophil activation and induced oxidative modification were observed in numerous biological matrixes. Recent studies found that significantly elevated protein-bound 3-BrY was recovered in sputum, bronchoalveolar lavage fluid (BAL) in asthmatic patients compared to the healthy controls [20, 31]. Elevated serum eosinophil is the hallmark of a chronic inflammatory in rhinosinusitis patients [2, 5]. In the current study, the tissue levels of 3-BrTyr were significantly elevated in RS patients compared to that in control group (3-BrTyr, RS (n=42) vs. Control (n=10), 871.1 μmol/mol vs. 556.9 μmol/mol, $p< 0.05$). However, half of RS patients (n= 21) had asthmatic symptoms. Therefore, the potential impact of asthma on protein oxidative damage in nasal tissue was investigated. Significantly elevated 3-BrTyr was detected in nasal mucosa in RS patients with or without asthmatic symptom compared with control groups (3-BrTyr (μmol/mol), RS with asthma vs. control, 861 vs.556.9, $p< 0.05$; RS without asthma, 881 vs.Control, 556.9, $p< 0.05$). But there was no significant different in 3-BrTyr in nasal mucosa between RS patients with or without asthma (3-BrTyr (μmol/mol), RS with asthma, 861 vs. RS without asthma, 881, $p= 0.856$). The present study strongly suggests that asthmatic inflammation has no significant impact on the augment of bromination in nasal mucosa in RS patients. Thus

the elevation of 3-BrTyr levels supports activation of eosinophils in RS pathophysiology. In this way, EPO-catalyzed oxidation may play central roles in fighting pathogens and inadvertently in inducing non-specific host tissue oxidation.

This report describes both nasal mucosal tissue and serum levels of a panel of oxidized tyrosine species in healthy control subjects as well as RS patients. Even in healthy controls, tissue levels of o-Tyr, 3-ClTyr and 3-BrTyr were significantly higher than the corresponding serum levels. Thus, under physiological conditions, nasal mucosa serves as a sanctuary site for oxidative stress, as measured by dramatic elevations of oxidized tyrosine residues in nasal mucosa from healthy subjects. The presence of evidence of oxidative stress in health nasal mucosa is not surprising in light of the barrier function provided by the nasal mucosa. The nasal cavity serves as a 'trap' for inhaled micro-organisms and particulate matter. Removal of this foreign material occurs through the active transport of mucus in the process of mucociliary clearance. Surveillance provided by the immune system also occurs in the interface provided by the mucosa. Since peroxidases released by inflammatory cells play an important role in the inactivation of invasive micro-organisms and particulate matter, evidence of their activity in healthy mucosa, where normal clearance of these non-self antigens is an active (and successful) process that should be expected.

In RS patients, m-Tyr, o-Tyr, 3-BrTyr, diTyr and 3-$NO_2$Tyr were all elevated in nasal tissue compared with that in serum, suggesting a more generalized elevation of oxidative stress in the tissues. This more generalized elevation of the oxidative stress in sinonasal mucosa in RS patients probably reflects the underlying RS disease process of inflammatory infiltration of the sinonasal mucosa.

To further investigate the involvement of each distinct oxidative pathway in nasal inflammation, RS patients were divided into two subgroups, allergic rhinosinusitis (ARS, n=17) and nonallergic rhinosinusitis (NARS, n=25). Sinonasal tissue 3-BrTyr level was significantly increased in NARS patients compared with controls (3-BrTyr (μmol/mol), NARS, 927.7 vs. Control, 556.9, $p < 0.05$). Sinonasal tissue levels of 3-BrTyr were elevated but not reach statistic significant in the ARS and control groups (3-BrTyr (μmol/mol), ARS, 787.8 vs. Control, 556.9, $p = 0.11$), and no significant differences in sinonasal tissue 3-BrTyr levels in NARS and ARS were noted (3-BrTyr (μmol/mol), NARS, 927.7 vs. Control 787.8, $p = 0.20$) (Figure 5.5 A.). In addition, sinonasal tissue di-Tyr was significantly increased in ARS patients compared with control subjects (di Tyr (μmol/mol), ARS, 5753.0 vs. Control, 2028.3, $p < 0.05$). Sinonasal tissue levels of di-Tyr were elevated but not statistic significant in the NARS and control groups (di Tyr (μmol/mol), NARS, 4970.9 μmol/mol vs. Control, 2028.3, $p = 0.08$), and no significant differences in sinonasal tissue di Tyr levels in ARS and NARS were noted (di Tyr (μmol/mol), ARS, 5753.0 vs. NARS, 4970.9, $p = 0.72$). (Figure 5.5B.). Since the mechanisms for nonallergic and allergic inflammation are often considered distinct, the failure to identify many differences between allergic and nonallergic RS is surprising. Perhaps, enhanced oxidative stress is a common feature of RS associated with allergic and nonallergic inflammatory mechanisms.

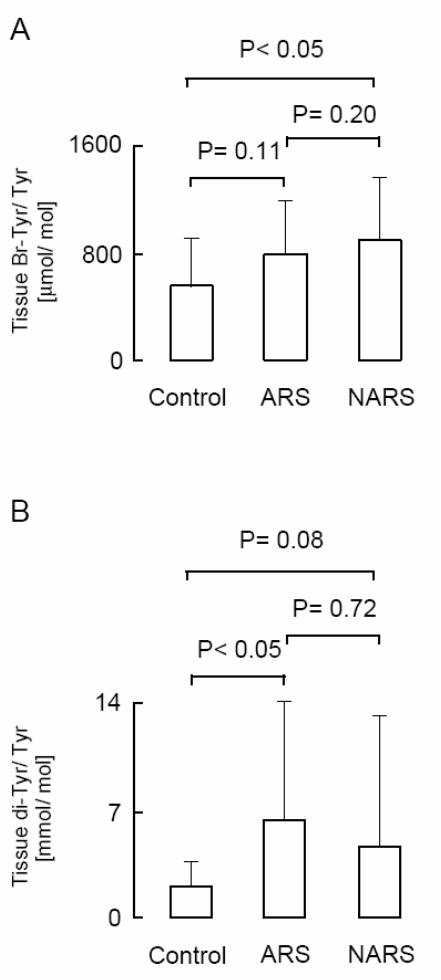


**Figure 5. 5 Distinct Oxidation Pathway Was Elevated in non-allergic Rhinosinusitis (NARS) and Allergic Rhinosinusitis (ARS) Compared with Control**

A, tissue 3-BrTyr levels in control (n=10), ARS (n=17) and NARS (n=25) were compared. Significantly elevated sinonasal tissue 3-BrTyr levels were only observed in NARS compared to control (NARS, 927.7 µmol/mol vs. Control, 556.9 µmol/mol, $p < 0.05$). In panel B, tissue levels of di-Tyr in control, ARS and NARS subjects were compared. Significantly elevated tissue level diTyr were observed in ARS patients compared to controls (ARS, 5753.0 µmol/mol vs. Control, 2028.3 µmol/mol, $p < 0.05$). No other significant differences were observed between ARS vs. Control and NARS vs. ARS.

Our previous study indicated that systemic level of protein-bound nitrotyrosine declined in response to the treatment of with statins [32]. The primary design of current study was not focused on the impact of anti-inflammation action of steroid on the observed levels of oxidative markers. But due to general steroid usages in RS patients is about 70%, it may have certain impact on reducing eosinophils, neutrophils and may modulate the observed levels of bromination at serum and tissue level. Therefore the serum level of 3-BrTyr was compared between RS patients with or without steroid usage. No significant difference in bromination was observed between RS patients with or without steroid usage at serum level (3-BrTyr (μmol/mol), RS with steroid vs. RS without steroid, 35.1 vs. 34.9, p= 0.95). However, in RS patients with tissue level 3-BrTyr ≤ 658.6 μmol/mol ($T_1$), 64% of them had steroid treatment. The steroid usage was increased to 86% when RS patients with tissue levels of 3-BrTyr were greater than 1027.9 μmol/mol ($T_3$). The trend did not reach statistic significant due to limit study number, various brands steroid usages. In addition, without the oxidative profile prior to treatment, the therapeutic impact of steroid at inflammation site is still unsolved. Future study the correlation of oxidative modification in nasal mucosa in response to steroid, especially nasal steroid treatment is necessary.

## 5.5 Conclusion

The elevations of oxidized tyrosine species in healthy nasal mucosa (compared with corresponding serum levels) suggests that oxidative stress occurs in nasal tissue under normal physiologic conditions. Furthermore, detection of end products of oxidative metabolism in normal tissue supports the concept that nasal mucosa is a sanctuary site for

host defenses against potentially pathogenic micro-organisms and other foreign antigens. RS patients show an even higher level of oxidative stress in nasal tissue. Thus, activation of oxidative pathways may contribute to RS pathogenesis.

## 5.6 References:


1. Infectious rhinosinusitis in adults: classification, etiology and management. International Rhinosinusitis Advisory Board. Ear Nose Throat J **1997,** 76, (12 Suppl), 1-22.
2. Zadeh, M. H.; Banthia, V.; Anand, V. K.; Huang, C., Significance of eosinophilia in chronic rhinosinusitis. Am J Rhinol **2002,** 16, (6), 313-7.
3. Gliklich, R. E.; Metson, R., The health impact of chronic sinusitis in patients seeking otolaryngologic care. Otolaryngol Head Neck Surg **1995,** 113, (1), 104-9.
4. Senior, B. A.; Glaze, C.; Benninger, M. S., Use of the Rhinosinusitis Disability Index (RSDI) in rhinologic disease. Am J Rhinol **2001,** 15, (1), 15-20.
5. Ponikau, J. U.; Sherris, D. A.; Kephart, G. M.; Kern, E. B.; Gaffey, T. A.; Tarara, J. E.; Kita, H., Features of airway remodeling and eosinophilic inflammation in chronic rhinosinusitis: is the histopathology similar to asthma? J Allergy Clin Immunol **2003,** 112, (5), 877-82.
6. Schultz, J.; Kaminker, K., Myeloperoxidase of the leucocyte of normal human blood. I. Content and localization. Arch Biochem Biophys **1962,** 96, 465-7.
7. Carlson, M. G.; Peterson, C. G.; Venge, P., Human eosinophil peroxidase: purification and characterization. J Immunol **1985,** 134, (3), 1875-9.

8. Weiss, S. J.; Test, S. T.; Eckmann, C. M.; Roos, D.; Regiani, S., Brominating oxidants generated by human eosinophils. Science **1986,** 234, (4773), 200-3.

9. Foote, C. S.; Goyne, T. E.; Lehrer, R. I., Assessment of chlorination by human neutrophils. Nature **1983,** 301, (5902), 715-6.

10. Bozeman, P. M.; Learn, D. B.; Thomas, E. L., Assay of the human leukocyte enzymes myeloperoxidase and eosinophil peroxidase. J Immunol Methods **1990,** 126, (1), 125-33.

11. Slungaard, A.; Mahoney, J. R., Jr., Thiocyanate is the major substrate for eosinophil peroxidase in physiologic fluids. Implications for cytotoxicity. J Biol Chem **1991,** 266, (8), 4903-10.

12. Jong, E. C.; Chi, E. Y.; Klebanoff, S. J., Human neutrophil-mediated killing of schistosomula of Schistosoma mansoni: augmentation by schistosomal binding of eosinophil peroxidase. Am J Trop Med Hyg **1984,** 33, (1), 104-15.

13. Beckman, J. S.; Koppenol, W. H., Nitric oxide, superoxide, and peroxynitrite: the good, the bad, and ugly. Am J Physiol **1996,** 271, (5 Pt 1), C1424-37.

14. van der Vliet, A.; Eiserich, J. P.; Halliwell, B.; Cross, C. E., Formation of reactive nitrogen species during peroxidase-catalyzed oxidation of nitrite. A potential additional mechanism of nitric oxide-dependent toxicity. J Biol Chem **1997,** 272, (12), 7617-25.

15. Hazen, S. L.; Zhang, R.; Shen, Z.; Wu, W.; Podrez, E. A.; MacPherson, J. C.; Schmitt, D.; Mitra, S. N.; Mukhopadhyay, C.; Chen, Y.; Cohen, P. A.; Hoff, H. F.; Abu-Soud, H. M., Formation of nitric oxide-derived oxidants by myeloperoxidase

in monocytes: pathways for monocyte-mediated protein nitration and lipid peroxidation In vivo. Circ Res **1999,** 85, (10), 950-8.

16. Brennan, M. L.; Wu, W.; Fu, X.; Shen, Z.; Song, W.; Frost, H.; Vadseth, C.; Narine, L.; Lenkiewicz, E.; Borchers, M. T.; Lusis, A. J.; Lee, J. J.; Lee, N. A.; Abu-Soud, H. M.; Ischiropoulos, H.; Hazen, S. L., A tale of two controversies: defining both the role of peroxidases in nitrotyrosine formation in vivo using eosinophil peroxidase and myeloperoxidase-deficient mice, and the nature of peroxidase-generated reactive nitrogen species. J Biol Chem **2002,** 277, (20), 17415-27.

17. Wu, W.; Chen, Y.; Hazen, S. L., Eosinophil peroxidase nitrates protein tyrosyl residues. Implications for oxidative damage by nitrating intermediates in eosinophilic inflammatory disorders. J Biol Chem **1999,** 274, (36), 25933-44.

18. Maskos, Z.; Rush, J. D.; Koppenol, W. H., The hydroxylation of phenylalanine and tyrosine: a comparison with salicylate and tryptophan. Arch Biochem Biophys **1992,** 296, (2), 521-9.

19. Wu, W.; Chen, Y.; d'Avignon, A.; Hazen, S. L., 3-Bromotyrosine and 3,5-dibromotyrosine are major products of protein oxidation by eosinophil peroxidase: potential markers for eosinophil-dependent tissue injury in vivo. Biochemistry **1999,** 38, (12), 3538-48.

20. Wu, W.; Samoszuk, M. K.; Comhair, S. A.; Thomassen, M. J.; Farver, C. F.; Dweik, R. A.; Kavuru, M. S.; Erzurum, S. C.; Hazen, S. L., Eosinophils generate brominating oxidants in allergen-induced asthma. J Clin Invest **2000,** 105, (10), 1455-63.

21. Hazen, S. L.; Heinecke, J. W., 3-Chlorotyrosine, a specific marker of myeloperoxidase-catalyzed oxidation, is markedly elevated in low density lipoprotein isolated from human atherosclerotic intima. J Clin Invest **1997,** 99, (9), 2075-81.

22. Podrez, E. A.; Abu-Soud, H. M.; Hazen, S. L., Myeloperoxidase-generated oxidants and atherosclerosis. Free Radic Biol Med **2000,** 28, (12), 1717-25.

23. van der Vliet, A.; Eiserich, J. P.; Kaur, H.; Cross, C. E.; Halliwell, B., Nitrotyrosine as biomarker for reactive nitrogen species. Methods Enzymol **1996,** 269, 175-84.

24. Giulivi, C.; Davies, K. J., Dityrosine: a marker for oxidatively modified proteins and selective proteolysis. Methods Enzymol **1994,** 233, 363-71.

25. Nair, U. J.; Nair, J.; Friesen, M. D.; Bartsch, H.; Ohshima, H., Ortho- and meta-tyrosine formation from phenylalanine in human saliva as a marker of hydroxyl radical generation during betel quid chewing. Carcinogenesis **1995,** 16, (5), 1195-8.

26. Pennathur, S.; Wagner, J. D.; Leeuwenburgh, C.; Litwak, K. N.; Heinecke, J. W., A hydroxyl radical-like species oxidizes cynomolgus monkey artery wall proteins in early diabetic vascular disease. J Clin Invest **2001,** 107, (7), 853-60.

27. Benninger, M. S.; Ferguson, B. J.; Hadley, J. A.; Hamilos, D. L.; Jacobs, M.; Kennedy, D. W.; Lanza, D. C.; Marple, B. F.; Osguthorpe, J. D.; Stankiewicz, J. A.; Anon, J.; Denneny, J.; Emanuel, I.; Levine, H., Adult chronic rhinosinusitis: definitions, diagnosis, epidemiology, and pathophysiology. Otolaryngol Head Neck Surg **2003,** 129, (3 Suppl), S1-32.

28. Hazen, S. L.; Crowley, J. R.; Mueller, D. M.; Heinecke, J. W., Mass spectrometric quantification of 3-chlorotyrosine in human tissues with attomole sensitivity: a sensitive and specific marker for myeloperoxidase-catalyzed chlorination at sites of inflammation. Free Radic Biol Med **1997,** 23, (6), 909-16.

29. Malencik, D. A.; Sprouse, J. F.; Swanson, C. A.; Anderson, S. R., Dityrosine: preparation, isolation, and analysis. Anal Biochem **1996,** 242, (2), 202-13.

30. Huggins, T. G.; Wells-Knecht, M. C.; Detorie, N. A.; Baynes, J. W.; Thorpe, S. R., Formation of o-tyrosine and dityrosine in proteins during radiolytic and metal-catalyzed oxidation. J Biol Chem **1993,** 268, (17), 12341-7.

31. Aldridge, R. E.; Chan, T.; van Dalen, C. J.; Senthilmohan, R.; Winn, M.; Venge, P.; Town, G. I.; Kettle, A. J., Eosinophil peroxidase produces hypobromous acid in the airways of stable asthmatics. Free Radic Biol Med **2002,** 33, (6), 847-56.

32. Shishehbor, M. H.; Brennan, M. L.; Aviles, R. J.; Fu, X.; Penn, M. S.; Sprecher, D. L.; Hazen, S. L., Statins promote potent systemic antioxidant effects through specific inflammatory pathways. Circulation **2003,** 108, (4), 426-31.